

AD-A036 904

FAIRCHILD REPUBLIC CO FARMINGDALE N Y
PULSED PLASMA PLUME STUDIES. (U)
MAR 77 W J GUMAN, M BEGUN

F/G 21/3

UNCLASSIFIED

AFRPL-TR-77-2

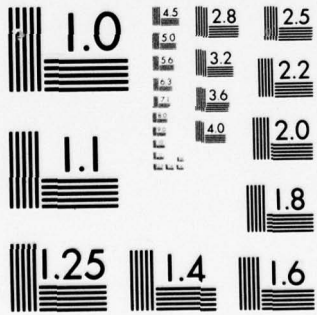
F04611-75-C-0037

NL

1 of 2
AD
A036904



3690



MICROCOPY RESOLUTION TEST CHART
NATIONAL BUREAU OF STANDARDS-1963-A

ADA036904

AFRPL-TR-77-2

12

PULSED PLASMA PLUME STUDIES

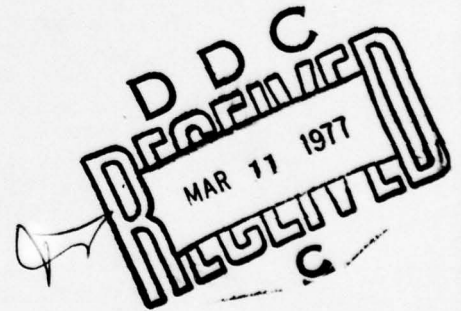
William J. Guman
Martin Begun

Fairchild Industries, Inc.
Fairchild Republic Company
Farmingdale, N. Y. 11735

March 1977

Final Report

APPROVED FOR PUBLIC RELEASE
DISTRIBUTION UNLIMITED



Prepared for
AIR FORCE ROCKET PROPULSION LABORATORY
DIRECTOR OF SCIENCE AND TECHNOLOGY
AIR FORCE SYSTEMS COMMAND
Edwards AFB, CA 93523

NOTICE

When Government drawings, specifications, or other data are used for any purpose other than in connection with a definitely related Government procurement operation, the United States Government thereby incurs no responsibility nor any obligation whatsoever; and the fact that the Government may have formulated, furnished, or in any way supplied the said drawings, specifications, or other data, is not to be regarded by implication or otherwise as in any manner licensing the holder or any other person or corporation, or conveying any rights or permission to manufacture, use, or sell any patented invention that may in any way be related thereto.

FOREWORD

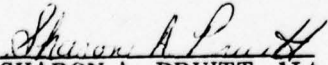
This final report was prepared by Fairchild Industries, Inc., Fairchild Republic Company under Air Force Contract F04611-75-C-0037, "Pulsed Plasma Plume Studies".

The research reported upon was supported by the Air Force Rocket Propulsion Laboratory. The program was monitored in the Liquid Rocket Division by Lt. Sharon Pruitt.

Work on this contract began in March 1975 and was completed in October 1976 and the pertinent studies of this period are reported herein. The report was submitted by the Authors in December 1976.

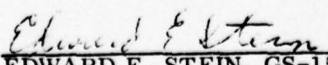
The authors wish to acknowledge the significant contributions of Mr. M. Katchmar and the assistance of Messrs. S. Pasternack and F. Carlson. Specific acknowledgement is made to the valuable contributions of Dr. R. Jahn and Dr. K. Clark of Princeton University who, as consultants, assisted in the development of the Langmuir probe. Appreciation is extended to Dr. R. Jakobsen of the Battelle Columbus Laboratories for assistance in carrying out the chemical analysis. The constructive comments and suggestions of Dr. Palumbo of Fairchild Republic are also gratefully acknowledged.

This report has been reviewed by the Information Office/DOZ and is releasable to the National Technical Information Service (NTIS). At NTIS it will be available to the general public, including foreign nations. This technical report has been reviewed and is approved for publication; it is unclassified and suitable for general public release.


SHARON A. PRUITT, 1Lt
Project Engineer


THOMAS W. WADDELL, GS-14
Chief, Satellite Propulsion Section

For The Commander


EDWARD E. STEIN, GS-15
Deputy Chief, Liquid Rocket Division

ACCESSION for	Write Section	<input checked="" type="checkbox"/>	<input type="checkbox"/>
	Subj Section	<input type="checkbox"/>	<input type="checkbox"/>
RTS			
DOC			
UNANNOUNCED			
JUSTIFICATION			
BY	DISTRIBUTION/AVAILABILITY CODES		
	Dist.	Avail. and/or SPECIAL	
		A	

UNCLASSIFIED

SECURITY CLASSIFICATION OF THIS PAGE (When Data Entered)

19 REPORT DOCUMENTATION PAGE		READ INSTRUCTIONS BEFORE COMPLETING FORM
18 1. REPORT NUMBER AFRPL TR-77-2	2. GOVT ACCESSION NO.	3. RECIPIENT'S CATALOG NUMBER
4. TITLE (and Subtitle) Pulsed Plasma Plume Studies	5. TYPE OF REPORT & PERIOD COVERED Final rept. March 1975 - November 1976	6. PERFORMING ORG. REPORT NUMBER
10 7. AUTHOR(s) William J. Guman Martin Begun	8. CONTRACT OR GRANT NUMBER(s) F04611-75-C-0037	
9. PERFORMING ORGANIZATION NAME AND ADDRESS Fairchild Industries, Inc. Fairchild Republic Company Farmingdale, N. Y. 11735	10. PROGRAM ELEMENT, PROJECT, TASK AREA & WORK UNIT NUMBERS JON305812TF 62302F	
11. CONTROLLING OFFICE NAME AND ADDRESS Air Force Rocket Propulsion Laboratory/LKDA Edwards AFB, CA 93523	12. REPORT DATE March 1977	13. NUMBER OF PAGES 105
14. MONITORING AGENCY NAME & ADDRESS (if different from Controlling Office) 12 IOPP	15. SECURITY CLASS. (of this report) Unclassified	15a. DECLASSIFICATION/DOWNGRADING SCHEDULE
16. DISTRIBUTION STATEMENT (of this Report) Approved for Public Release, Distribution Unlimited		
17. DISTRIBUTION STATEMENT (of the abstract entered in Block 20, if different from Report)		
18. SUPPLEMENTARY NOTES None		
19. KEY WORDS (Continue on reverse side if necessary and identify by block number) Space Propulsion, Rocket Plumes, Electric Propulsion, Plasma Propulsion, Solid Propellant, Spacecraft Contamination		
20. ABSTRACT (Continue on reverse side if necessary and identify by block number) The exhaust plume of a millipound thrust level pulsed plasma thruster was studied in a vacuum chamber having all walls cooled by liquid nitrogen. This thruster has a propulsive performance capable of meeting North-South station-keeping requirements of satellites. The major source of contamination of a surface located in the facility was identified to be mainly due to mass being scattered off the walls of the test facility because the walls were incapable of absorbing the highly energetic plume on the first encounter with the wall. Using a Langmuir probe		

D D C
R E P O R T
M A R 11 1977
R E C E I V E D

DD FORM 1473 1 JAN 73 EDITION OF 1 NOV 68 IS OBSOLETE S/N 0102-014-6601

UNCLASSIFIED
SECURITY CLASSIFICATION OF THIS PAGE (When Data Entered)

use → 408278

18

TABLE OF CONTENTS

<u>Section</u>		<u>Page</u>
1.0	INTRODUCTION	3
2.0	DESCRIPTION OF FACILITY, THRUSTER AND MAJOR INSTRUMENTATION	6
2.1	Vacuum Test Facility	6
2.2	Thruster	11
2.3	Instrumentation	13
2.3.1	Instrumentation Rake	13
2.3.2	Quartz Crystal Microbalance (QCM)	16
2.3.3	Microbalance	19
2.3.4	Thrust Balance	20
2.3.5	Langmuir Probe	20
3.0	EXPERIMENTAL STUDIES	21
3.1	Mass Distribution Studies	21
3.1.1	Quartz Crystal Microbalance Measurements	21
3.1.1.1	QCM Temperature Test	21
3.1.1.2	QCM Survey of the Plume	22
3.1.2	Mass Distribution by Glass Capture Cup Measurements	27
3.1.2.1	Experimental Studies with Glass Capture Cups	32
3.1.2.1.1	Pre-test Checks	32
3.1.2.1.2	Tests with the Cups Being Exposed to the Plume	34
3.2	Ion Density Measurements	39
3.2.1	Langmuir Probe Design	40
3.2.2	Experimental Set-up for Ion Density Measurements	44
3.2.3	Langmuir Probe Data Reduction	45
3.2.4	Ion Density and Electron Temperature Distribution	50
3.3	Back Flow Measurements	55
3.4	Thruster Propulsive Performance	58
3.5	Solar Cell Contamination Studies	58
3.6	Thermal Control	71
3.6.1	Emissivity Changes by an In-Situ Calorimetric Technique	72
3.6.2	Absorptance Measurements	75
3.6.3	Beam Energy Distribution Study	79
3.7	Chemical Analysis of Test Surfaces	88
4.0	CONCLUSIONS AND RECOMMENDATIONS	95
5.0	REFERENCES	98

LIST OF ILLUSTRATIONS

<u>Figure</u>	<u>Page</u>
1. General Geometry of Test Facility	6
2. Test Facility with Thruster and Instrumentation Rake	7
3. Temperature History of Test Facility	9
4. Test Facility Pumping Capacity	10
5. Thruster, Front View, Covers Removed	14
6. Thruster, Rear View, Covers Removed	15
7. Angular Notation Used	17
8. QCM Temperature Test Results	23
9. QCM Survey, 140° Acceptance Angle	25
10. QCM Survey, Reduced Acceptance Angle	26
11. Glass Capture Cup Container, Cover Removed	35
12. Glass Capture Cup Experimental Set-up	36
13. Distribution of Captured Mass from Cup Experiments	38
14. Langmuir Probe	42
15. Langmuir Probe Current Detection Circuit Schematic	42
16. Schematic of Probe Cleaning Circuit	44
17. Schematic of Experimental Set-up with Langmuir Probe	46
18. Langmuir Probe Characteristic for Earlier Time	48
19. Langmuir Probe Characteristic for Later Time	49
20. Ion Density Variation in the Plume	52
21. Electron Temperature Variation in the Plume	53
22. Ion Density Variation in the Flow Direction	54
23. Ion Density Variation with Time	54
24. Thruster Discharge Port Near Anode	59
25. Solar Cell Contamination Test	63
26. Solar Cell SN 5 Calibrations	66
27. Solar Cell SN 7 Calibrations	67
28. Solar Cell SN 9 Calibrations	68
29. Discharge Current and Light Pulse	70
30. Discharge Current and Shorter Light Pulse	70
31. Calorimetric Disc	80
32. Temperature Variation for Angles θ and ψ	82
33. Temperature Variation Comparison	83
34. Axial Variation of Temperature	85
35. Effect of Cone Geometry	86
36. Temperature of Discs and Rake	87
37. Absorptance Spectra by FR-IR Technique	91
38. Subtracted Absorptance Spectra by FR-IR Technique	92

1.0 INTRODUCTION

This study examines the exhaust plume produced by the millipound thrust level pulsed plasma thruster. The specific questions that were studied included: a) a definition of the character of the plume, b) an examination of the effects of the exhaust plume on functional surfaces of a spacecraft and c) an identification of the source of contamination.

The pulsed plasma thruster has several features which require special consideration in order to carry out a meaningful plume contamination study. The pulsed plasma thruster generates and accelerates plasma which is ejected from a nozzle in the form of a highly concentrated blob. The flow time of this blob of mass is of the order of a few tens of microseconds and its forward directed mass averaged velocity is about 17,000 meters/sec. The total mass ejected per discharge is roughly 1.5 milligrams. The time averaged mass flow rate of propellant during the flow time is approximately 30 gr/sec. Because events at a given point in the plume are constantly changing and mass expulsion occurs in such a short time, conventional instrumentation normally used to examine exhaust plumes cannot be used. The present study was therefore confronted with several basic problems. One pertained to the development of instrumentation that could be used to give the information sought as well as the technique of using and interpreting the results from such instrumentation. Plume studies of ion engines [1, 2, 3, 4, 5, 6] or colloid thrusters [7] provided no useful information on transient measuring techniques. The other basic problem concerned itself with an assessment of the interaction of the plume with the walls of the vacuum chamber and how such an interaction would affect the results being sought.

During the course of the present program the independent studies and laboratory measurements revealed that wall scattering was significant. Such scattering is attributed to the exhaust beams concentrated energy level and the associated gas-dynamic interactions at the liquid nitrogen cooled walls of the vacuum chamber. The liquid nitrogen cooled walls which completely surrounded the thruster were not capable of reducing scattering to an acceptable level. Based upon information presented in Ref. 8, some scattering was expected but not to the extent observed. Using experimental data generated during the present studies, simple order-of-magnitude

considerations revealed that the exhaust beam might even be too energetic to be absorbed during the first encounter with the walls of the MOLSINK and that some scattering might be expected in that facility before the mass is ultimately absorbed by the walls.

High speed photographs [9] of the interaction of the plasma ejected by a pulsed plasma accelerator with downstream located metal surfaces have shown the formation of a shock wave which moves against the incident mass thereby serving as a screen preventing the incoming plasma to reach the metal surface freely. Such a gasdynamic wall interaction would allow plasma to flow parallel to the wall in a thin layer upstream of the wall and be a mechanism of wall scattering in a cryogenically cooled test facility.

After these observations were noted, collimators were incorporated on the instrumentation thereby enabling meaningful data to be obtained. Such a technique was also used at NASA Lewis Research Center during their studies⁴ of contamination due to ion engines.

The results of the present study have provided some insight in the characteristics of the plume and effects on spacecraft surfaces. However, additional studies are desirable in order to answer some of the questions that have not yet been examined. Some of these questions include: a) the effect of the thruster's exhaust cone geometry on the results, b) the fluid dynamical behavior (i. e., shocks and wakes) around diagnostic instruments, c) the effect of exposing test samples to air prior to the chemical analysis and d) the effect of wall scattering of the incident plume, e) the development of instrumentation capable of following the transient behavior of the plume.

Quite generally, Langmuir probe data, collimated QCM data and data taken of the energy distribution of the wake indicates that the plume is located within a cone angle of about $\pm 30^\circ$ to $\pm 40^\circ$ about the geometric centerline of the nozzle. Expansion transverse to the forward directed motion is minimal and both ion density and electron temperature drop off rapidly in the forward direction. The mass itself is ejected as a time varying highly concentrated "blob" of mass in the forward direction.

It is believed that the results of the present study have advanced the state of knowledge of plume effects of pulsed plasma thrusters significantly beyond the state of knowledge existing at the time Ref. 10 was written.

None of the test data generated during this study revealed the plume of the pulsed plasma thruster to be "dirty" or highly contaminating. It has been shown that scattered mass off the walls of the test facility to be the primary source of contamination noted with the pulsed plasma thruster. However, like with an ion engine, erosive effects are noted on surfaces located within the roughly $\pm 40^\circ$ cone angle of the relatively sharply defined outer edges of the plume.

2.0 DESCRIPTION OF FACILITY, THRUSTER AND MAJOR INSTRUMENTATION

2.1 Vacuum Test Facility

All thruster tests were carried out in a vacuum chamber whose interior bounding surfaces are cooled by liquid Nitrogen. Figure 1 shows the general geometry of the test facility. Figure 2 shows the actual test facility with the

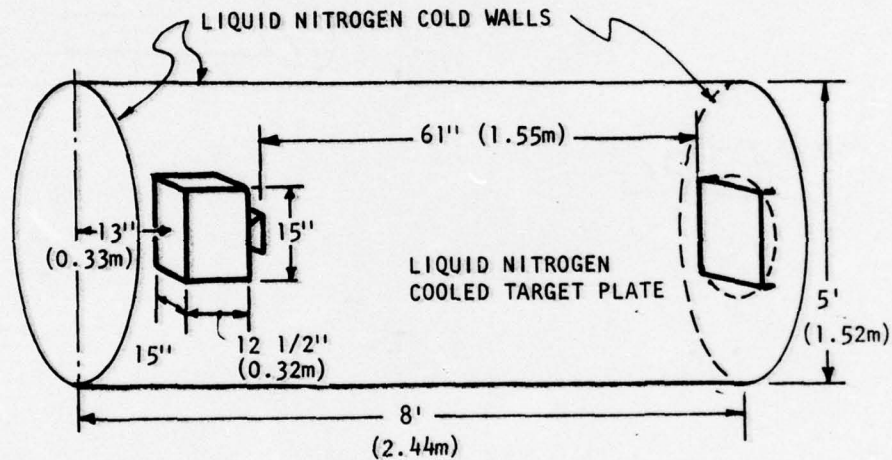


Figure 1. General Geometry of Test Facility

thruster and instrumentation rake in position. The test area is cylindrically shaped 5 ft (1.52 m) in diameter and 8 ft long (2.44 m). The distance from the thrusters exhaust plane to the downstream wall is 5½ ft (1.68 m). The interior surfaces were painted with Nextel 401-C10 black paint manufactured by the 3M company. Two 20 inch diffusion pumps having liquid freon cooled baffles are used to evacuate the chamber. To minimize contamination from sources other than the thruster's plume, all interior instrumentation and power leads were Kapton coated.

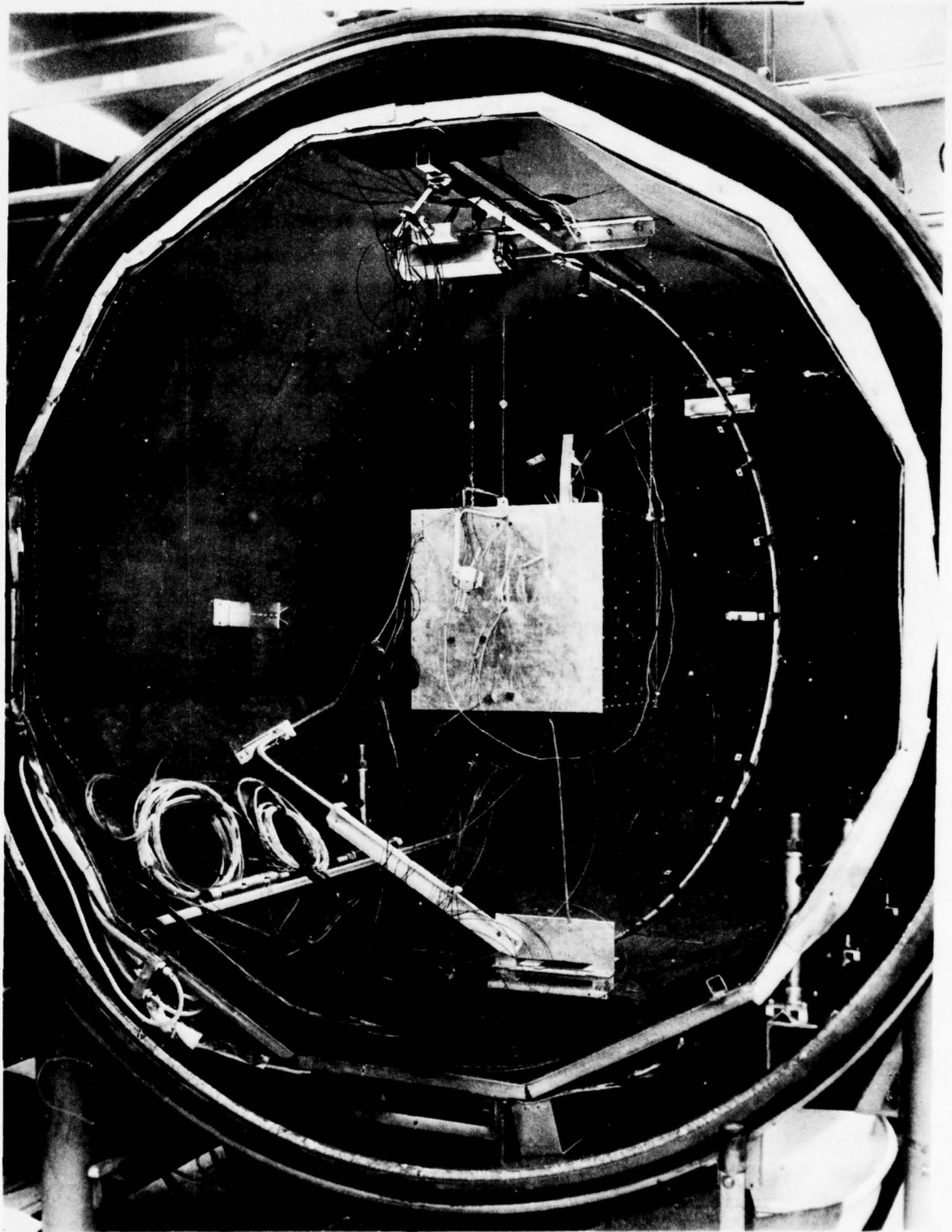


Figure 2. Test Facility with Thruster and Instrumentation Rake

Typical operational procedures for a test would be to evacuate the facility overnight and to initiate the flow of liquid Nitrogen by a timer approximately 5 A. M. the following morning. This approach enabled a full 8 hour working day to be realized with the facilities cold wall at about -185°C . A safety interlock was incorporated to stop the flow of liquid Nitrogen in the event of an electrical power failure. To prevent water from condensing inside the chamber after completion of a test, two infrared heating coils were used to heat up the interior of the chamber to room temperature after the liquid Nitrogen was turned off and before the chamber was opened. In order not to overheat the thruster and test instrumentation during this heating cycle these were connected to a temperature controller with the thermal sensing element located on top of the thruster enclosure. The controller is set to turn off the infrared heaters whenever the thruster's enclosure exceeds 90°F . This technique enables the chamber to be safely opened approximately 6 hours after the liquid Nitrogen is turned off.

Figure 3 presents experimental data of the temperature history of the thruster and the cold walls of the test facility during a typical test. It is seen that the test facility is at the coldest temperature in about $3\frac{1}{2}$ hours and that the temperature of the thruster can be kept essentially constant at the temperature preset at the temperature controller.

Figure 4 presents the measured mass pumping capacity of the LN cooled test facility. Also shown is a line showing the equivalent steady state mass throughput of the thruster when it is pulsed once every 6.77 seconds (110.8 watt power level of operation). The intersection of these two curves shows that the average equivalent steady state background pressure in the facility is expected to be about 3×10^{-5} Torr when the thruster is operated steadily at the indicated pulse rate. Instantaneous mass flow rates generated by the thruster are orders-of-magnitude higher than this time averaged mass flow rate. For purposes of this plume study it is really this instantaneous mass flow rate ejected by the thruster that determines whether or not wall scattering will be present. Some order-of-magnitude calculations of the actual mass flow rate ejected by the thruster can be made utilizing experimental data generated during the program. The actual flow rate averaged over the thruster discharge time may be approximated as:

$$\text{discharge time averaged flow rate} = \frac{\text{Mass discharged per pulse}}{\text{pulse duration}}$$

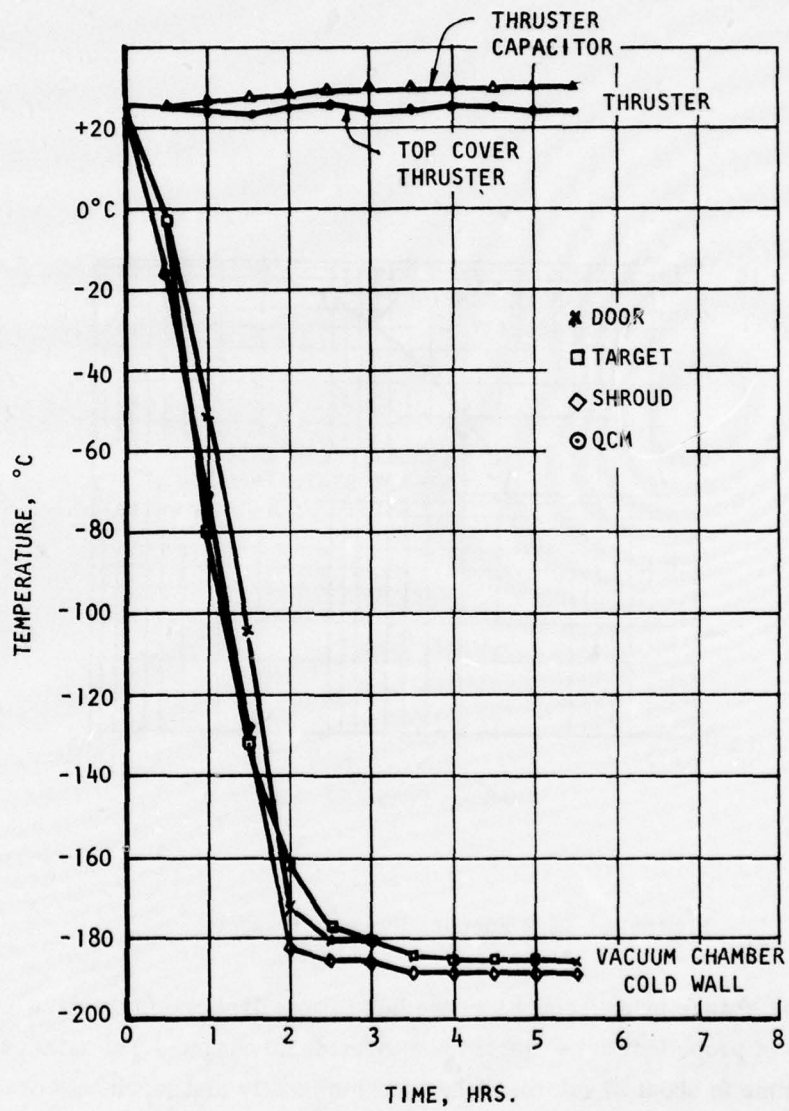


Figure 3. Temperature History of Test Facility

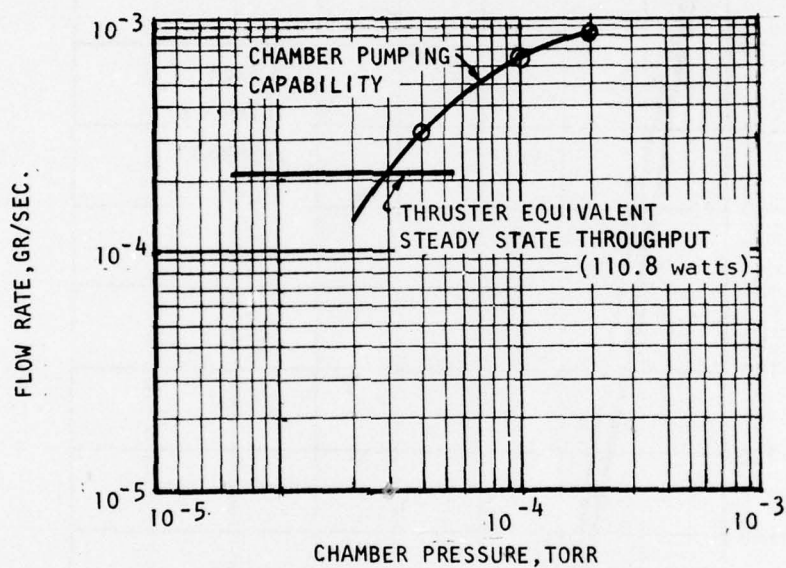


Figure 4. Test Facility Pumping Capacity

From weight change measurements of the solid propellant one finds about 1.5 milligrams of propellant to be ejected per thruster discharge. The total current discharge time is about 27 microseconds and luminosity measurements of the thrusters exhaust show the major part of the pulse to be about 30 microseconds long with a total duration of about 45 microseconds. From this data, the major part of the mass flow rate ejected by the thruster is of the order of 50 grams/sec (0.11 lb/sec). This energetic (i.e., average velocity of the order of 17,000 meters/sec) jet of mass encounters the downstream wall of the test facility during a thruster discharge. These elementary considerations reveal that scattering

can be expected in the LN cooled test facility. A literature search revealed that the plume is most likely even too energetic to be absorbed during the first encounter by the walls of a liquid Helium cooled test facility (i. e. , NASA Marshall Space Flight Center's facility (11) or the JPL MOLSINK). An experimental study presented in Ref. 12 with gaseous hydrogen reported that the capture coefficient of hydrogen impinging upon a L He cooled panel was observed to decrease as the mass flow rate of impinging hydrogen was increased beyond a certain limit. More important, it was found that above certain impinging flow rates the capture coefficient even became negative, indicating that gas which had already been Cryo-pumped was being eroded and added to the background gas load in the test facility.

The various independent measuring techniques employed during the present study also revealed that wall scattering of plume mass was taking place. Presently it is not known if any test facility exists in which no wall scattering would take place of the impinging plume mass of the pulsed plasma thruster. Even a small amount of such scattering could result in erroneous conclusions to be drawn on contamination effects over very long periods of thruster operation. It was not possible in the present program to provide a quantitative measure of the amount of scattering that was present. Collimating techniques, to be discussed, were used to minimize the effects of such scattering.

2.2 Thruster

The thruster used during the present study was designed specifically for the plume contamination studies. The thruster nozzle and exhaust cone geometry are configured to be identical as the corresponding items on the millipound thrust level propulsion system (13) of program F04611-72-C-0053. Several mechanical design improvements were incorporated in the Plume studies thruster. The entire electrical insulating assembly around the strip line extensions were modified to eliminate the electrical breakdown problems encountered with the design used prior in the large total impulse thruster. Furthermore, the electrode nozzle design was improved so that the electrodes could easily be removed without a major disassembly of the propulsion system. Finally, the electrode-Mykroy interfaces were redesigned in the nozzle to reduce the severe erosion previously noted to occur at such interfaces.

Since a large total impulse system was not required for the present studies, short independently fed straight propellant rods were used instead of the costlier helically coiled ones in the high total impulse system. Sufficient propellant has been provided for about 2680 lb-sec (11920 N-sec) of total impulse before the system would have to be refueled. Furthermore, four low cost off-the-shelf Mylar capacitors were used instead of four high energy density K-film capacitors. The capacitance, discharge energy and the general construction of both propulsive systems are otherwise essentially identical. Propulsive performance comparisons carried out during the program (see section 3.4) verifies that both thrusters can be considered equivalent to each other.

All studies of the thruster exhaust plume were carried out with a background temperature of about -185°C . Because this background temperature is considerably below the freezing point of the dielectric fluid in the capacitor, it was necessary to enclose the entire thruster inside a temperature controlled aluminum box. Figure 2 shows the test ready configuration of the thruster located inside the temperature controlled box suspended in the vacuum chamber. Figure 5 shows a front view of the thruster with the exterior covers removed from the structural frame of the box. Figure 6 shows a rear view of the thruster assembly inside the box. Eight 1 ohm resistors connected in series were attached to the inside panels of the box. These resistors were powered by a 25 volt 3 amp D.C. power supply and a Fenwall model 194 temperature controller. The controller's thermal sensor was installed inside the box and the controller was set to maintain the box at 65°F when it was located in the cold wall test facility. This temperature controlled box also served as the heat sink for the thruster. Similar to the millipound propulsion system, two copper straps attached to Beryllium Oxide slabs on the anode and cathode strip lines intercept heat from the thruster's nozzle and transfer it to the temperature controlled box. These two vertical copper straps can be seen in Fig. 5. This approach of thermally controlling the thruster worked flawlessly throughout the program. Six Kapton coated copper-constantan thermocouples were attached at the following locations: on one upper capacitor, on one lower capacitor, at the upper heat sink extension on the aluminum box, at the lower heat sink extension on the box, on the Be O cathode stripline plate and on the Be O anode stripline plate. These thermocouples, as well as all leads, were brought out of the thruster box through NEMA G-10

fiber glass bushings located in the back cover of the aluminum box. These leads can be seen in Figure 2. The exterior of the aluminum box was left unpainted and all material selected for the thruster and its enclosure were of flight quality and low out-gassing.

The thruster discharge circuit is electrically isolated from the aluminum box. The capacitors and the electrical discharge circuit are supported by two NEMA G-10 fiber glass plates (See Figs. 5 and 6) from the aluminum box. Besides this isolation, the aluminum box was isolated from the vacuum chamber. Each of three suspension wires had a NEMA G-10 isolating ring in it (see Fig. 2) so that electrical isolation was realized. The thruster capacitors were charged through a resistive bank during most of the studies by a high voltage power supply having a floating high voltage output. These precautions of electrically isolating the thruster prevented electric current returning through the plume and chamber walls.

Considerable effort was spent in hermetically sealing all seams of the off-the-shelf commercial capacitors to prevent silicone oil impregnant of the capacitors from leaking out of the capacitors during vacuum operation. Shell Epon 828 epoxy was molded over the fill plug of the capacitor (see Fig. 6), an aluminum ring was epoxied over the welded seam of the rear lid (see Fig. 6) and epoxy was also molded over the soldered joint at the ceramic bushing and high voltage stud of the capacitor. Despite these precautions one capacitor was found to have developed a small leak after having been used for many months in the program. Using spotcheck developer Type SKD-NF manufactured by the Magnaflux Corp. it was found that a minute leak was present at one of the four welds which fasten the ground ring of the capacitor to the capacitor can. Such a leak can be prevented if the ground ring were brazed instead of welded to the capacitor can. Furthermore, it has become evident that the base of the ground ring should be epoxy sealed to the capacitor can in instances when the ground ring is welded to the capacitor can.

2.3 Instrumentation

2.3.1 Instrumentation Rake. A remotely controlled instrument supporting rake was designed and built in order to be able to sweep out the surface of a hemisphere centered about the thruster's discharge exit plane. Figure 2 shows this semicircular

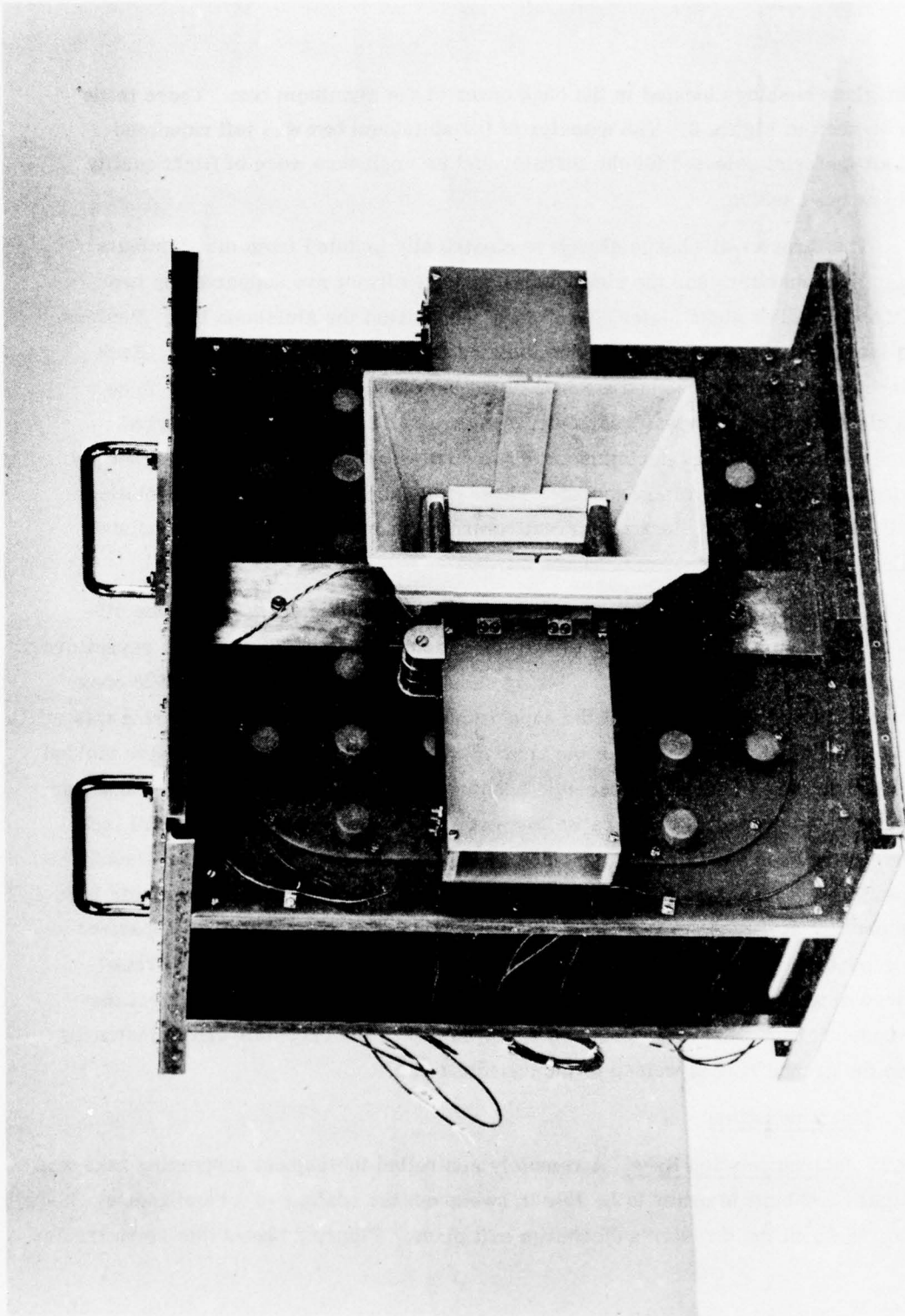


Figure 5. Thruster, Front View, Covers Removed

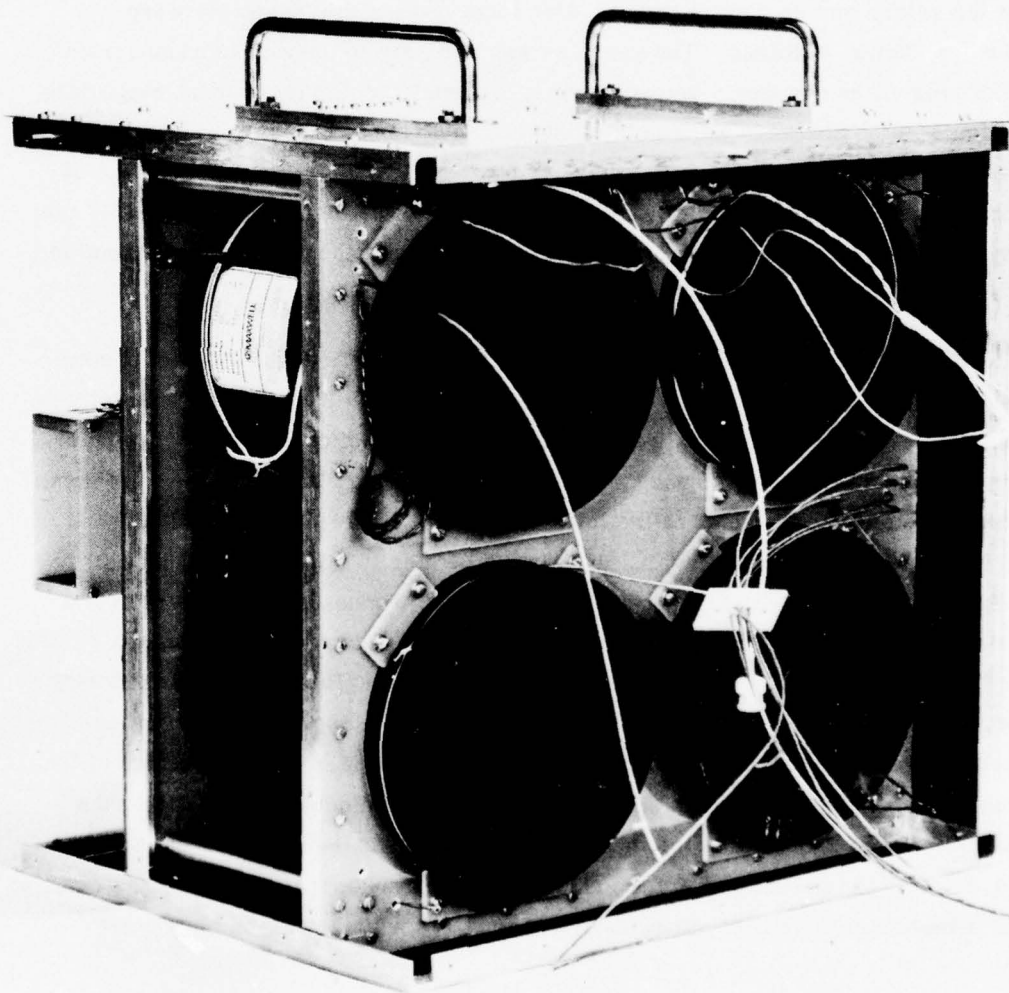


Figure 6. Thruster, Rear View, Covers Removed

rake with eight mass capturing cup containers mounted on it. This rake can be rotated from outside the vacuum chamber to any angular location within about 1/2 degree when the rake is rotated $\pm 90^\circ$ about the axis of rotation. This system worked flawlessly at the cryogenic temperatures generated inside the chamber. The rotary motion was transferred through a vacuum feedthrough to a gear box mounted on the floor of the cold wall. Three complete turns on an external crank rotates the internal rake by 1° . Three stainless steel bellows* were used to transmit the rotary motion around bends. Aluminum rods of this assembly were guided by Teflon bushings. The gear box was used dry to prevent lubricant from solidifying at the cryogenic temperature. The semicircular instrument supporting section was fabricated of aluminum tubing and instrument supporting holes directed at the geometric center of the nozzle were located at 5° intervals. The radius of the rake was 28 inches (71 cm). Another fixed rake was located 56 inches (142 cm) downstream in order to be able to examine variations in the downstream direction.

The angular notation used during this study is defined in Fig. 7.

2.3.2 Quartz Crystal Microbalance (QCM). A Celesco** Model 700A QCM sensor was used for the QCM studies of this program. This unit has a mass sensitivity of 4.43×10^{-9} gr/cm² per Hertz, and the allowable range of crystal temperature is from 78°K to 333°K. The viewing angle of the crystal port is 140° . The total measuring system was comprised of the latter crystal, a Model 700B control unit and the Model 700C signal processor. In order to be able to utilize the full capability of the QCM, the beat frequency output of the signal processor was connected to a Fluke Model 1900A Multicounter which has a digital readout. This technique allowed the QCM beat frequency to be read digitally to within one Hertz at any time during a test. The response of this system is not fast enough to display the true instantaneous rate of mass deposition on the crystal of the QCM. Only a measure of the amount of mass deposited by a single thruster pulse can be detected. Using the calibration data provided by the manufacturer, the mass deposited on the crystal is $1.4 \times 10^{-9} \Delta f$ grams with Δf the change in beat frequency due to the mass change. The detection capability of our system was thus 1.4×10^{-9} grams.

*FM-384 Flex-metal manufactured by Abbeon Cal., Inc., Santa Barbara, Calif.

**IBC - Celesco, Irvine, California

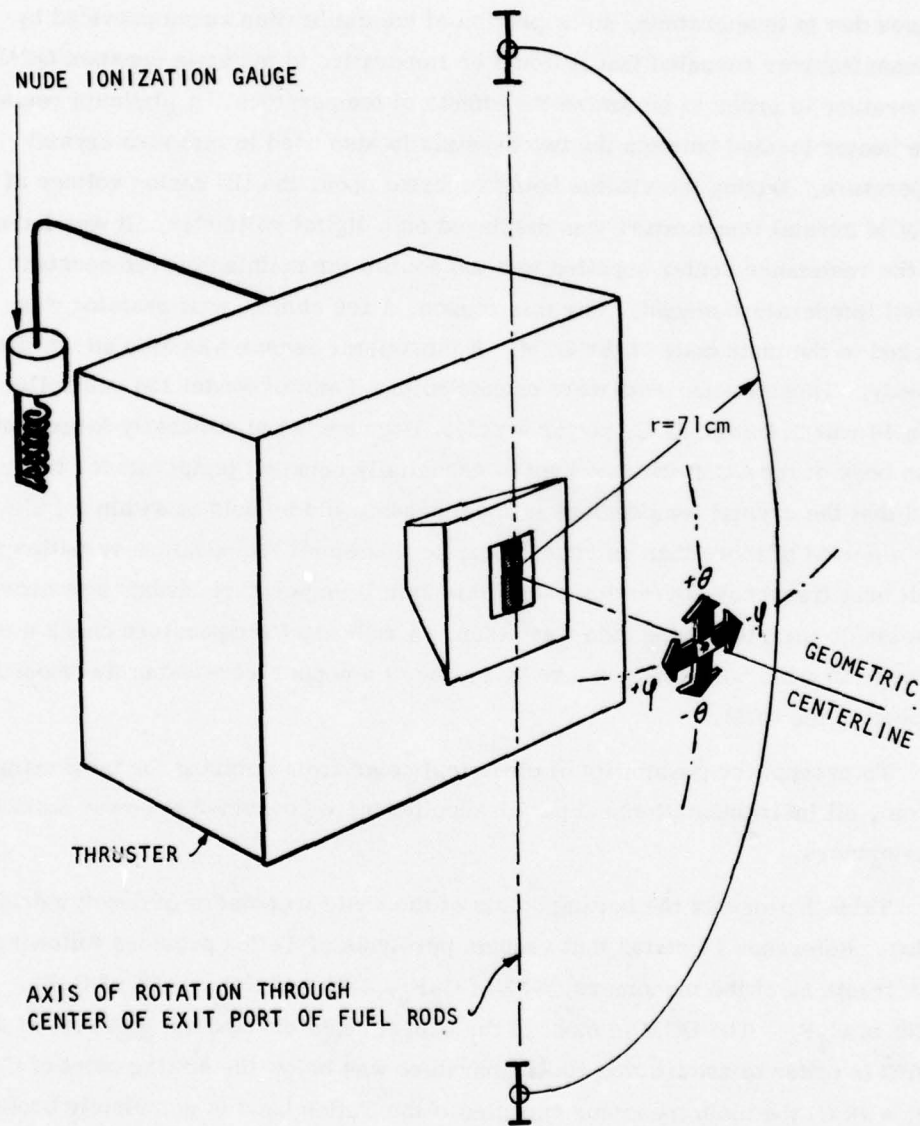


Figure 7. Angular Notation Used

Since the output beat frequency varies with temperature independent of the changes due to mass, it is important that the crystal temperature be known. Even though the Model 700A QCM utilizes two crystals to minimize frequency changes due to temperature, an inspection of the calibration curve provided by the manufacturer revealed that it would be imperative to maintain constant QCM temperature in order to minimize the effects of temperature. A platinum resistance heater located between the two crystals is also used to measure crystal temperature. During the studies being reported upon, the DC analog voltage of the QCM crystal temperature was displayed on a digital voltmeter. It was found that the resistance heater supplied was too coarse for maintaining the constant crystal temperature sought. For this reason, a 100 ohm 15 watt resistor was attached to the main body of the QCM. A thermistor sensor was also attached to the body. These components were connected to a Fenwall Model 194 controller and a 40 volt 0.4 amp. D.C. power supply. Because the significantly larger mass of the body of the QCM could be kept at essentially constant temperature, it was found that the crystal temperature in most cases could be held to within $\pm 1^\circ\text{C}$ over a period of more than an hour. Despite this small temperature variation a small beat frequency correction due to this small temperature change was necessary when single thruster firing data was taken. A redundant temperature check was made of the QCM body temperature by means of a copper-constantan thermocouple attached to the QCM.

To prevent the possibility of electrical noise from entering the measuring system, all instrumentation and power supplies were connected to power isolation transformers.

Table 1 presents the boiling points of the basic monomers of depolymerized Teflon. Reference 14 states that vacuum pyrolysis of Teflon provides following mole fractions of the monomers: 94% of C_2F_4 , 0.86% of CF_4 , 2.6% of C_3F_6 , 0.73% of C_4F_8 . The QCM in most of the experiments carried out was kept at about -100°C in order to assure that its temperature was below the boiling point of C_2F_4 (i. e. -76°C) the main monomer expected if the Teflon band is completely broken into the basic monomers.

TABLE 1
Boiling Points of Monomers

<u>Monomer</u>	<u>Name</u>	<u>B. P. (°C)</u>	<u>(°K)</u>
CF ₄	Tetrafluoromethane	-128	145
C ₂ F ₄	Tetrafluoroethylene	- 76	197
C ₂ F ₆	Hexafluoroethane	- 79	194
C ₃ F ₆	Hexafluoropropene	-129	144
C ₄ F ₈	Octafluorocyclobutane	- 4	269

Two approaches were used during the program to drive any possible water condensation off the crystal of the QCM. One approach was to heat up the crystal by means of the self contained heating circuitry of the Celesco unit. The second approach was simply to elevate the entire body of the QCM by means of the heater resistor and temperature control circuit that was incorporated by Fairchild Republic. The second approach is better than the first and recommended in future studies⁴. Such pre-test heating of the QCM was carried out under vacuum conditions and with the test facility's cold wall in operation. Rapid cooling of the QCM after this "boil-off" cycle was accomplished by rotating the QCM on the rake until it made contact with a V-shaped cold finger attached directly to the cold wall of the vacuum chamber. This cold finger can be seen in Figure 2 to be located and extending into the chamber from the left wall of the chamber. The QCM temperature was monitored during this cool down cycle and when the desired temperature was reached, the QCM was rotated away from the cold finger and the QCM temperature controller was turned on to maintain a desired crystal temperature. It was found that the duration of this pre-test in-situ preparation of the QCM could be kept to within roughly two hours. During this time interval the thruster was usually also allowed to operate for roughly 200 thruster firings in order to outgas all of its surfaces. The QCM was located roughly 90° to the side of the thruster exhaust during this thruster "conditioning" period.

2.3.3 Microbalance. A Perkin-Elmer Model AD-2 autobalance was used for total mass capture measurements. This electronic microbalance has a digital readout with four ranges of measuring capability. These ranges and the corresponding resolution are: + 1mg with a resolution of 0.1 microgram, ± 10mg with a resolution

of 1 microgram, ± 100 mg with a resolution of 10 micrograms and ± 1000 mg with a resolution of 100 micrograms. The glass capture cups used for total mass capture measurements weighed typically 300 milligrams. Instead of making direct weight measurements of these capture cups, a measuring technique was developed which enabled a resolution of 1 microgram to be realized with these cups instead of 100 micrograms. The technique developed was to make all mass capture cup weight measurements as a differential measurement. Each capture cup was differentially counter balanced by a set of calibrated weights to within about 5 milligrams or less. These weights were recorded and used as the reference weight against which the reweighed capture cup was compared during later measurements.

2.3.4 Thrust Balance. Thruster propulsion performance was periodically monitored during the program. A direct impulse bit measuring thrust stand was used. Details of this balance have been described previously (15). Because this balance uses a damping fluid which would solidify at the cold temperatures being used during the contamination studies, the balance is periodically placed in the vacuum chamber and propulsive performance was measured under vacuum conditions but at room temperature.

2.3.5 Langmuir Probe. A double Langmuir probe was developed specifically for this program to measure electron temperature and ion density in the plume. Since a significant effort went into the development of the probe and the experimental technique, all details of the probe will be presented in section 3.2 of this report.

3.0 EXPERIMENTAL STUDIES

3.1 Mass Distribution Studies

3.1.1 Quartz Crystal Microbalance (QCM) Measurements. Six different studies were carried out with the QCM:

- (a) A study of the effect of QCM crystal temperature on captured mass.
- (b) A QCM survey across the exhaust plume at $\theta = 0^\circ$ with angle ϕ varying from -90° to $+90^\circ$.
- (c) A test to check test facility back scattering with the QCM at $\theta = 0^\circ$ and angle ϕ varying from -90° to $+90^\circ$.
- (d) A QCM survey of the plume using a collimating tube to reduce test facility scattering effects.
- (e) Tests to examine the effect of downstream test facility wall geometry on back scattered mass.
- (f) An exploratory test to examine the effect of thruster exhaust cone geometry on mass deposition 90° to one side of the exhaust cone.

3.1.1.1 QCM Crystal Temperature Test. Table 1 presents the boiling points of the monomers expected of completely depolymerized Teflon. It is seen that if all mass capturing tests are carried out with a crystal temperature well below -76°C (197°K) it would be expected that most of the mass (i.e., C_2F_4) captured by the crystal should not boil off. The first study performed was to determine if the deposit captured by the QCM at -100°C during thruster firing could be boiled off if the QCM, after thruster firing has ceased, is subsequently raised to roughly room temperature under vacuum conditions. The QCM was positioned at $\theta = 0^\circ$ and $\phi = -85^\circ$ for this test. Figure 8 presents the results of this study. With exception of the beat frequency change at constant temperature denoted by section 4-5, all other beat frequency changes noted are due to changes in the crystal temperature realized by heating and cooling of the QCM by the QCM heater control circuitry. The approach taken in this test was to capture mass during thruster firing (i.e., section 4-5) with the QCM crystal temperature held constant at -104°C . Thruster firing was stopped and with the facility cold wall in operation and under evacuated conditions, the QCM crystal temperature was raised over a period of 45 minutes from -104°C to about $45^\circ\text{C} \pm 3^\circ$. It was kept at this latter temperature for 23 minutes before the temperature of the QCM was restored to the original test temperature of -104°C . It was reasoned that if the deposit is C_2F_4 , the temperature rise to 45°C

should boil off the C_2F_4 as well as the other monomers and upon subsequently restoring the original $-104^\circ C$ capture temperature one should not restore data point 5. Instead, one might expect data point 5 to shift towards and possibly coincide with data point 4.

The test conditions presented in Figure 8 are as follows:

- Section 1-2: Pre-test (i. e., before thruster firing) heating of the QCM under vacuum conditions and cold wall operation to drive off any possible condensibles which may be on the crystal.
- Section 2-3: The QCM is moved against the cold finger on the cold wall and cooled from $53^\circ C$ to $-103^\circ C$.
- Section 3-4: The QCM is moved away from the cold finger to $\phi = -85^\circ$ and the QCM body temperature is controlled to maintain $-104^\circ C$ crystal temperature.
- Section 4-5: The thruster is operated for 255 pulses at a constant crystal temperature of $-104^\circ C$. Thruster firing is stopped at point 5. This operation produced a beat frequency change of 95Hz (1.33×10^{-7} gr).
- Section 5-6: The resistive heater on the body of the QCM was activated to raise the crystal temperature from $-104^\circ C$ to $48^\circ C$.
- Section 6-7: The QCM is rotated against the cold finger after the heater circuit is turned off. The QCM is cooled back to the original cold temperature.

The results of this test revealed that test point 5 was essentially reestablished (i. e., to within 9 Hz). The agreement was within 1.26×10^{-8} grams. This result indicates that whatever mass was deposited on the 140° acceptance angle QCM during the 255 thruster discharges was not boiled off by raising the temperature from $-104^\circ C$ to $48^\circ C$. If the deposit on the QCM was due to any of the 5 main monomers of Teflon, it would have been expected that they should have been boiled off. Three possible explanations can be offered: 1) The exhaust plume is composed of heavier molecular components of Teflon whose boiling point is below $-104^\circ C$ ($169^\circ K$). 2) The mass captured by the QCM is comprised of a significant quantity of back scattered mass including black paint from the cold wall whose boiling points are below $-104^\circ C$. 3) A combination of both of these sources of mass. Since the viewing angle of the QCM was 140° , a large area of the test chamber is being viewed by the QCM. Subsequent independent tests revealed that mass was indeed being back scattered in the test facility.

3.1.1.2 QCM Survey of the Plume. With the QCM (acceptance angle 140°) on the rake at $\theta = 0^\circ$, the rake was moved from $\phi = -75^\circ$ to $\phi = -35^\circ$ stopping at the following locations: -75° , -65° , -55° , -45° and -35° . The thruster was fired for 100 pulses

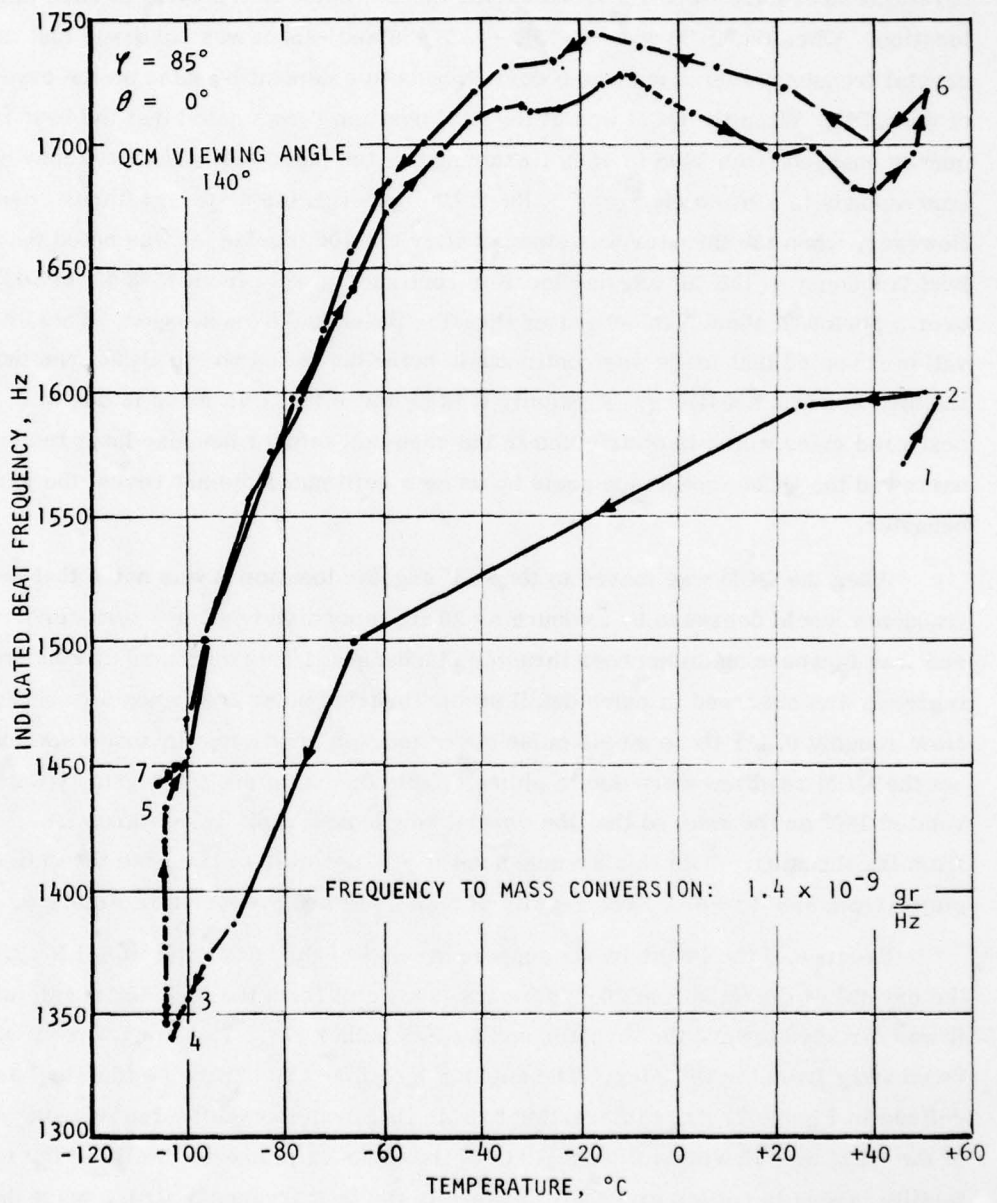


Figure 8. QCM Temperature Test Results

at each of these angular locations (except the -35° case). The beat frequency and crystal temperature were recorded during the 100 pulse firing cycle at each angular location. When the QCM was at -75° , -65° , -55° and -45° it was observed that the crystal frequency increased which corresponds to a deposit of mass on the crystal of the QCM. When the QCM was at the -45° position it was noted that the beat frequency changed from 1498 to 1580 Hz during the 100 pulse test (this frequency change corresponds to a mass change of 1.138×10^{-7} gr or 1.148×10^{-9} gr/thruster pulse). However, when the thruster was stopped after the 100th pulse, it was noted that the beat frequency at the 45° angular location continued to rise from 1580 Hz to 1623 Hz over a period of about a minute after thruster firing had been stopped. This observation revealed that mass was continuously being deposited on the QCM even though the thruster was not firing. Presently it is believed that this mass is due to scattered mass which is distributed in the vacuum chamber because later tests which narrowed the QCM acceptance angle by using a collimator did not reveal the same behavior.

When the QCM was moved to the -35° angular location it was noted that the beat frequency would decrease by as much as 20 Hz immediately after a thruster firing and then increase again between thruster discharges. This decrease and subsequent increase was observed in more detail as the thruster pulse frequency was changed from roughly 0.147 Hz to single pulse operation. In an attempt to resolve whether or not the QCM readings were due to plume effects or due to scattering, the QCM was rotated 180° on the rake so that the crystal now looked radially outward, i. e., away from the thruster. With this arrangement it was possible to traverse the entire plume from -85° to $+65^\circ$. The results of both tests are presented in Figure 9.

Because of the length of the support bracket of the QCM, the radial location of the crystal of the QCM was $26\frac{1}{8}$ inches (66.4 cm) from the thruster nozzle when it was directed toward the thruster and $30\frac{3}{8}$ inches (77.2 cm) away when it was faced away from the thruster. The angular locations are otherwise identical as defined in Figure 7. It is interesting to note that even though the 140° viewing angle of the QCM was viewing different parts of the thruster plume and walls of the test facility, there is not too great a difference in the beat frequency (i. e., mass deposited in the crystal) when the QCM was facing either toward or away from the thruster exit plane. Even the inflection in data between -60° and -75° was reproduced. The mass

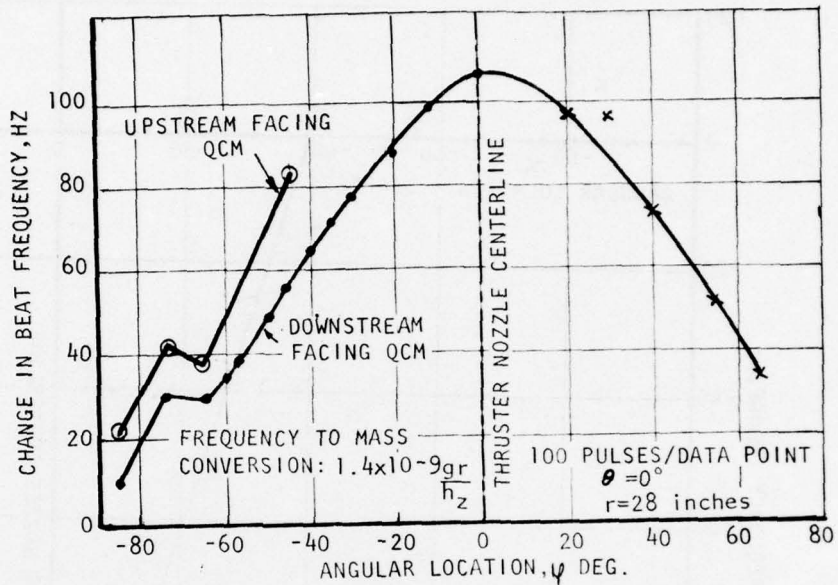


Figure 9. QCM Survey, 140° Acceptance Angle

distribution deposited on the downstream facing QCM was not expected and can only be explained by either of two mechanisms; 1) plume mass is scattering off the LN cooled walls of the test facility or 2) flow disturbances due to the presence of the QCM in the plume causes a backflow in the wake of the QCM which causes mass to be deposited on the downstream facing crystal of the QCM. In any case, it was quite clear that additional studies with the QCM would have to be carried out to resolve the question raised and attempt to obtain a true measure of the total mass distribution in the plume.

It was reasoned that if the results noted were due to scattered mass, reducing the viewing angle of the QCM from 140° to a smaller angle would reduce the amount of mass deposited on the QCM. A collimating tube 5.03 in. (12.8 cm) with a bore of 0.43 inches (1 cm) was placed over the entrance port of the QCM. The QCM was then placed on the rake facing the thruster and a survey was made of the mass deposited on the crystal with this reduced viewing angle system. Figure 10 presents

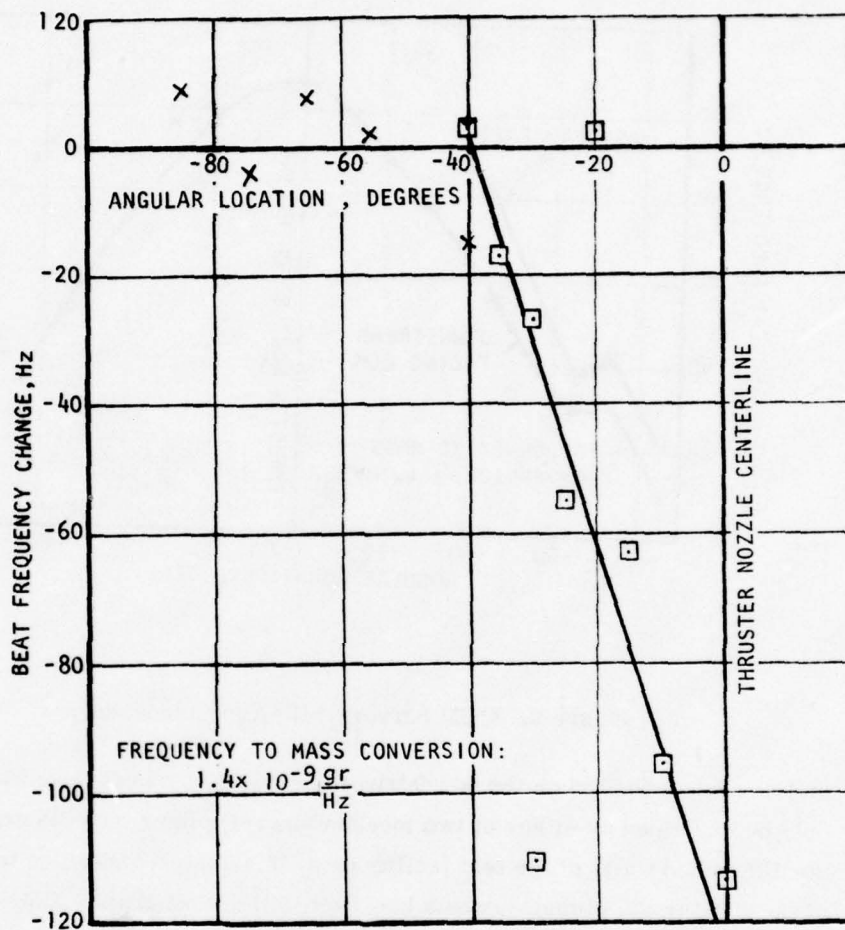


Figure 10. QCM Survey, Reduced Acceptance Angle

the results of this survey. The results obtained were unlike any of the earlier QCM data discussed above. Instead of mass being deposited on the crystal, it was noted that mass was being removed from the crystal face by the impinging plasma plume as the QCM was moved from the thruster nozzle centerline ($\phi = 0$) to about $\phi = -40^\circ$. At about 40° off to the side of the geometric centerline of the plume virtually no change in beat frequency due to mass changes was noted.

The result that mass is removed from an object placed within the plume was not surprising as earlier total mass measurements with glass capture cups also revealed that mass is removed from a target placed within the fairly sharply defined highly energetic plume mass. It is interesting to note that such an erosive action within the exhaust beam has also been reported [3] for an ion thruster. Sufficient evidence exists to believe that the results presented in Figure 10 are more representative of the plume of the millipound thrust level pulsed plasma thruster (with the present exhaust cone geometry) than the 140° acceptance angle QCM data presented in Figure 9. Despite this belief, the QCM study has raised several questions for further study beyond the scope of the present effort. For example, it is known that the QCM and collimating tube are located in a high velocity nonsteady flow regime. It was not possible with the present rake design to remotely swivel the QCM about some point on the rake in order to probe for the local direction of flow within the plume. In the study performed, the QCM was always directed at the geometric center of the thruster nozzle. Another question that could not be resolved is what fraction of the mass intercepted by the open port of the collimating tube actually becomes deposited on the crystal of the QCM. It is quite possible that because of the high speed nonsteady nature of the plume not all of the mass interacts with the face of the crystal. Furthermore, the effect of aspect ratio of the collimating tube was not evaluated. Even though the latter questions can be raised, subsequent studies carried out with the Langmuir probe (section 3.2), calorimetric type discs (section 3.6) and glass capture cups indicate that the outer boundaries of the pulsed plume are indeed located in the vicinity of $\pm 40^\circ$ from the geometric center line of the thruster nozzle such as observed (see Figure 10) with the collimated QCM.

Unlike thermal type propulsive devices, the roughly 17,000 m/sec forward directed velocity realized by body forces in a pulsed plasma thruster is significantly higher than the transverse velocity due to the thermal velocity. The result that the transverse thermal velocity is much smaller than the forward directed velocity in a pulsed plasma accelerator has been noted previously [9]. In that study the accelerator was configured as a coaxial nozzle and gaseous propellants were used.

3.1.2 Mass Distribution by Glass Capture Cup Measurements. A knowledge of the mass distribution within the plume is important. Once this distribution and the manner in which it is deposited on surfaces is known, one can locate spacecraft

surfaces so that their thermal and optical properties will not be changed by the plume. If such surfaces cannot be relocated, one can establish what effect the beam would have on the operational capability of the surface.

The technique that was used to measure the mass distribution in the transient plume of the pulsed plasma thruster is based on the concept that if one puts a small capture cup within the plume, then after N thruster pulses an amount of mass M will be deposited on it. Then if one knows the effective capture area, one can compute the mass deposited per thruster pulse per unit area. This approach assumes that the cup or capture device is not disturbing the local flow and that all material which impinges upon the cups surface is captured and that the cup simulates a typical spacecraft surface. Type 7740 Borosilicate (Pyrex) glass cups were used during this study.

Unlike most propulsion devices, the plume of a pulsed plasma thruster is a transient phenomena of extremely short duration. Results of the present study reveal that mass may be passing a given point in the plume for a time of the order of only 50 microseconds (50×10^{-6} sec) per thruster pulse. To deliver 37,000 lb-sec (165,000 N-sec) of total impulse only 6.2×10^6 thruster pulses are required. Thus a point within the plume is really only being exposed to an equivalent steady flow of plume mass for a total duration of about 310 seconds during a typical 5 to 7 year mission time. Thus in capture cup studies, the cups will be exposed timewise longer to test facility background effects by orders-of-magnitude than to direct plume effects. Such simple considerations point out the difficulty of carrying out mass capture measurements in a vacuum chamber. A technique was developed for deposited mass measurements which for certain test conditions early in the program appeared to provide the information sought. Later in the program it was found that the technique that was developed had shortcomings. Never-the-less, the results obtained by the mass capture technique qualitatively provided the same information as the more accurate techniques involving the Langmuir probe and the Quartz Crystal Microbalance (QCM).

The experimental technique developed during this program is based upon making 3 direct weight measurements of the cups: 1) before the cup is subjected to the plume, 2) after it is subjected to the plume, 3) after the "contaminated" cup has been cleaned. From these three weight measurements one can, in principle, determine the amount of mass deposited in the cup and also the amount of mass eroded from the cup by sputtering.

Originally, as the technique was being developed, it was believed that three weight measurements would define captured and eroded mass in accordance with following relations:

$$W_A = W_{\text{cup}}$$

$$W_B = W_{\text{cup}} + W_{\text{deposit}} - W_{\text{eroded}}$$

$$W_C = W_{\text{cup}} - W_{\text{eroded}}$$

hence the mass deposited in the cup and the eroded mass would be given by the relations:

$$W_{\text{deposited}} = W_B - W_C$$

$$W_{\text{eroded}} = W_A - W_C$$

where W_A denotes the capture cup weight before testing

W_B denotes the capture cup weight after testing

W_C denotes the capture cup weight after testing and cleaning

To obtain the weighing accuracy required with this technique, a differential weighing technique was developed.

The micro-balance (see section 2.3.3) used is capable of resolving a weight to 0.05 micrograms. Its absolute accuracy is determined by the class of calibration weights used for the calibration. The calibrating weight that was used is 100 mg accurate to .005% i.e. 5 micrograms.

The weight of a typical glass capture cup ranged between 300 and 500 milligrams. This latter weight would have required that weight changes of the order of 100 micrograms be detected if one were to use the 1000 milligram range of the balance. This difficulty was overcome by differentially balancing out the weight of the cup by a counterweight. A given cup's weight was counterbalanced so that a reading could be made on the 10 milligram range of the balance. This approach allowed us to detect changes of the order of 1 microgram.

Initially, the weighing technique cited above was evaluated with microthrusters and subsequently with a 200 joule thruster with the glass capture cups at room temperature. In these cases the technique was found to be feasible. However, when the same technique was applied to the 750 joule plume thruster in the LN cooled

test facility it was noted that repeatability of weight change data of plume total mass measurements was not too good. The data and experimental technique was therefore carefully re-examined. It was established that the final cleaning technique used to remove the deposit at the end of testing does not remove all of the mass deposited inside the capture cup. This variable quantity of residual mass apparently was the cause for poor repeatability of weighing data. Analytically, the later observations governing the technique should be expressed as follows:

$$W_A = W_{\text{cup}} + \Delta W_1$$

$$W_B = W_{\text{cup}} + W_{\text{deposit}} - W_{\text{eroded}} + \Delta W_2$$

$$W_C = W_{\text{cup}} - W_{\text{eroded}} + W_{\text{residue}} + \Delta W_3$$

Where: $W_{\text{residue}} = W_{\text{deposit}} - W_{\text{removed by cleaning}}$

Hence
$$W_{\text{deposit}} = (W_B - W_C) + \underbrace{W_{\text{residue}} + (\Delta W_3 - \Delta W_2)}_{\text{new terms}}$$

$$W_{\text{eroded}} = (W_A - W_C) + \underbrace{W_{\text{residue}} + (\Delta W_3 - \Delta W_1)}_{\text{new terms}}$$

The ΔW terms are the very small (typically of the order of a few to a few tens of micrograms) weight changes apparently due to (careful) handling and humidity effects. For example, we noted on a given clean cup the following weight changes:

<u>Date</u>	<u>Residual Weight (Milligrams)</u>	<u>Date</u>	<u>Residual Weight (Milligrams)</u>
6/18	0.868	7/8	0.800
6/18	0.860	7/8	0.796
6/23	0.881	7/8	0.797
6/24	0.886	7/13	0.804
6/28	0.885	7/16	0.790
6/29	0.889	7/20	0.853
7/2	0.844	7/20	0.852
7/6	0.892	7/21	0.859
7/7	0.802	7/22	0.867
7/7	0.803	7/26	0.871

The effect of the ΔW weight changes, while real, is most likely a second order effect because of the manner in which they appear in the final analytic expressions for the deposited and eroded mass. The residual weight has now been shown to possibly be the main reason for the poor repeatability. Our original cleaning procedure to remove the deposit utilized Nitrobenzene-MEK cleaning fluid. It has now been established that this cleaning solution does not remove all of the material deposited inside the cup. Since the plume is most likely depositing some form of fluorocarbon, it was decided to use a mild sodium etchant solution to clean the glass cups. Chemgrip treating agent distributed by Chemplast was used. This agent is used to prepare Teflon surfaces for epoxying in that the sodium solution reacts with Fluorine in the Teflon leaving carbon behind. When this new "cleaning" procedure was used, it was noted that an additional reduction occurred in the weight of a "cleaned" cup. The data noted is as follows:

Cup cleaned by Nitrobenzene/MEK:	0.745 Milligram residual
(Placebo cup weight at that time):	0.867 Milligram
Cup subsequently cleaned by etchant:	0.712 Milligram residual
(Placebo cup weight at that time):	0.871 Milligram

A further weight reduction of 33 micrograms occurred when this new "cleaning" procedure was used. It should be noted that the ΔW contribution due to handling and humidity of the placebo cup was only 4 micrograms.

An additional contamination test (Log 170-27) was performed over two days of continuous thruster operation (24635 pulses) at liquid Nitrogen temperatures. No improvement in the results were noted despite doubling the mass collection time. While we believe we can now explain the poor repeatability of the data from the above analytic considerations it is still puzzling why the experimental technique used earlier in the program with the microthruster and the 200 joule thruster apparently provided better data. The earlier mass data was collected with the cup at room temperature and in a different vacuum chamber. Whether or not capture cup temperature can account for the differences has as yet not been resolved.

A procedure was developed for Pre-test and Post-test cleaning of the glass capture as required for the weighing technique described.

The capture cups were cleaned in three stages:

- 1) A one percent solution of nitrobenzene and MEK (Methyl Ethyl Ketone) was used to remove material which deposited in the cup. This solution has been found effective in removing deposits which accumulated in the normal course of our work (this solution worked well in removing the deposited material which was collected in the cups during the preliminary experiments but not with the 750 joule plume thruster).
- 2) The cups were then washed in MEK.
- 3) The cups were given a final wash in Carbon Tetrachloride (spectro quality).

After the final wash, the cups were blown dry with a commercial "clean air" called microduster. This material is freon which is converted to gas and is used for fine cleaning. This gas was given a final filtering before using.

3.1.2.1 Experimental Studies with Glass Capture Cups.

3.1.2.1.1 Pre-test Checks. In an effort to understand the effect of the cleaning procedure and the vacuum environment on the accuracy of the weighing technique, two tests were carried out:

Test 1 - Effect of Pre-test Cleaning on the weight of a given cup: the cups were cleaned with MEK, alcohol, and distilled water, and were weighed by the residual technique. They were then placed in an oven at 72°C for 15 minutes. The residual weight (i.e., the difference in weight between the glass tube and a fixed tare weight) was recorded as soon as the glass tube was removed from the oven. Table 2 presents a set of data. The residual weight stabilized after about 8 minutes of weighing. The results indicate that the cleaned cups picked up a measurable amount of moisture as they cooled in the laboratory. It was noted, however, that the final 0.141 mg residual was the same value that was recorded before the cleaned cup was placed in the oven. This result suggests that the pre-test cleaning procedure does not leave any volatile residues on the cup, but that moisture can be picked up by a heated cup which is allowed to cool in air.

Test 2 - Effect of a Vacuum Exposure on the weight of a cup: The residual weights of three glass capture cups were determined and the cups were then placed in a vacuum chamber (no cold wall) and evacuated for 20 hours. The cups were then removed and the residual was recorded. Table 3 presents the results of this

TABLE 2

WEIGHT CHANGE OF CLEANED CAPTURE CUP DURING COOLING

Time Difference Between Weighing (Minimum)	Residual Weight (Milligram)
-	0.540
1	0.120
1	0.136
1	0.140
1	0.140
4	0.141

test. The results show that all cups gained weight (2% to 7%). To check whether or not this weight gain was due to a volatile substance, the cups were subsequently heated in an oven at 80°C for about 15 minutes. They were then allowed to cool to room temperature before they were reweighed. Table 4 presents a comparison of the residual weight before exposing the cup to a vacuum and after the post evacuation heat treatment. With the exception of the first reading (suspected to include a minor weighing error), it can be seen that any volatiles picked up by the cup during its exposure to the vacuum environment were subsequently driven off by the post evacuation heat treatment.

TABLE 3

WEIGHT CHANGES DUE TO VACUUM EXPOSURE

Cup	Residual Before Evacuation (mg)	Residual After Evacuation (mg)
1	0.224	0.239 (+6.7%)
2	0.319	0.336 (+5.8%) 0.339 (+5.8%)
3	0.626	0.639 (+2.1%)

TABLE 4

COMPARISON OF PRE- AND POST-EVACUATION TESTS

Residual Before Evacuation (mg)	Residual After Evacuation and Heat Treatment (mg)
0.224	0.234 (+4.4%)
0.319	0.316 (-0.9%)
0.626	0.626 to 0.627 (0%)

3.1.2.1.2 Tests with the Cups Being Exposed to the Plume. Early in the program as the mass capturing technique was being developed, a microthruster was used while the plume thruster was being built. During these exploratory studies the capture cups were placed at three positions in the plume. After several thousand thruster pulses, the cups were removed and weighed. The mass distribution that was determined indicated that the greatest mass was deposited on the geometric center line of the thruster, and then dropped off to the sides in some manner which was not calculated. After these exploratory experiments established feasibility of the approach, experiments were subsequently tried with a 200 joule millipound thruster. These experiments indicated that within the core of the plume the rim of the glass capture cups had to be protected from the impinging flow to prevent it from sputter eroding. To prevent such erosion, a copper container was constructed into which the glass capture cup was placed. The container also had three aperture plates which helped to collimate the flow into the cups (see Figure 11). The diameter of the holes in the aperture plates were slightly smaller than the glass cups' inside diameter, and thus protected the rim of the cups from erosion.

The final series of tests were carried out with the plume thruster in the liquid Nitrogen cooled test facility to determine the total mass distribution in the exhaust plume. Eight cups were located on the rake at $\theta = +85^\circ, +40^\circ, +30^\circ, +15^\circ, 0^\circ, -30^\circ$ and -40° , respectively. One cup was also placed on top of the thruster looking downstream at the cold target and another was placed on the target looking upstream into the thruster nozzle (see Figure 12). Each glass cup was located inside the holder which had collimating plates (Fig. 11). A thermocouple was attached to each holder. On one sample ($\theta = -60^\circ$), a thermocouple was located on the glass cup as well as the holder. This latter unit provided data on the temperature gradient that exists between the holder and the glass cup. Seven tests with the capture cups were carried out in the test facility. Table 5 summarizes these.

As stated earlier, repeatability of weight change data was not too good. It was finally concluded that the original cleaning procedure did not remove all of the deposits formed in the glass cups and therefore errors were introduced by the technique. Since the QCM and Langmuir probe studies were considered to be more reliable diagnostic techniques, further refinements in the glass cup capture technique were not made. It is now believed that instead of standard counterbalance weights

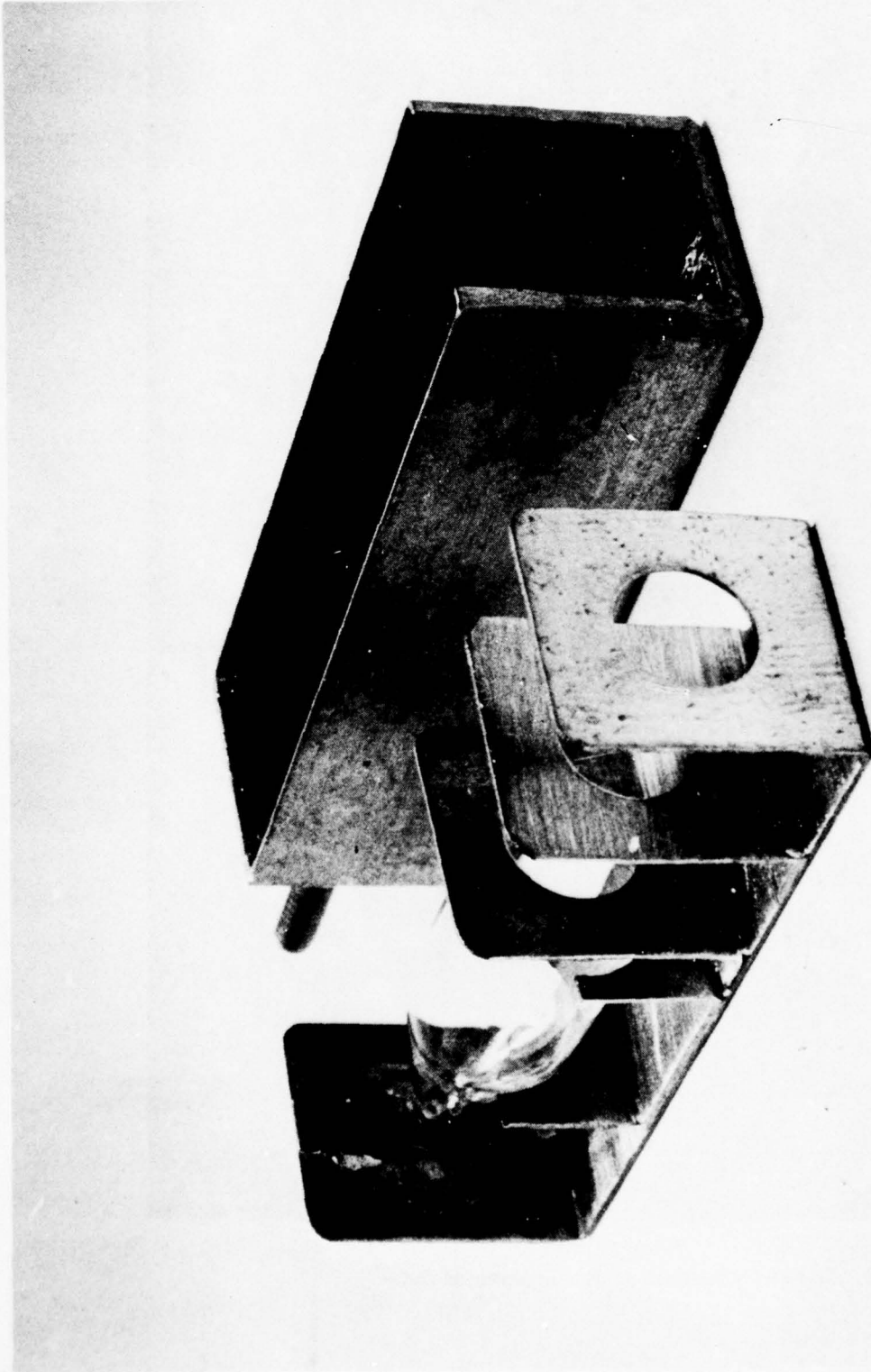


Figure 11. Glass Capture Cup Container, Cover Removed

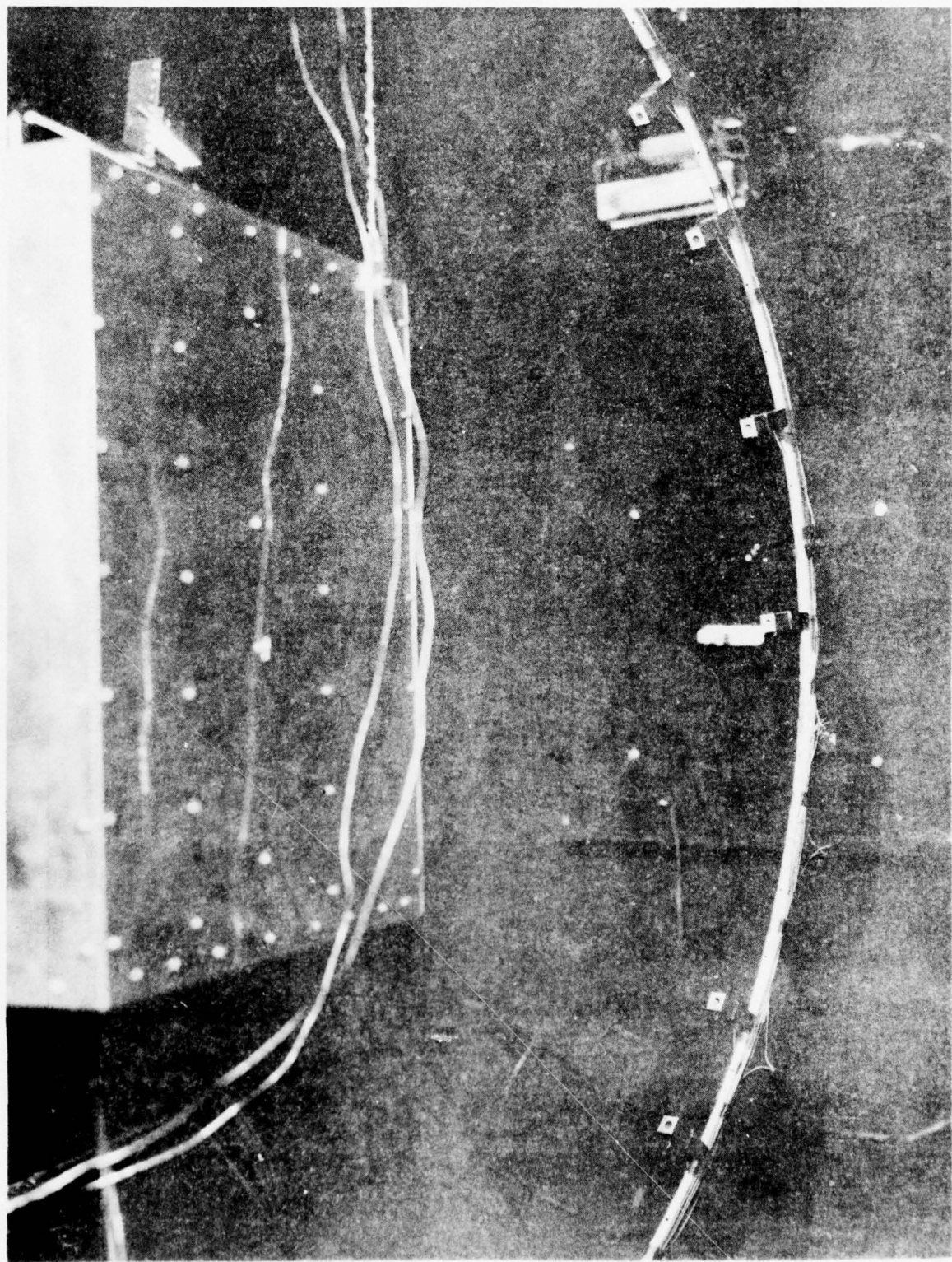


Figure 12. Glass Capture Cup Experimental Set-Up

TABLE 5

GLASS CAPTURE CUP TESTS WITH THE PLUME THRUSTER

<u>Log</u>	<u>Number of Pulses</u>	<u>Test Duration (hrs)</u>	<u>Location of Rake</u>	<u>Comment</u>
170-21	4,008	8	$\phi = 0^\circ$	-
-22	12,064	24	$\phi = 0^\circ$	-
-23	12,044	24	$\phi = 0^\circ$	repeat of -23
-24	12,064	24	$\phi = 0^\circ$	repeat of -23
-25	12,085	24	$\phi = 15^\circ$	-
-26	12,012	24	$\phi = 30^\circ$	-
-27	24,635	48	$\phi = 0$	-

it might have been desirable to use a placebo glass cup which had been subjected to the same temperature and vacuum environment as the test cup. In any case, the final cleaning process must remove all traces of whatever deposits are formed.

The experimental data of deposited mass that was obtained is shown in Figure 13. The results presented show the deposited mass at any angular location θ normalized with respect to the value on the geometric center line of the thruster (i.e. $\theta = 0^\circ$, $\phi = 0^\circ$). The data presented is for test Log numbers 170-22, 23, 24 and 27, respectively. It should be noted that the downstream capture cup (#9) on top of the thruster also indicated mass deposition. In the same normalized notation *this cup which is outside of the plume* provided the following values 0.39, 0.322, 0.306 and 0.167 respectively. These latter values reveal that this downstream facing capture cup also captured material. This result agrees with the general observation by all of the experimental techniques of this program that material is being scattered off the downstream walls of the test facility. Since the mass deposited on capture cups located outside angular locations θ of about 30° to 40° is of the same value as the level of backscattering noted, it is reasonable to say that all of the plume mass as determined by the glass capture technique is within a cone angle of roughly $\pm 30^\circ$ to $\pm 40^\circ$. It should be noted that this result is in complete agreement with the QCM and Langmuir probe data of this program.

Backscattering was measured at another location besides on top of the thruster. During the 48 hour test (Log-27) one capture cup was placed on the rake at $\theta = 5^\circ$, $\phi = 0^\circ$ but directed downstream instead of toward the thruster. During the same test measurements were made on a cup located on the rake at $\theta = 0^\circ$, $\phi = 0^\circ$ but facing

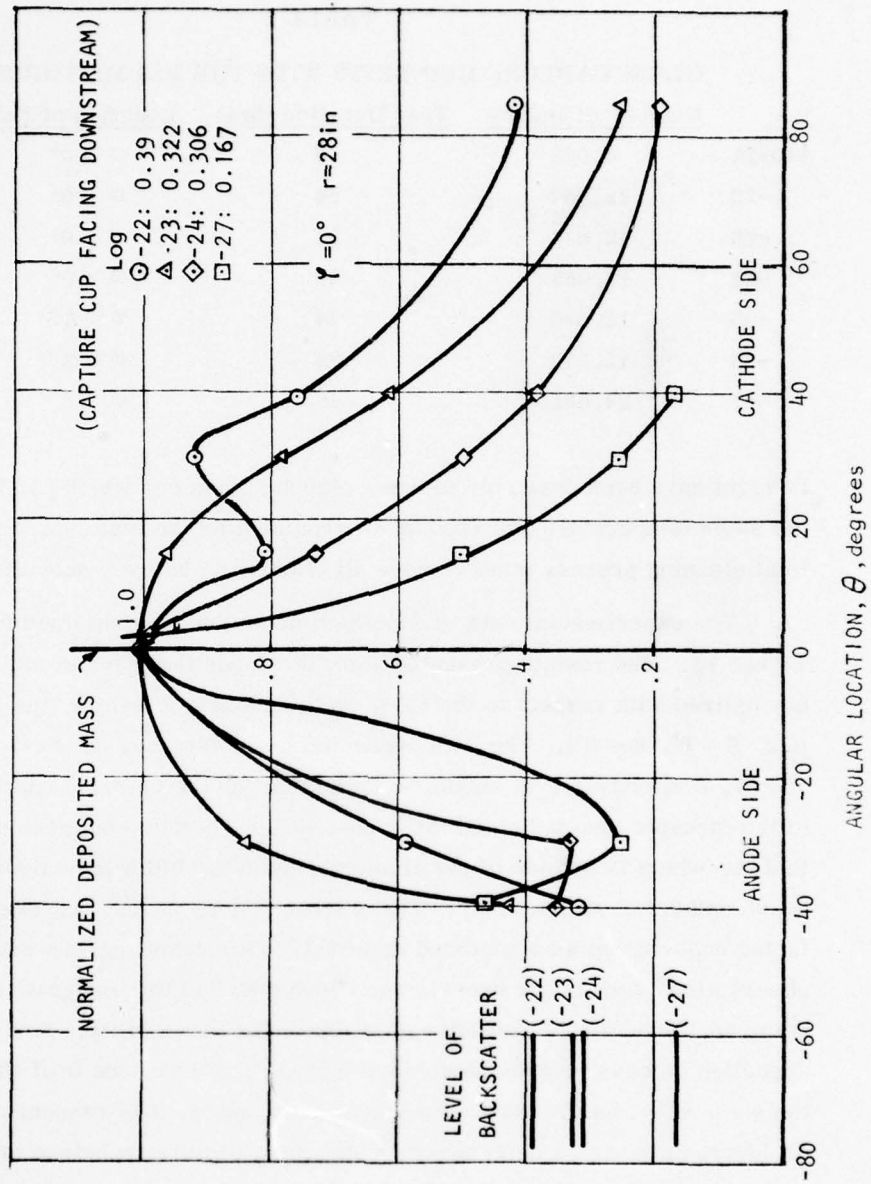


Figure 13. Distribution of Captured Mass from Cup Experiments

the thruster and also on the cup located at $\theta = 0^\circ$, $\phi = 0^\circ$ at the downstream target plate. This latter cup also faced upstream but from a distance of 61 in. (1.55 m) instead of 28 in. (0.71 m). The weight deposited on these three cups during this test is as follows:

- 1) $\theta = 0^\circ$, $\phi = 5^\circ$ looking downstream: 0.037 milligr.
- 2) $\theta = 0^\circ$, $\phi = 0^\circ$, $r = 28$ in. looking upstream: 0.036 milligr.
- 3) $\theta = 0^\circ$, $\phi = 0^\circ$, $r = 61$ in. looking upstream: 0.035 milligr.

This latter result again revealed that the downstream looking cup at $\theta = 5^\circ$ was being deposited by the same amount of mass as the upstream facing cups at $\theta = 0^\circ$.

Another observation that was made during these glass cup capture measurements was a discoloration of the face plate of the container box after prolonged exposure to the plume. In particular it was noted that the high velocity exhaust plume would polish these plates if they were located roughly along the geometric center line ($\theta = 0^\circ$) of the thruster. Such sputter erosion of material has also been noted with ion propulsion devices [4] and also during our studies with the QCM (see section 3.1.1.2).

Despite all the precautions taken, the glass cup capture technique is not considered to have the accuracy of the other techniques developed during this program. However, the results obtained with the cups qualitatively confirm the results obtained by the other techniques that were used pertaining to the outer boundaries of the plume, erosion in the core of the beam and scattering of mass by the walls of the test facility.

3.2 Ion Density Measurements

A double Langmuir probe [16] was used to probe the time varying ionized portion of the plume. The Langmuir probe allows one to obtain the characteristics of a plasma in a localized region of space, which is required for the description of the ionized portion of the plume. The double probe technique has the advantage of sampling the plasma with respect to its own electrode system rather than using one of the thrusters electrodes for reference. As a consequence one draws much smaller currents from the plasma thereby reducing the perturbation of the plume due to the probe. The double probe also has good inherent time resolution since time resolution is limited only by the ion transit time across the probes electrodes.

The application of Langmuir probes to flowing plasma should take into account the orientation of the probe with respect to the local flow direction, since the saturated ion current is orientation sensitive [17]. In order to apply simple probe theory, the probe should be aligned in the flow direction. The following relationship has been verified for Langmuir double probes. [18]

$$I_{\alpha} = I_{11} + (I_1 - I_{11}) \sin \alpha$$

where I_{α} = Saturated ion current for the probe oriented at the angle α to the flow
 I_1 = Saturated ion current with the probe oriented at right angles to the flow
 I_{11} = Saturated ion current with the probe oriented parallel to the flow

In our experiment the probe pointed at the geometric center of the thrusters electrode nozzle for all values of θ and ϕ . We could not check the alignment error because the rake design did not have the capability of allowing instruments to be remotely swiveled about a point on the rake. It is reasonable to assume that the alignment error would increase as one moves away from the central region of the plume. This implies that our data for the density distribution should actually fall off faster than observed, thus our ion density distribution is conservative.

The peak electron density at any time along the thruster axis (i.e. $\theta = 0$, $\phi = 0$) is 5.65×10^{13} el/cm³ for $r = 142$ cm (56 in.) and 3.35×10^{14} el/cm³ for $r = 71$ cm (28 in). These values were evaluated from the maximum transient Langmuir probe signal observed. The decrease in the peak density at $r = 71$ cm & $\theta = 0^\circ$ for variations in ϕ are 3.5×10^{14} el/cm³ for $\phi = 0^\circ$ and a density less than 2×10^{11} el/cm³ for $\phi = 90^\circ$. These values were also taken from the maximum time varying signals.

Plume contamination of the Langmuir probe was a problem during the earlier parts of the program. A technique was developed to clean the probe in place under vacuum conditions. This technique consisted of heating the probe wires by electron bombardment.

3.2.1 Langmuir Probe Design. The Langmuir probe was designed on the basis of the following criteria:

$$1) \quad r_p / \lambda_D \gg 1$$

$$2) \quad \ell_c / r_p \gg 1$$

where r_p is the probe radius, λ_D is the Debye length and ℓ_c is the electron mean free path. The 1st condition allows one to use simple probe theory for analysis, and the second allows one to assume low pressure theory. Our results are consistent with the above assumptions. Consider the following:

$$T_D \sim 10^{-4} \text{ cm for } T_e = 23600^\circ\text{K (2ev)}$$

$$r_p = 1.27 \times 10^{-2} \text{ cm}$$

The 1st criterion is then $r_p / \lambda_D \sim 10^2 \gg 1$

One can estimate the second criterion as follows. Assume a cross section of the order of 10^{15} cm^2 , and assume that 10^{14} el/cm^3 represents 10% ionization. For such a case we have $\ell_c = \frac{1}{N\sigma} = \frac{1}{10^{15} \times 10^{-15}} = 1 \text{ cm}$. This leads to a value of $\ell_c / r_p \sim 10$. This value of ℓ_c / r_p implies that high pressure corrections should be used, but even in this case these corrections are not significant for our plume [19]. These estimates are upper bounds and imply that our measurements are consistent with simple probe theory.

The probe dimensions are $r_p = 1.27 \times 10^{-2} \text{ cm}$ and $L = 1.0 \text{ cm}$ where r_p is the probe radius and L is the probe length. Fig. 14 is a photograph of the probe including the emitter which was used in the cleaning procedure. The emitter is shown as 3 circular coils which are attached to nickel posts. These posts carry the heater current which brings the emitter up to the probes temperature for electron emission.

In our application a time dependent probe signal is generated because of the time varying flow conditions in the plume as it sweeps over the probe. The source of power for driving the probe is a coaxial set of batteries which are manually changed when one wishes to change the applied probe voltage. The resultant signal output of the Langmuir probe is detected by a wide band current transformer. The coaxial battery holder can accommodate 12 batteries for a total voltage of 18 volts. Each battery can deliver a pulsed current of several hundred milliamps for times of the order of 10-20 m.s. without appreciable change in its terminal voltage. The peak current was detected by a wide band current transformer and displayed on an oscilloscope. Fig. 15 is a schematic of the probe current detection circuit that was used.

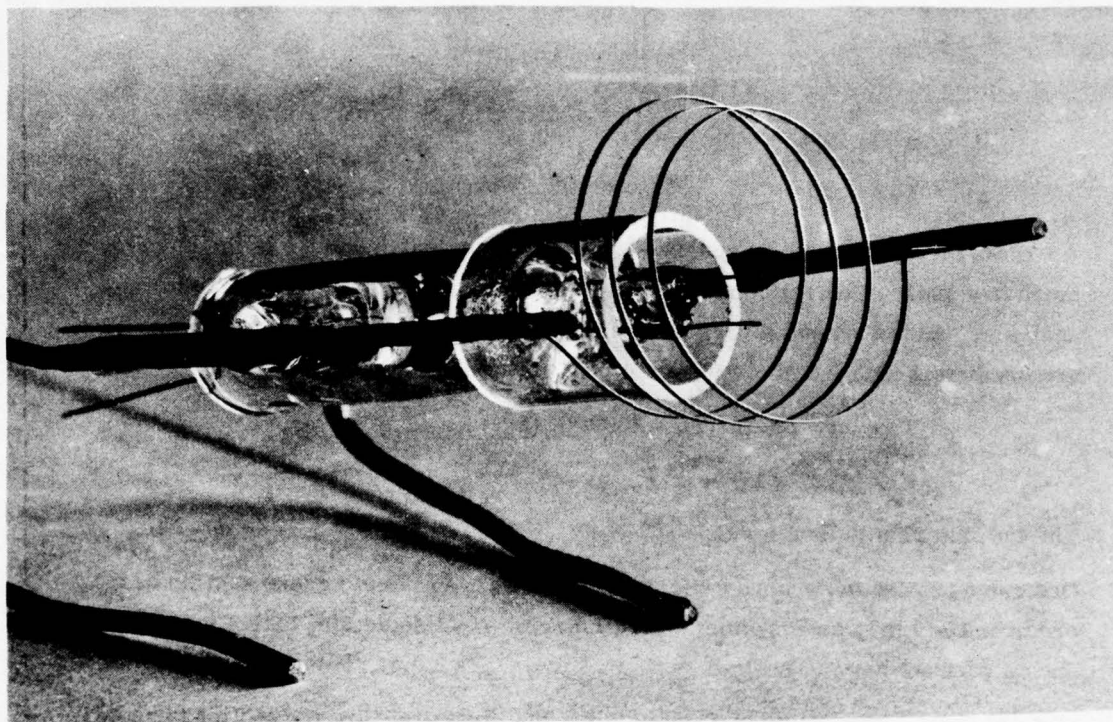


Figure 14. Langmuir Probe

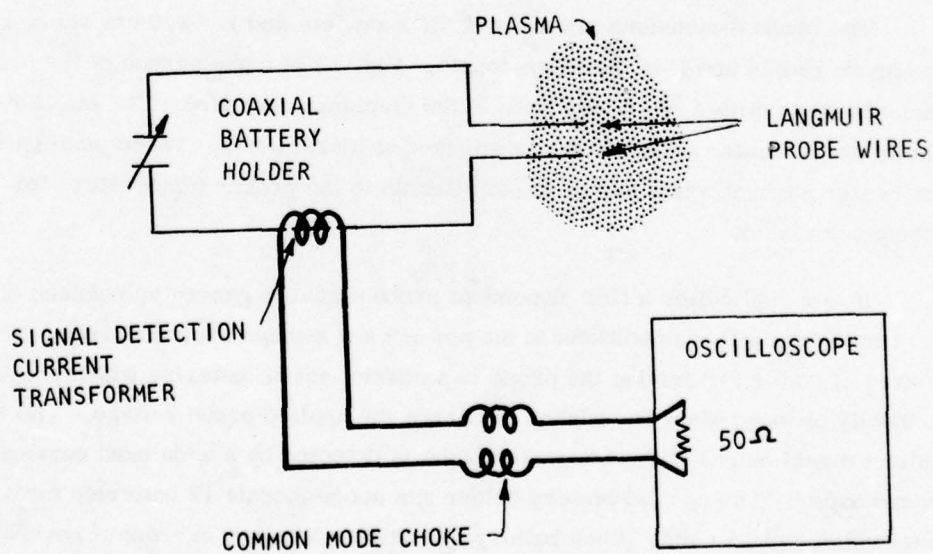


Figure 15. Langmuir Probe Current Detection Circuit Schematic

Typical photographs of the probe signal and the probe voltage show a small drop due to battery loading. These drops have the effect of changing the shape of the knee of the probes current-voltage curve, but not the slope or the saturation level which is used to analyze the data.

During the earlier studies with the Langmuir probe technique we noticed a deterioration of the probe signal after it was exposed to a number of pulses of the thruster plume. We concluded that material from the plume was being deposited on the electrodes of the probe. A closer evaluation revealed that this effect became pronounced after about roughly 20 shots of the thruster. A technique was subsequently developed at Fairchild Republic for cleaning the probe in place under vacuum conditions. A circular spiral of tungsten ribbon was located coaxially about the probe tips. This spiral served as an electron emitter when heated. In order to clean the probes electrodes, a high voltage is applied between the tips of the probe and the electron emitter thereby causing the tips of the Langmuir probe to be bombarded by an electron current. This bombardment heated the probe tips sufficiently to cause the probe to be cleaned. The emitter was heated by A. C. to a temperature which allowed 60 to 70 ma to be drawn at 600 volts. The heater power used was about 230 watts. This power level allowed us to obtain an emitter temperature in excess of 2300°C. This technique for cleaning the electrodes of the Langmuir probe worked fairly well over the course of the ion density studies (2500 shots). Toward the end of the ion density studies a discoloration due to a deposit near the tungsten-glass interface was noticed. This deposit caused a resistance of several thousand ohms to be formed across the probe. It should be emphasized that the probe was constantly checked during the experimental studies both visually, when the vacuum test chamber was opened, and also electrically at frequent intervals during testing. The cleaning procedure resulted in a clean matte finish over most of the probe wire. Figure 16 is a schematic of the probe cleaning circuitry.

The probe data was displayed on an oscilloscope. One channel of the oscilloscope was used to monitor the thruster's discharge current by means of a Rogowski coil. The second channel of the oscilloscope was used to monitor the Langmuir probe current. The thrusters discharge current that was displayed represents only one quarter of the total discharge current since the current from only one capacitor of the capacitor bank was monitored. Monitoring this discharge current served two purposes. It is useful as a timing reference of events and also indicates

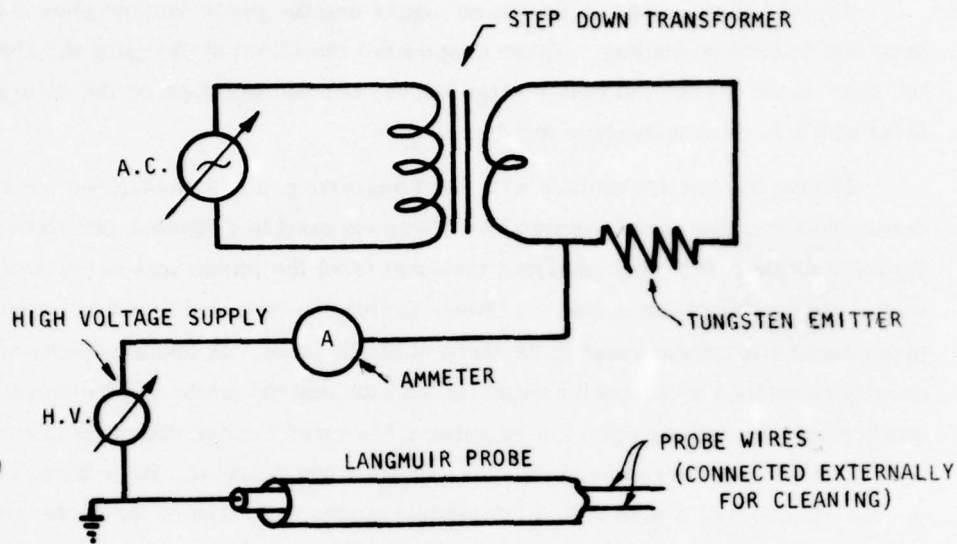


Figure 16. Schematic of Probe Cleaning Circuit

the general repeatability of the thrusters discharge. At each position of the Langmuir probe in the plume a minimum of three thruster pulses were fired. All of these discharges were recorded on a single photograph. In most cases the data that was recorded superimposed each other very well. In those instances where they did not overlay very well we averaged the data.

3.2.2 Experimental Set-up for Ion Density Measurements. The ion density studies with the Langmuir probe were performed in the liquid nitrogen cooled vacuum chamber described in section 2.1. All probe data was taken with the cold wall in operation. The test facility has two instrumentation rakes (section 2.3.1). One of these is located at .71 meters and can be rotated relative to the geometric center of the thruster. The other rake is fixed further downstream at 1.42 meters. The orientation of the fixed rake is in the plane $\phi = 0^\circ$. The thruster was operated at the design discharge energy of 750 joules (2414 volts) to obtain the charged particle characteristics of its plume.

Data was obtained at .71 meters for various angular positions ϕ and θ . Only one angular position was examined for the 1.42 meter rake. The crosses in Table 6 represent the positions in the plume that were studied with the Langmuir probe.

TABLE 6

Langmuir Probe Positions Studied

a) RAKE RADIUS = .71 meters

ϕ / θ	0°	$+15^\circ$	-15°
0°	X	X	X
$+15^\circ$	X	X	X
$+30^\circ$	-	X	X
$+45^\circ$	-	X	X
$+90^\circ$	-	X	X
-15°	X	X	X
-30°	X	X	X
-45°	X	X	X
-90°	X	X	X

b) RAKE RADIUS = 1.42 meters

ϕ / θ	0°
0°	X

Figure 17 presents a schematic of the experimental set-up.

3.2.3 Langmuir Probe Data Reduction. The experimental probe data was generated as follows. At a given applied probe voltage an oscilloscope photograph was taken of the response of the probe to the plume. This photograph then represents the time dependent probe response for a given probe voltage. If one takes a whole series of such photographs, each for a different probe voltage, the resulting set of photographs represents the total time dependent history of current-voltage (I-V) characteristic of the probe. The next task was to determine the I-V characteristic at specific times. This was done as follows:

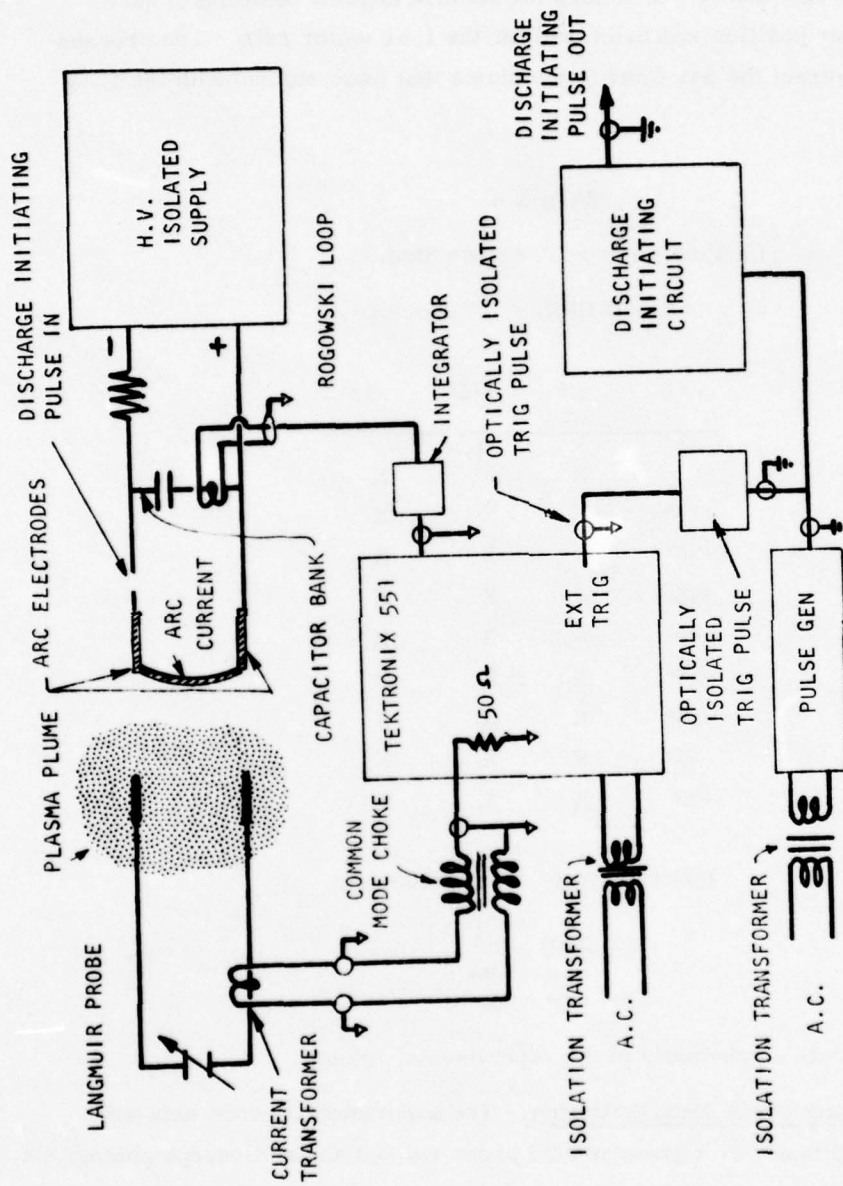


Figure 17. Schematic of Experimental Set-up with Langmuir Probe

Each photograph was traced on a replica of the scope grid. Two tracings were made, one for positive probe voltages, and the other for negative probe voltages. The two traces were then fitted so that the maximum and the initial points matched; although the maximum was used as the main criteria. A complete I-V characteristic was then generated at a specific time by drawing a vertical line through the curves and picking off the probe currents at that specific time. Since each curve had been identified with respect to its probe voltage, a complete characteristic could be generated. It should be pointed out that the underlying assumption here is that at a given time the I-V characteristic is the same as would have been generated under steady conditions, i.e. we assume quasi-static conditions hold. Figures 18 and 19 are examples of the probes current-voltage (I-V) characteristics for the indicated time after thruster discharge initiation and probe position. These times intervals are measured from the onset of the thruster discharge current as measured by the Rogowski coil.

The electron temperature in the thrusters plume was determined from the slope of the I-V curve at $V = 0$. Consider the following:

$$\left. \frac{dI}{dV} \right|_{V=0} = \frac{e}{kT^{\circ}(\text{K})} \frac{i_1 i_2}{i_1 + i_2} \quad (1)$$

where $\left. \frac{dI}{dV} \right|_{V=0}$ represents the slope of the I-V curve at $V = 0$

- and e = the electronic charge
 k = Boltzman constant
 $T(k)$ = Electron temperature in degrees Kelvin
 $i_1 + i_2$ = the saturated probe current as determined by the
 2 tangent method

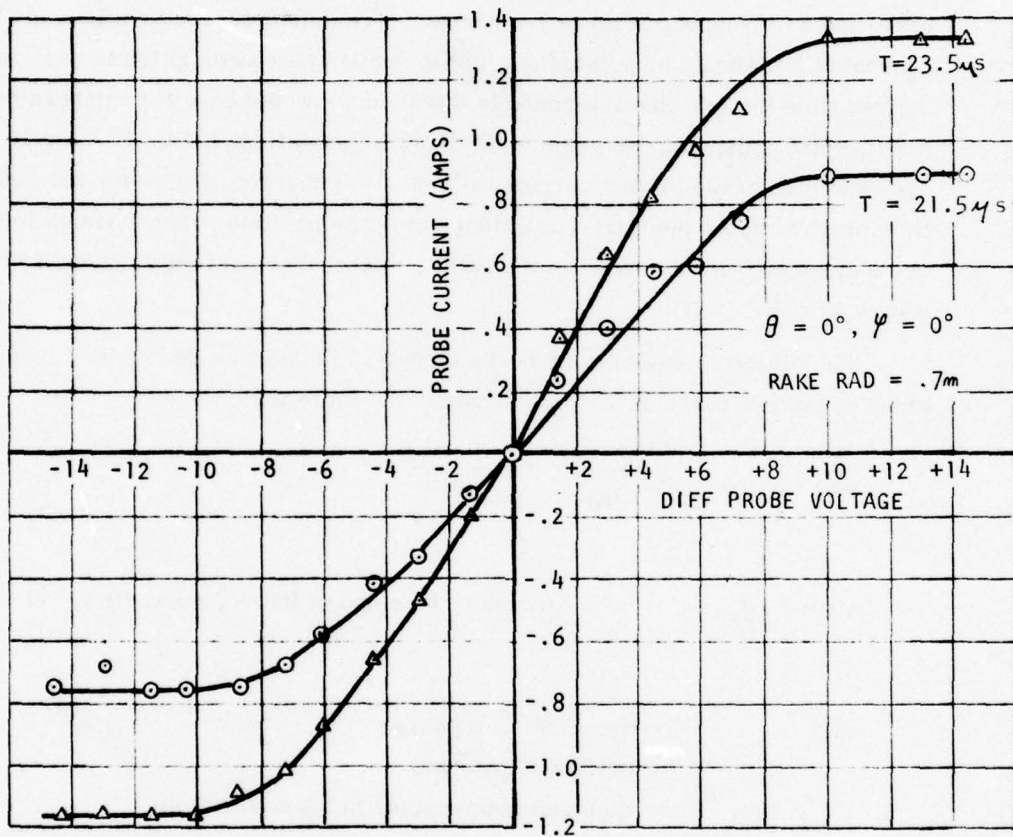


Figure 18. Langmuir Probe Characteristic for Earlier Time

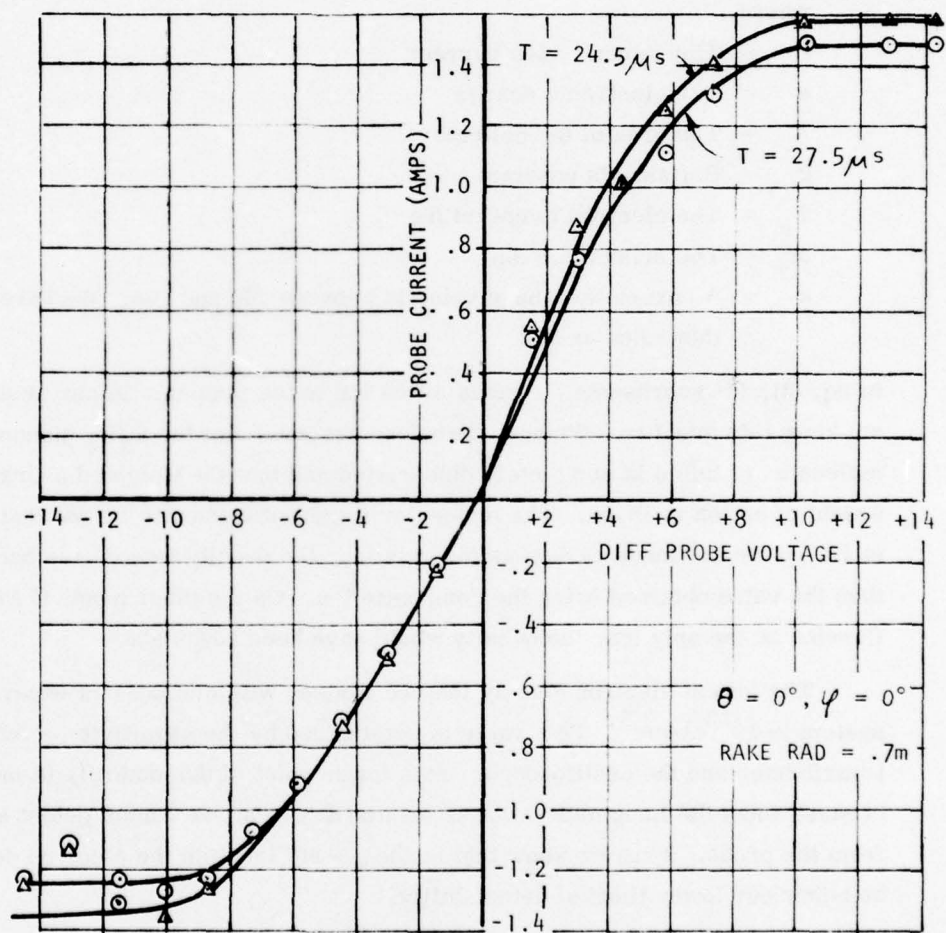


Figure 19. Langmuir Probe Characteristic for Later Time

All the quantities are known except the electron temperature. Equation 1 then determines the electron temperature. The corresponding electron density is determined by the equation [19]:

$$i = x n e A \frac{k T_e}{M_+} \quad (2)$$

where

- i = The saturated ion current
- e = The electronic charge
- A = The area of the collector
- k = Boltzman's constant
- T_e = The electron temperature
- M₊ = The mass of an ion
- x = A parameter whose value is between .56 and .60. We have taken this value as 1/2

In eq. (2), M₊ represents the mass of the ion in the plasma. In our studies we do not know this quantity. We have therefore assumed that the C₂F₄ monomer molecule of teflon is completely dissociated and that the weighted average molecular weight of an ion is 16.66. The molecular weight of carbon is 12 and that of fluorine is 19. If we had taken carbon as the only ion, the density would have been 7% lower than the value obtained using the composite ion. On the other hand, if we had taken fluorine as the only ion, the density would have been 15% higher.

The lowest electron density that we can see with our present experimental system is 10¹² e1/cm³. This value is determined by the sensitivity of our current transformer and the oscilloscope. This lower point of detectability is mentioned because when the Langmuir probe is located at φ = 90° we cannot detect a signal from the probe. Thus we know that at the φ = 90° location the electron density must be below our lower limit of detectability.

3.2.4 Ion Density and Electron Temperature Distribution. Langmuir probe theory allows one to obtain electron temperature from the I-V characteristic and then to calculate the ion density from a theory of ion saturation current. We have assumed that the inherent charge neutrality of a pulsed plasma thruster holds in the plume plasma.

The charge particle density, Fig. 20, is shown in the plane $\theta = 0^\circ$ as a function of angle ϕ for a radius of .7 meters. If one extrapolates the data of this figure to $\phi = 90^\circ$ one might expect a density varying somewhere from 10^9el/cm^3 to 10^{11}el/cm^3 . These values are based on taking the density at $t = 21.5 \mu\text{s}$ for $\phi = 90^\circ$. The dotted portion of the density variation has been included so that one can see the possible overall distribution of the charged particles across the plume. The dotted line presented is a reflection of the curve for the data points on the right hand side of the graph i.e., $\phi = +30^\circ, +45^\circ$.

Figure 21 presents the electron temperature as a function of ϕ at $\theta = 0^\circ$ and $r = .7 \text{ m}$ at different times. This result reveals that the electron temperature drops as one moves into the outer edges of the plume.

Figure 22 presents the change in peak ion (or electron) density in the flow direction at $\theta = 0^\circ, \phi = 0^\circ$ at a rake radius of .7 meters and at 1.4 meters. These values of electron density correspond to the maximum measured values. Only the maximum values of the time varying density have been presented in Figure 22.

Figure 23 represents the variation in time of the charged particle density at a given location $\theta = 0, \phi = 45^\circ$. This variation has been included to indicate the way in which the pulsed plume particle density rises and decays in a region that might have a spacecraft surface in this region. This result substantiates the observation that the plume is ejected as a concentrated energetic blob.

The probe data can also be used to determine the average forward speed of the plume. The times corresponding to the maximum signals observed at the two radii were used to determine this average speed. This value is $2.49 \text{ cm}/\mu\text{s}$. This value was compared against the speed as measured from the time of arrival for the probe mounted on the rake located at 0.7 m. This latter value is $2.4 \text{ cm}/\mu\text{s}$. These two numbers are quite consistent. The thruster propulsive performance data indicates a specific impulse of 1700 sec. This translates into an overall mass average speed of $1.7 \text{ cm}/\mu\text{s}$ for the total efflux of material from the thruster. This latter average speed compares very well with the speed measured with the probe and strongly suggests that most of the plume mass is moving in the forward direction.

The double Langmuir probe is a useful experimental technique for studying the ionized portion of the plume from a pulsed plasma accelerator. The probe that was used for this work can be improved in two areas. The first is in the construction

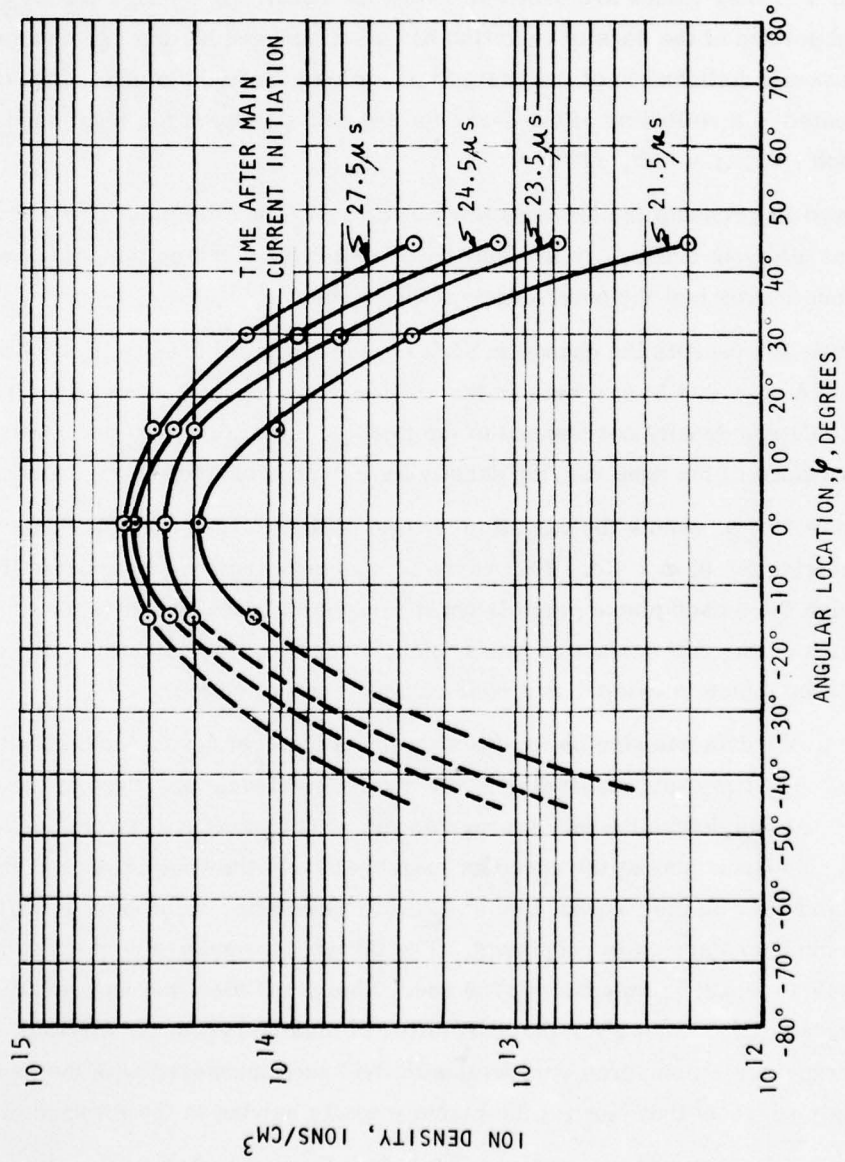


Figure 20. Ion Density Variation in the Plume

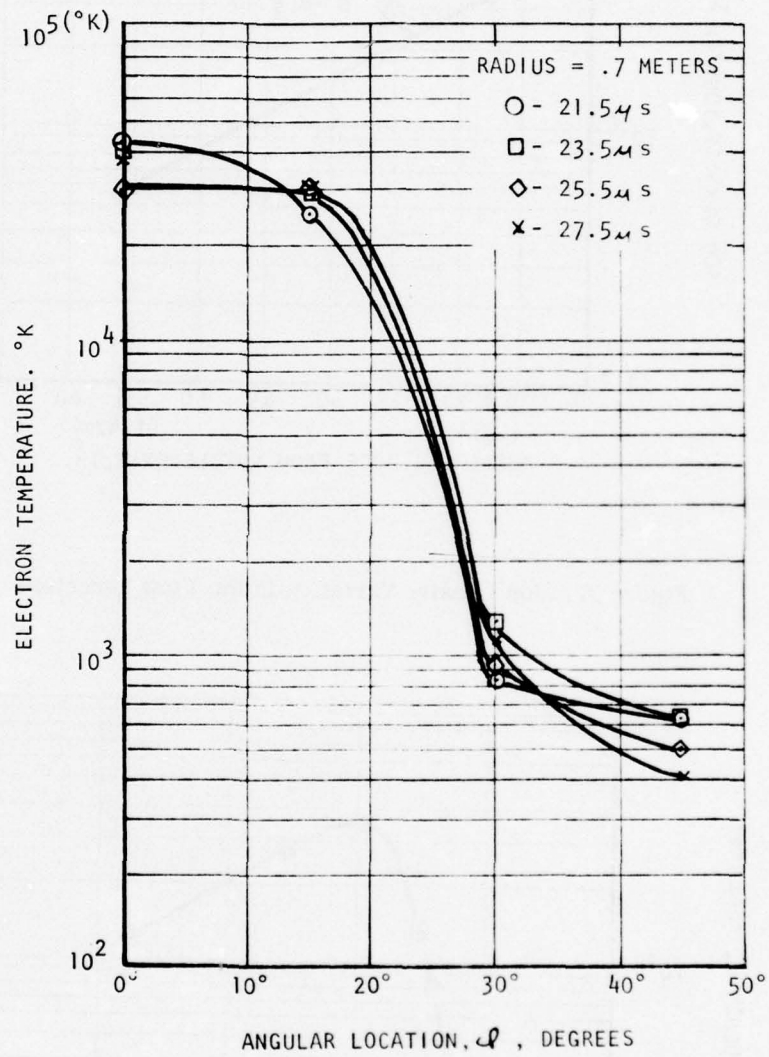


Figure 21. Electron Temperature Variation in the Plume

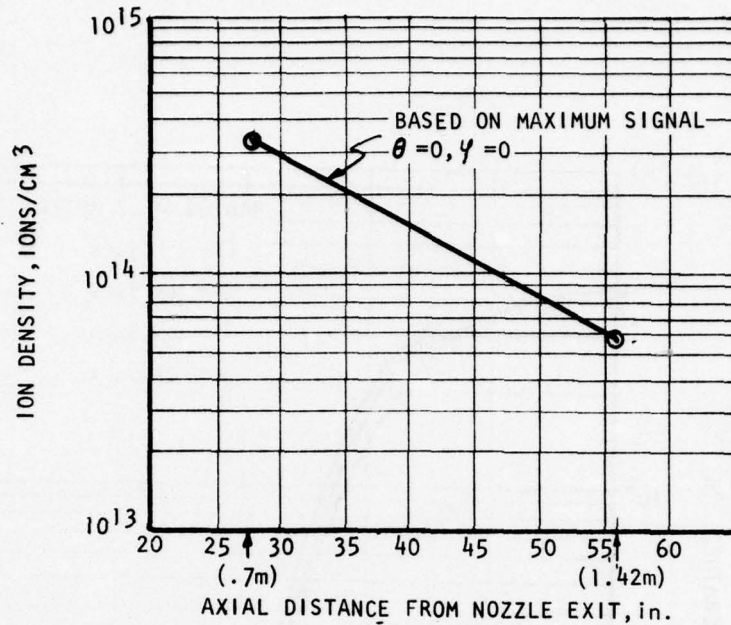


Figure 22. Ion Density Variation in the Flow Direction

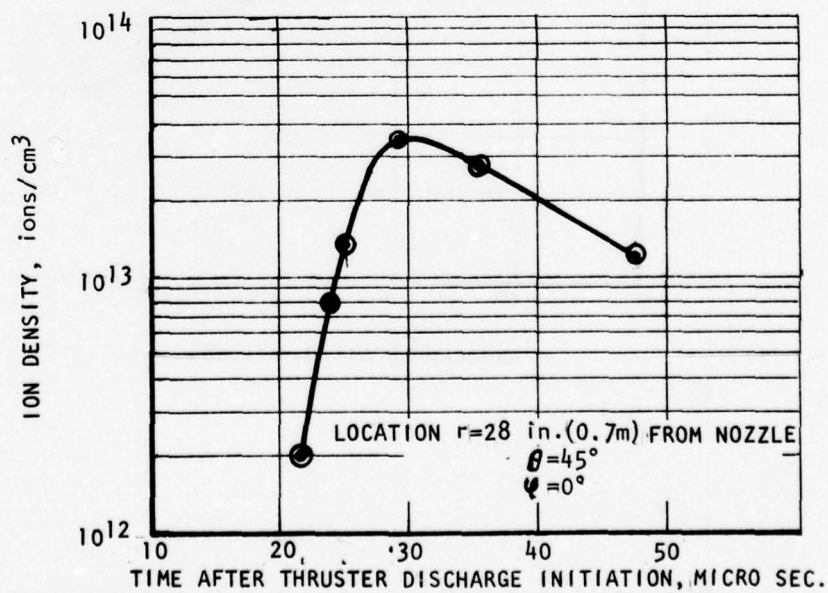


Figure 23. Ion Density Variation with Time

of the probe. At the present time a tungsten emitter was used to clean the probe. This emitter operates at very high temperatures and eventually damages the interface between the probe wires and the glass structure. It is believed that one can significantly improve on this technique by using a lower temperature electron emitter such as thoriated tungsten. The second area of improvement is in the operation of the probe. At the present time it is extremely time consuming to collect and analyze the data. It is believed that a pulsed probe can be built which would allow one to display the entire probe characteristics at specified times during the transient flow of the plume. Such a diagnostic system would be more complex than the present arrangement, but would reduce the data taking process and analysis by one to two orders of magnitude. It probably would also reveal the effects of the plume/wall interaction after the main pulse of plume mass has gone past the probe.

3.3 Back Flow Measurements

Tests were performed to determine if plume mass could be found in areas behind the thruster cone. One test in particular provided results which raised doubt on the validity of any back flow detected and supported the conclusion that the energetic plume is scattered to some extent by the liquid nitrogen cooled wall upon impact. The test in question involved locating a nude ionization pressure gauge behind the thruster enclosure (see Figures 2 and 7). An aluminum 90° angle support bracket was attached at the center top of the rear panel of the thruster enclosure. The nude ionization gauge was supported by this bracket near the center of the rear panel so that any back flow expanding around the edges of the exhaust cone would have to subsequently also expand at the front top and rear top edges of the thruster box. This latter type of expansion is virtually impossible. During actual thruster operation with the cold wall of the test facility at -183°C it was noted that the pressure recorded by the concealed nude ion gauge increased from 3.4×10^{-5} Torr to 5.8×10^{-5} Torr after only 32 thruster discharges when operated at a pulse rate of 0.138 Hz. This result revealed that any type of back flow measurements in regions behind the exhaust cone would also be comprised of an unknown amount of mass scattered off the walls of the test facility.

Despite the conclusion that wall scattering was taking place, two additional tests were carried out with the QCM located in regions behind the exhaust cone. The first test involved locating the QCM on a bracket positioned on the top panel of the thruster

enclosure (see Figure 2). The 140° viewing angle QCM was positioned 3 inches (7.6 cm) above the top panel and 10-1/4 in. (26 cm) behind the exit plane of the exhaust cone. This location places the entrance port of the QCM 5 in. (12.7 cm) behind the imaginary line connecting the upper lip of the exhaust cone with the front top edge of the front panel of the thruster enclosure. With the walls of the test facility at -187°C and the QCM crystal temperature at -33°C to -34°C it was noted that the beat frequency increased by 45 counts for 200 pulses of the thruster. This increase in frequency corresponds to 6.3×10^{-9} gr of mass being deposited on the crystal while the thruster was pulsed 200 times. An attempt was subsequently made to determine if this mass could possibly be due to wall scattering as established by the test with the nude ionization gauge. From theoretical considerations [20] one could in principle calculate the number of molecules that strike a unit area per unit time due to the increased facility background pressure due to wall scattering. The rate at which these molecules will actually condense on a surface requires knowing the accommodation coefficient. Since neither the molecular composition of the background mass nor the accommodation coefficient are known, it is not possible to carry out any meaningful calculations at this time of the amount of mass deposited on the QCM due to the scattered background pressure.

Some consideration was also given to establish the feasibility of displaying the gauge current of a nude ionization gauge on an oscilloscope in an attempt to develop a fast pressure gauge to resolve effects from scattered material. The developmental effort was considered beyond the scope of the present study and therefore was not undertaken.

Some additional studies were carried out with the QCM located in the exit plane of the exhaust cone but 9 in. (22.9 cm) above the top edge of it (i. e. 90° off the centerline of the nozzle). The axis of the QCM was tilted slightly downward so as to intersect an imaginary line extended through the geometric center of the thruster nozzle. The intersection of these two lines occurred 61 in. (1.55 m) downstream at the face of the liquid nitrogen cooled square target plate (see Figure 1). Four tests were carried out in an attempt to determine whether or not the geometry and surface configuration of either the downstream target or the thruster's exhaust cone geometry had any effect on the mass deposited on the QCM. The four tests that were performed are:

- 1) Operation with the downstream target plate in its normal configuration (see Figure 1).

- 2) Operation with the normal to the surface of the target plate tilted 14° downward.
- 3) The same as the second test except instead of a black surface a shiny aluminum surface was facing toward the thruster.
- 4) The same as test 2 except the four downstream edges of the thruster's exhaust cone were extended horizontally by about 2 in. (5 cm).

The 14° tilt was selected so that the normal at the center of the downstream target plate projected upstream below the lower front edge of the thruster enclosure. The thruster was operated for 150 pulses three times during each of the four tests. QCM data was taken during the 150 pulse tests. Table 7 presents a summary of the data.

TABLE 7. QCM DATA FOR GEOMETRIC CHANGES

Number of Thruster Pulses	Test 1 (Normal) (gr)	Test 2 (Tilted 14°) (gr)	Test 3 (14°, Aluminum Surface) (gr)	Test 4 (Cone Extension) (gr)
0	0	0	0	0
10	5.6×10^{-9}	6.3×10^{-9}	4.9×10^{-9}	4.9×10^{-9}
20	13.3	11.9	11.2	5.6
40	25.2	23.8	23.8	12.6
50	30.8	27.3	26.6	21
70	41.3	29.4	34.3	28
80	46.2	30.8	36.4	34.3
100	56	44.8	44.8	54.6
120	68.6	58.1	55.3	64.4
130	74.9	63.7	61.6	60.9
150	88.2	75.6	74.9	68.6

The mass changes presented are the numerical average of the three series of 150 pulses for the particular configuration. The data of the tests performed are too close to each other to draw any other tentative conclusion that either local geometric changes to the exhaust cone or downstream geometric changes to the target plate had essentially no effect on the mass seen by the QCM. Such a result would be compatible with the hypothesis that wall scattering is dispersing plume mass throughout the chamber.

The conclusion drawn from the studies performed on the presence of mass behind the cone is most probably due to scattering of the plume off the liquid nitrogen cooled walls of the test facility.

3.4 Thruster Propulsive Performance

The propulsive performance of the plume thruster was monitored periodically during the program. The impulse bit amplitude was measured on the thrust balance (see section 2.3.4). Table 8 presents a summary of the data that was taken.

TABLE 8. THRUSTER PROPULSIVE PERFORMANCE DATA

Log	Pulses Since Assembly	Propellant Mass Per Discharge (gr)	Impulse Bit Amplitude (mlb-sec)	Specific Impulse (sec)	Thrust Efficiency (%)
170-1	3,697	1.490×10^{-3}	-	-	-
170-2	7,698	1.367×10^{-3}	-	-	-
170-3	9,161	1.297×10^{-3}	5.073	1773	26.07
170-5	10,087	-	5.964	-	-
170-6	13,712	1.68×10^{-3}	5.786	1558	26.3
170-28	127,063	1.44×10^{-3}	-	-	-
170-30	129,076	-	6.106	-	-
170-39	217,470	-	6.078	-	-

With the exception of the first impulse bit reading at 9161 pulses, the remaining readings were about 5.98 milli-lb-sec $\pm 3\%$. Like the data noted during the 12,000 lb-sec test of program F04611-72-C-0053 the impulse bit amplitude is seen to be essentially constant. The upstream located Teflon propellant rods used in the present program did not use Teflon cement at an interface. The accelerator nozzle cavity in the plume thruster was noted to be uniformly shaped and the six propellant rods remained quite symmetric about the fuel retaining shoulder during the 217,470 pulses (1300 lb-sec) produced by the thruster during the present study. Figure 24 shows the discharge port between the Teflon rods near the fuel retaining shoulder. The increased spacing about the fuel retaining shoulder is clearly evident.

3.5 Solar Cell Contamination Studies

Flight quality solar cells have previously been exposed to the exhaust plume of pulsed plasma microthrusters and all previous evidence obtained indicated that the solar cell is only negligibly affected by the plume. In one of these cases [21] four microthrusters were located around the periphery of the LES-6 satellite. In this spin stabilized satellite the entire cylindrical peripheral surface was covered by solar cells. Flight data and a few years of space operation did not reveal a degradation due to contamination in excess of what normally was expected. Limited laboratory vacuum chamber tests with another microthruster and flight quality solar cells also revealed

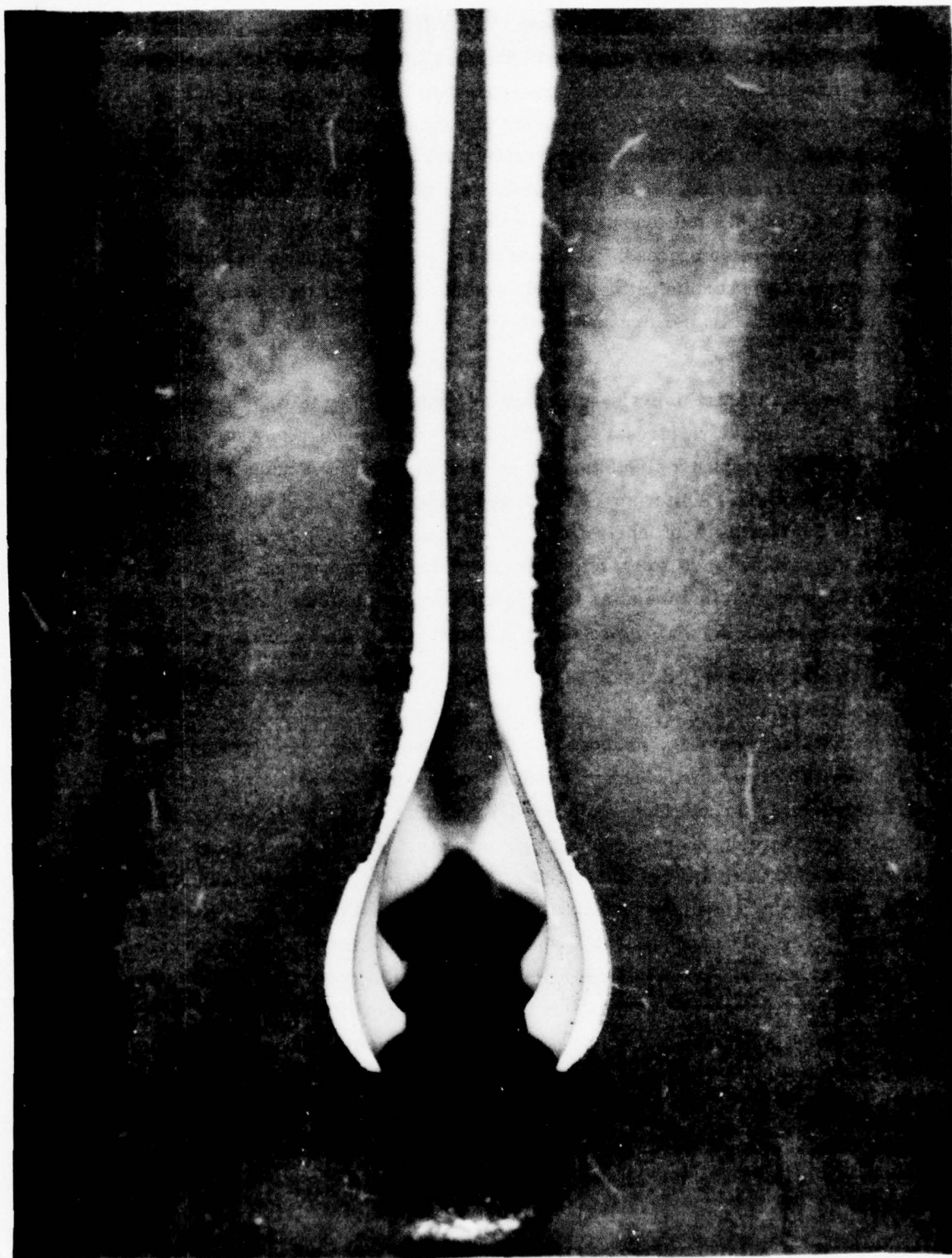


Figure 24. Thruster Discharge Port Near Anode

negligible degradation due to the plume. Mr. Allen of the Johns Hopkins University Applied Physics Laboratory suggested [22] that perhaps deposits of the pulsed plasma microthruster are optically transparent in the cells regime of maximum spectral response. Reference [23] cites that the spectral response of solar cells is such that an appreciable amount of incident solar radiation is not of wavelengths which are efficiently converted in the cell. In a typical cell solar radiation of wavelengths less than 0.4 microns or greater than 1.1 microns contribute very little to the power conversion process. Thus one of the relevant items to be considered in the present plume contamination study is whether or not any thruster plume deposits reduce the solar cells performance in the range of solar radiation extending from 0.4 to 1.1 microns.

The requirement of evaluating solar cell performance in regime .4 to 1.1 microns of radiation requires a solar simulator corresponding to AM0 (air mass zero) conditions. Such a simulator was not available in the vacuum test facility at Fairchild Republic. A literature search and study were carried out in an effort to establish the feasibility of fabricating a solar simulator which could possibly be used for in-situ calibration of solar cells exposed to the thruster plume. Some of the errors one could encounter in simulating the Johnson curve with either carbon arc, xenon lamp or mercury-xenon lamp were presented in Reference [23].

To simulate AM0 (air mass zero) conditions it would be necessary to simulate the Johnson solar curve of irradiance as a function of wavelength. The emissive power of a black body has, in accordance with Planck's law, a peak value which is a function of temperature. The distribution of the emissive power as a function of wavelength of AM0 conditions would require a source temperature of roughly 6000°K. Carbon arc sources, short arc xenon light sources, and tungsten-halogen sources have been used in an attempt to simulate AM0 conditions. A comparison of the spectral distributions of these sources was made in Reference [24]. It was concluded by Fairchild Republic that it would be beyond the scope of the present program to build and use a solar simulator which would reasonably present the amplitude of 140 mw/cm^2 of solar irradiance. The short arc xenon and the tungsten-halogen sources because of their lower source temperature, have a displaced spectral distribution compared with that of the Johnson solar curve. A carbon source while more nearly matching the Johnson curve is more difficult to control. It would

appear that the only in-situ calibrations which could possibly be carried out are observations of the changes in some relevant characteristics of either solar cells or thermal control material when irradiated by either a tungsten-halogen or short arc xenon light source located in the vacuum chamber but operated at a lower power level than the value corresponding to AM0 conditions.

The task of constructing a suitable solar simulator for in-situ calibrations of solar cells was finally assessed to be beyond the scope of the present program. However, an experimental technique for carrying out in-situ calibrations and tests with such a simulator was formulated. The main features of this technique can be briefly described as follows. Two flight quality solar cells would be used for in-situ contamination studies. One cell could be the sample located on the rake and exposed to the plume. The other cell would be protected from the plume and used only as an instrumented reference cell to be used to adjust the electrical power to the solar simulator during calibrations to assure "constancy" of the simulator during prolonged in-situ testing and calibrations. The geometric deployment and protection of the reference cell and light source would be roughly 90° to the side of the exhaust cone and at a radial distance which would allow the "contaminated" test cell to be rotated by means of the rake. One ohm resistive loads would be placed across both cells. The short circuit current of the contaminated cell could then be compared against that of the reference cell. The latter reference value would be kept constant by adjusting the voltage and current to the light source. Typical in-situ studies would entail periodically remotely rotating the "contaminated" cell into the "calibrating" position and subsequently returning it to the "test" location.

Since the latter in-situ study could not be carried out, ex-situ calibrations were carried out instead. Ten 2 cm x 2 cm N/P flight quality solar cell modules were procured from Spectrolab (Sylmar, CA). These cells had Dow 7940 cover slides with magnesium fluoride anti-reflective coating on the exposed surface. The cells were bonded with Dow 63-489 adhesive. The completed cells were subsequently bonded to 3.8 cm x 3.8 cm fiberglass substrates with GE-RTV 511 adhesive. Each unit had connections to allow electrical calibrations to be made. Spectrolab serialized each unit and provided a continuous current-voltage calibration curve for each cell at 25°C ±2° under AM0 (air mass zero conditions).

The QCM test results (see section 3.1.1) revealed that the effects of wall scattering could apparently be reduced by using an aluminum collimating tube over the test surface being evaluated. Therefore, the solar cell studies were also provided with collimating tubes have a square cross section in order to match the square configuration of the solar cell. Since the QCM tests also revealed that the exhaust beam could be erosive within a cone angle of about $\pm 40^\circ$, the collimating tube was designed so that the interior edges of the collimating tube facing the solar cell extend about 0.040 in. (1 mm) inward toward the cell at all edges. This approach was used to prevent the thruster's plume from possibly sputtering any of the solar cells fiberglass substrate onto the surface of the cell. Furthermore, the end of the collimating tube was terminated about 0.040 in. (1 mm) above the surface of the cell to prevent the aluminum tube from contacting the surface of the solar cell. The aspect ratio of the tube was about 10. The terminals and solar cell were located inside a sealed box at the lower end of the collimating tube to prevent scattered material from contacting the solar cells. Each cell was provided with one of these collimators. Five such collimators were located on the instrument supporting rake at $\theta = 80^\circ, 45^\circ, 30^\circ, 15^\circ$ and -45° , respectively. Figure 25 shows these units in the test ready configuration located at $\varphi = 0^\circ$. The geometric centerline of each collimating tube is directed to intersect the geometric center of the thruster nozzle where plasma is ejected from the cavity between the propellant rods. The solar cell located at $\theta = -45^\circ$ was electrically wired so that the light pulse output could be monitored on an oscilloscope. Besides these cells, another cell in a collimating tube was located behind the thruster (see Figure 25) approximately in the same location as the nude ion gauge used in an earlier test (see Figure 2).

Just prior to these installations, it was noted that the surface of the solar cells had become contaminated by the plastic wrapping material used by Spectrolab. In accordance with Spectrolab's recommendations, the cells were carefully cleaned with reagent grade MEK (Methyl Ethyl Ketone).

Because in-situ calibrations could not be carried out, questions arise regarding the effects of exposing the contaminated cells to air and also the long time lapse (about 8 months) between the original calibration (27 February 1976) and the recalibration (10 October 1976). In an effort to answer the question what effect the 8 month lapse would have on the validity of the calibration, one cell (SN 10) was kept as a reference placebo and never used during the present contamination studies. Another unit

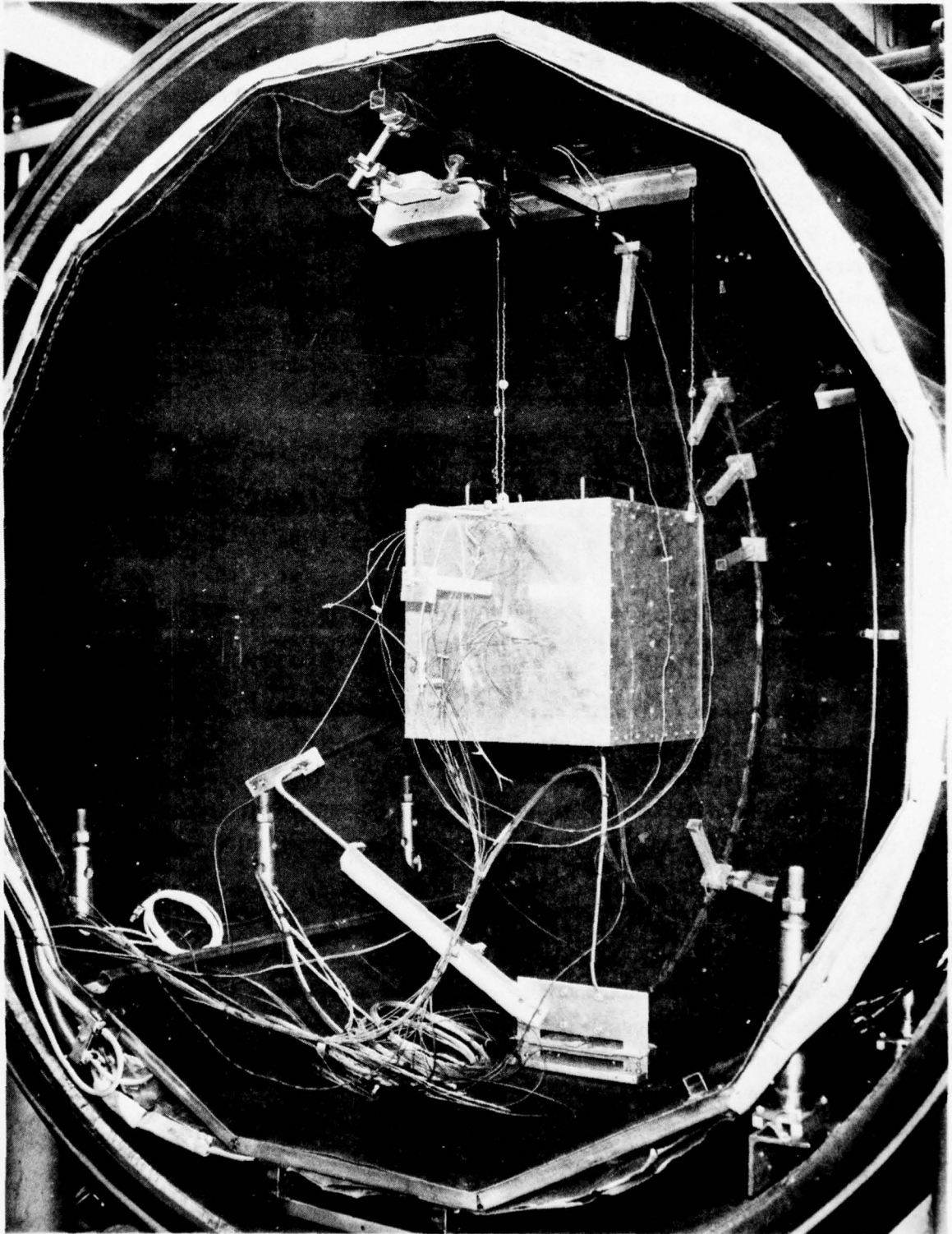


Figure 25. Solar Cell Contamination Test

(SN 9) was located in the collimating support tube behind the thruster. Its entrance port was 2.1 in. (5.3 cm) from the rear cover of the thruster. In essence, this unit would be exposed only to the large temperature excursions of the test facility and the varying pressure changes due to the evacuation cycle of the vacuum test chamber. This cell was used to monitor the effects of such environmental changes only. Of the remaining eight solar cells, four were located at $r = 28$ in. (0.7 m), $\phi = 0^\circ$, $\theta = 15^\circ$, 30° , 45° and 80° , respectively, and subjected to the plume for 8 hours of thruster firing (4072 thruster pulses). The remaining units were positioned at the same locations but exposed for 24 hours of continuous thruster firing (12,212 thruster pulses). Each solar cell test assembly had a thermocouple attached to it so that temperature could be monitored. The temperature variation which each solar cell underwent during the test is presented in Table 9.

TABLE 9
Temperature History of Solar Cells

Solar cell SN	1	2	3	4	5	6	7	8
Angular location, θ , deg.	80	45	30	15	80	45	30	15
Hours of exposure, Hr.	8	8	8	8	24	24	24	24
Temp. at Start, ($^\circ\text{C}$)	-17 $^\circ$	-16 $^\circ$	-16 $^\circ$	-18 $^\circ$	-40 $^\circ$	-38 $^\circ$	-38 $^\circ$	-39 $^\circ$
Temp. at End, ($^\circ\text{C}$)	-103 $^\circ$	-89 $^\circ$	-71 $^\circ$	-51 $^\circ$	-143 $^\circ$	-110 $^\circ$	-83 $^\circ$	58 $^\circ$

Since the solar cell holder intercepted the thruster plume, energy was transferred to it during thruster operation. Similarly, the rake to which the solar cells were attached also intercepted the plume (see Fig. 25). Thus one notes that the cells closest to the geometric centerline of the thruster ($\phi = 0^\circ$, $\theta = 0^\circ$) become warmer than the cells further out. More careful studies of this effect will be discussed in detail in section 3.6.

An attempt was made to keep the time interval after the solar cells were removed from the vacuum chamber until they were recalibrated by Spectrolab at a minimum. The 8 hour contamination test occurred on September 22, 1976 and the 24 hour test from September 23 to September 24, 1976. The recalibration occurred on 1 October 1976. Thus the contaminated cells were exposed from 7 to 9 days to air before being recalibrated by Spectrolab.

Figures 26, 27, and 28 present the A MO voltage-current calibration curves as supplied by Spectrolab for cells 5, 7 and 9, respectively. While such curves were supplied for cells 1 through 10, the ones presented are typical. These calibrations were performed by Spectrolab on their LAPSS (Large Area Pulsed Simulator System). According to Mr. Moffett [25] of Spectrolab, the calibrations are accurate to within 2%. Changes in the short circuit current are generally due to contamination effects. The short circuit current and the open circuit voltage of the ten cells are presented in Table 10.

TABLE 10
Solar Cell Short Circuit Current and Open Circuit Voltage

Solar Cell No.	Location (θ , Deg)	Initial Short Circuit Current (ma)	Initial Open Circuit (Volts)	Final Short Circuit Current (ma)	Final Open Current Voltage (Volts)
1	80	148	0.565	147.6	0.560
2	45	145	0.564	143.8	0.560
3	30	147	0.565	146.4	0.564
4	15	145.2	0.564	144.4	0.562
5	80	145	0.564	144.8	0.563
6	45	145	0.560	144.4	0.562
7	30	145	0.565	143.8	0.561
8	15	145.4	0.567	143.8	0.566
9	hidden	144	0.562	144.4	0.563
10	placebo	148	0.562	148	0.560

Two sets of calculations can be made from the calibration data. One entails evaluating the ratio of the final to initial short circuit current, the other the ratio of the 24 hour short circuit value to the 8 hour short circuit values. The result of these calculations are presented in Table 11.

TABLE 11
Short Circuit Current Ratio

Cell location θ (degrees)	Short Circuit Current Ratio			
	8 hours (I_8/I_0)	24 hours (I_{24}/I_0)	24 hour/8 hour I_{24}/I_8 I_8/I_0	
80°	0.997	0.999	0.981	-
45°	0.992	0.996	1.004	-
30°	0.996	0.992	0.982	-
15°	0.994	0.989	0.996	-
Vacuum Placebo	-	1.003	-	-
Air Placebo	-	-	-	1.000

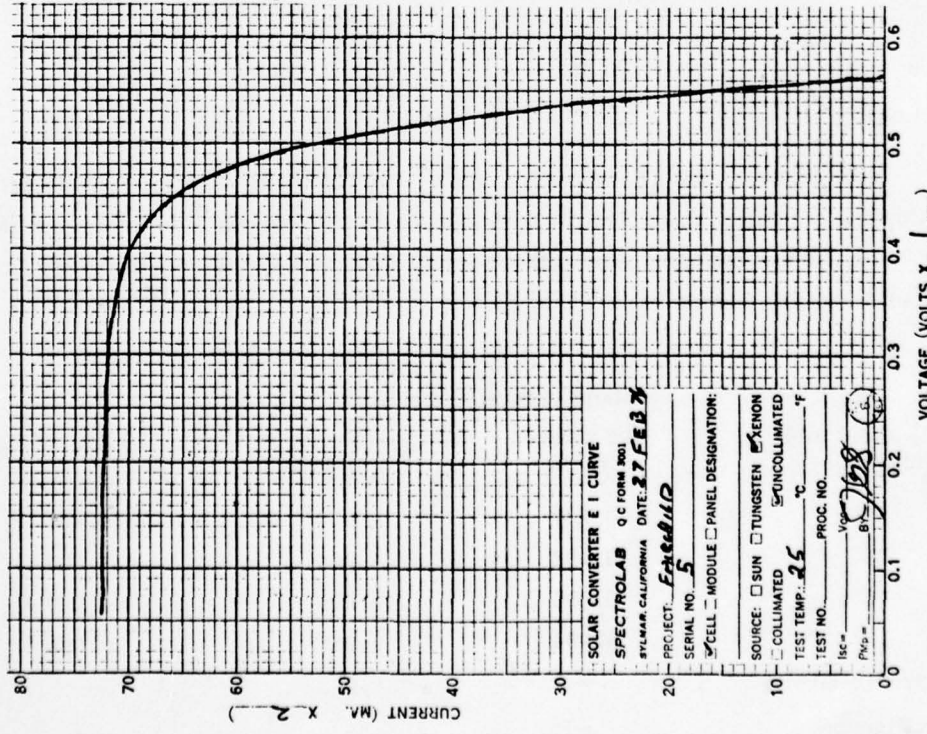
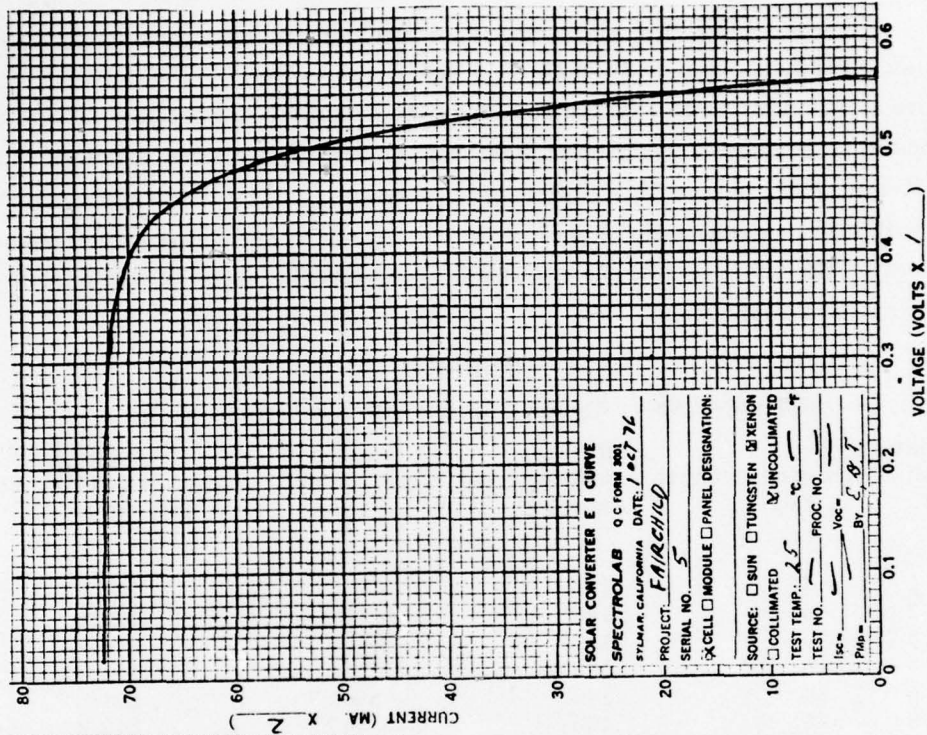


Figure 26. Solar Cell SN 5 Calibration

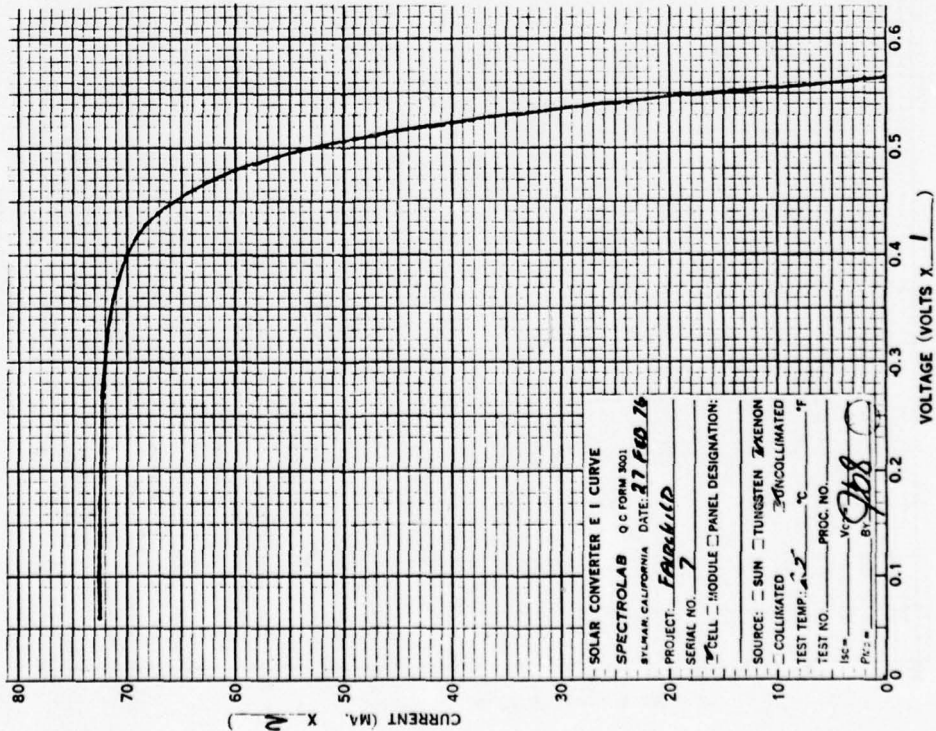
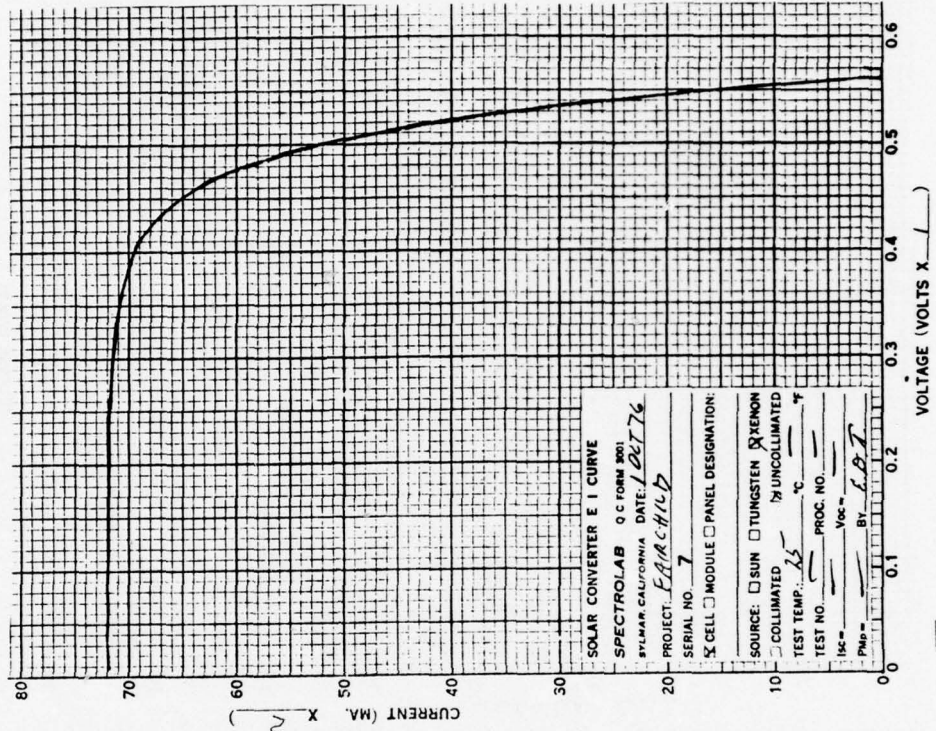


Figure 27. Solar Cell SN 7 Calibrations

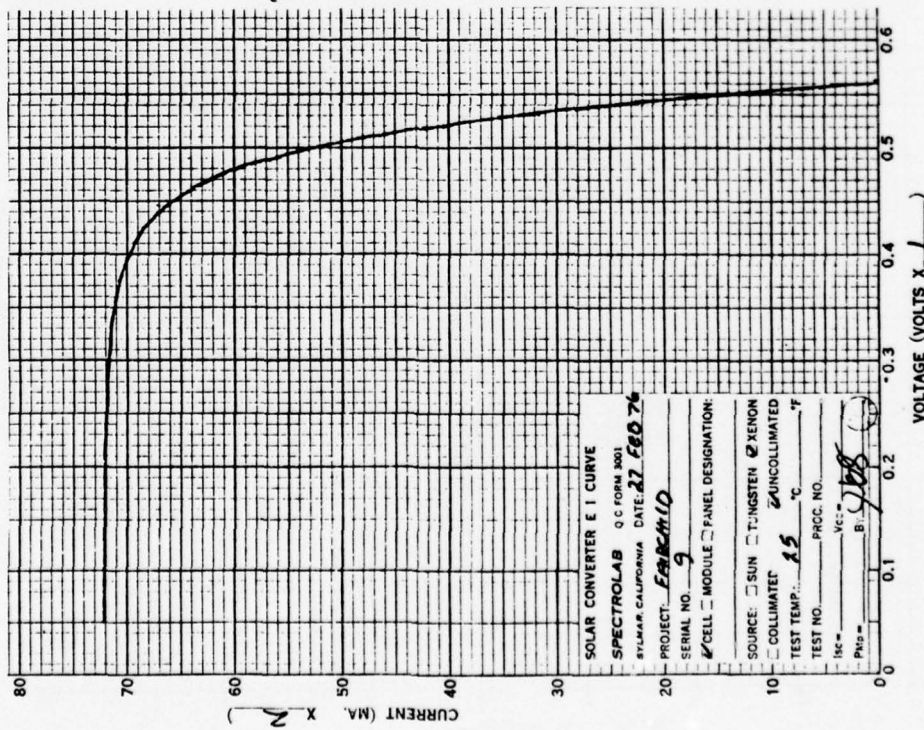
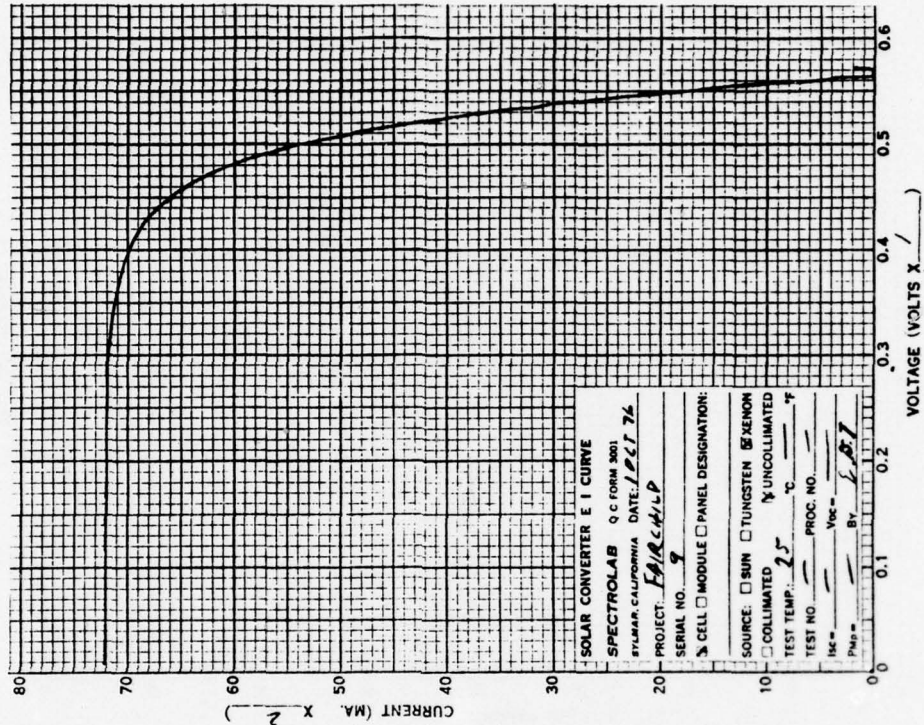


Figure 28. Solar Cell SN 9 Calibrations

All of the values presented in Table 11 fall within the 2% accuracy of the calibration. Therefore any minor differences or apparent trends could easily be due to the calibration. The 8 hour and 24 hour testing times were selected in order to be able to make a direct comparison³ with the results obtained with the 1.5 meter ion thruster. In the latter study it was found that the short circuit current dropped to roughly one quarter of its initial value after a 24 hour exposure to the plume. By comparison, the present solar cell contamination studies with the millipound thrust level pulsed plasma thruster have not shown any changes that could be directly attributed to plume effects. The results presented should not be interpreted that no adverse effects will ever be experienced when using a pulsed plasma thruster, but only that for the test durations and cell locations examined as well as with the ex-situ calibration technique used no changes could be noted. The test results presented suggest that longer duration tests should be carried out and if possible, in-situ A MO calibrations should be performed in order to detect under what conditions, if any, changes in solar cell characteristics will be noted.

The pulsed plasma thruster ejects mass as a puff over a time of the order of a few tens of microseconds. Studies with the Langmuir probe (see Fig. 23) shows this to be the case. Independently, one can show that the duration of the light pulse due to thruster firing is also of the same time duration or less than that measured by the Langmuir probe. During this study a photocell was used to obtain the duration of the light pulse. A photocell was directed at the exhaust plane of the thruster and the current across a $1\frac{1}{2}$ ohm load resistor was monitored on an oscilloscope. The thruster discharge current of one of the four thruster capacitors was also displayed on the oscilloscope. Figures 29 and 30 show two typical oscilloscope traces. The light pulse on the lower trace is seen to be of the nature of a square wave with a maximum duration of about 30 microseconds. The discharge current on the upper trace is seen to be about 27 microseconds in duration. The order-of-magnitude of the duration of the presence of the plume as measured by the Langmuir probe and the photocell are consistent with the duration of the thrusters electrical discharge current which produced and accelerated the mass within the plume. These all reveal a time duration of a few tens of microseconds showing that the thruster indeed ejects puffs of mass of extremely short duration.

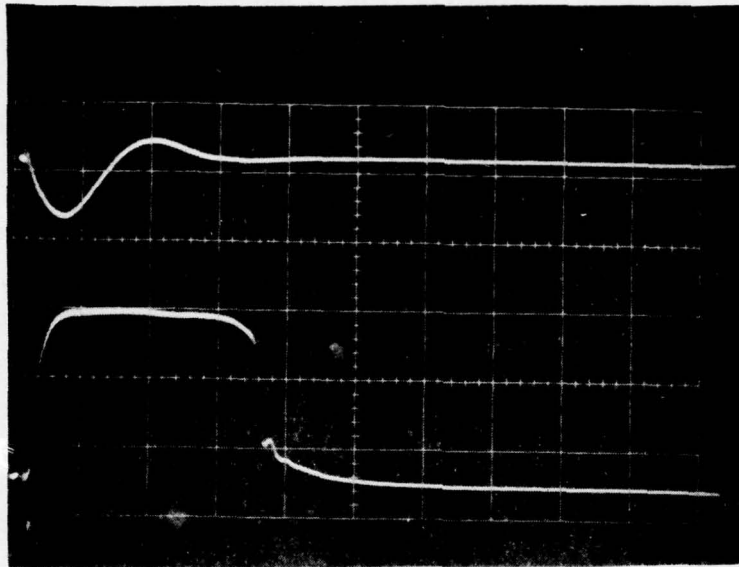


Figure 29. Discharge Current and Light Pulse
 Upper Trace: Discharge Current, Sweepspeed 10 Micro Sec/Cm
 Lower Trace: Light Pulse, Sweepspeed 10 Micro Sec/Cm

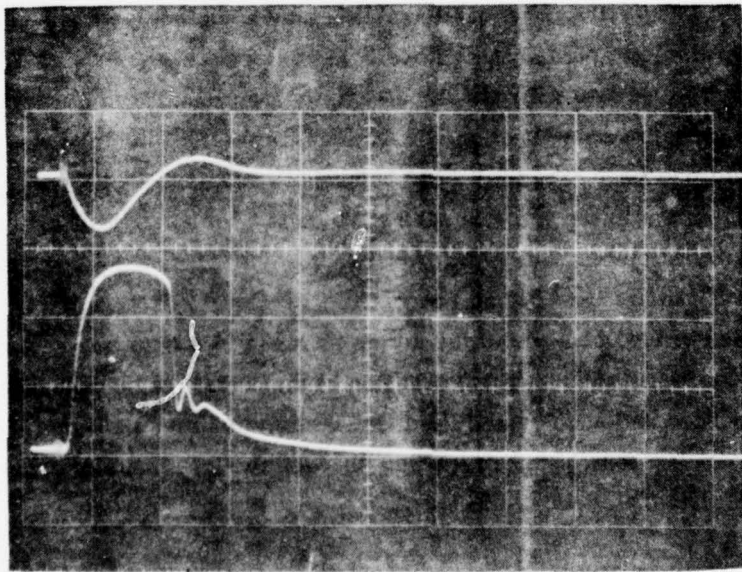


Figure 30. Discharge Current and Shorter Light Pulse
 Upper Trace: Discharge Current, 10 Micro Sec/Cm
 Lower Trace: Light Pulse, 10 Micro Sec/Cm

3.6 Thermal Control Contamination Studies

Two fundamental approaches of realizing spacecraft temperature control are by active and by passive means. Passive control is achieved by utilizing material and geometry as the basic parameters. A contamination study would be primarily concerned with passive means of spacecraft control. Ref. [26] classifies thermal control material into four general categories.

- Solar Reflector - Surface which reflects the incident solar energy while emitting infrared energy, low α_s high emittance ϵ , low α_s/ϵ
- Solar Absorber - Surface which absorbs solar energy while emitting only a small percentage of the infrared energy, high α_s low ϵ , high $\alpha_s/\epsilon < 1$
- Flat Reflector - Surface which reflects the energy incident on it throughout the spectral range from ultraviolet to far infrared, low α_s and ϵ , $\alpha_s/\epsilon = 1$
- Flat Absorber - Surface which absorbs the energy incident on it throughout the spectral range from ultraviolet to far infrared, high α_s and ϵ , $\alpha_s/\epsilon = 1$

It is seen that the solar absorptivity α_s and emissivity ϵ are the principal parameters of passive temperature control. Some representative material used for thermal control of satellites include the following:

Cat-a-lac black paint	(Amine cured epoxy)
3M 401-C10 Velvet black paint	(Polyester)
PV 100 white paint	(Silicone-Alkyd Resin;TiO ₂ pigment)
Z 93 white paint	(Potassium Silicate + ZnO)
S 13G white paint	(Methyl Silicone + ZnO)
Aluminized Kaptan 1 mil or 2 mil thick	
a) Kaptan facing space or	
b) Aluminum facing space	
Aluminized Teflon 1/2, 1, 2, or 5 mil thick	
Silvered Teflon 2, 5 mil thick	
Quartz and 2nd surface vapor deposited Aluminum	
Corning 0211 Microsheet with 2nd surface vapor deposited Aluminum	
Polished 6061T6 Aluminum	
Gold Plating on Aluminum	

Perhaps another general classification that can be made is with respect to the location of thermal control surfaces. One finds the use of thermal control on either the exterior surface of the satellite or on surfaces located exterior to the satellite payload. In the latter case one is generally concerned with the underside of a solar cell panel and also the cover plate region over the solar cell.

These passive temperature control surfaces may, dependent upon the mission, be subjected to a temperature ranging anywhere from -250°F up to +200°F in extreme cases and more typically from -150°F up to +100°F.

The above general considerations reveal the large number of parameters that a general contamination study of thermal control surfaces could embrace.

Because of the importance of the basic parameters solar absorptance (α) and emissivity (ϵ), considerable effort has gone into the development of instrumentation which can accurately determine these parameters in the solar spectral range of wavelengths. The calibrating instruments most commonly used include: Gier-Dunkle Reflectometer or a Lyons Reflectometer for emissivity measurements and a Beckman DK-2a Spectrophotometer for absorptivity measurements.

During this program it was concluded that because of the unavailability of these latter instruments, it would not be possible to carry out in-situ assessments of plume contamination with these instruments. However, an analytic study was carried out to determine the feasibility of performing tests and in-situ calibrations for establishing relative changes in the emissivity and absorptivity of thermal control surfaces when exposed to the exhaust plume. The analysis is presented below.

3.6.1 Emissivity Changes by an In-Situ Calorimetric Technique: If in the evacuated vacuum chamber one can neglect *heat conduction through the test plate supports, heater wires and thermocouple wires, the radiation heat loss under steady state condition from the test plate will quite generally be given by

$$q = AF_A F_\epsilon \sigma (T_h^4 - T_c^4)$$

where A is the test plate area, σ the Stefan-Boltzman constant (0.1714×10^{-8} Btu/ft² hr R⁴), T_h and T_c the absolute temperature of the test plate and cold sink, respectively. F_A is the geometrical or shape factor of radiation heat transfer and is commonly referred to as the area factor. F_A can in some cases be a complicated

* As will be shown, this assumption has to be carefully evaluated in order to be satisfied.

expression but is a constant for a fixed geometric arrangement and geometric shapes of the test plate and cold sink, respectively. F_{ϵ} is known as the emissivity factor and takes into account that both bodies are not perfectly black and that either body may have a corresponding emissivity, reflectivity and transmittivity. In our testing, F_{ϵ} could change due to surface contamination of the test plate being exposed to the thruster plume. This latter emissivity factor not only depends upon the geometric configuration and relative position of the test plate and heat sink, but also depends upon their respective emissivities.

Since a typical test plate area ($\sim 2 \text{ in.}^2$) is negligibly small compared to the surrounding vacuum chamber wall area, it would appear one could simply use $F_{\epsilon} = \epsilon_h$. However, in an experimental study with the thruster, the test plate will always be viewing the roughly $15\frac{1}{2} \times 15\frac{1}{2}$ inch cubical thruster enclosure from a radius of about 27 inches. To assure that the test plate will always be viewing a cold black body during calibration, the test plate would have to be rotated from the test location to a location $\phi = 90^\circ$ off the thrust axis into a position which is parallel and behind a square surface which is painted black and kept at the cold wall temperature. This latter plate would be located between the thruster and the test sample. In this calibrating position the test surface of the test sample and its edges would only be viewing black surfaces which are at the cold wall temperature.

For this calibrating arrangement $F_{\epsilon} \approx \epsilon_h \epsilon_c$

$$\text{Hence, } q = \sigma A F_A \epsilon_h \epsilon_c (T_h^4 - T_c^4)$$

Two in-situ experiments are possible to determine the change in emissivity due to plume contamination: 1) Calibrating at constant power input to the sample plate (i. e., variable temperature), 2) Calibrating at constant sample plate temperature (i. e., variable power input). The former would simulate having to dissipate a fixed power on a spacecraft, the latter would simulate maintaining a constant temperature environment.

Case 1: Constant Power Experiment: In this case, the power P into the sample plate will equal the power P radiated before and after exposure to the plume.

Since the geometric factor F_A and area A will not change,

$$\epsilon_{h_o} \epsilon_{c_o} (T_{h_o}^4 - T_{c_o}^4) = \epsilon_{h_f} \epsilon_{c_f} (T_{h_f}^4 - T_{c_f}^4)$$

Since the emissivity of the vacuum chamber wall is not expected to vary, one obtains the relation

$$\frac{\epsilon_{h_f}}{\epsilon_{h_o}} = \frac{T_{h_o}^4 - T_{c_o}^4}{T_{h_f}^4 - T_{c_f}^4}$$

where subscripts o and f denote before and after exposure to the plume; respectively. The ratio of the emissivity can thus be evaluated by a measurement of the test sample and sink temperatures under equilibrium conditions, respectively. A constant heater power would be required before and after exposure to the plume.

Case 2: Constant Temperature: In this case it will be necessary to vary the input power P to the test sample in order to maintain a constant test sample temperature T_h i.e. $T_{h_o} = T_{h_f}$

Then when $\epsilon_{c_o} = \epsilon_{c_f}$:

$$\frac{P}{\sigma A F_A F_E} + T_c^4 = T_h^4 = \text{constant}$$

or,

$$\frac{\epsilon_{h_f}}{\epsilon_{h_o}} = \frac{P_f/P_o}{1 + T_{c_o}^4 - T_{c_f}^4} \frac{T_{h_o}^4 - T_{c_o}^4}{T_{h_o}^4 - T_{c_o}^4}$$

When $T_{c_o} = T_{c_f}$ (NOTE $T_{h_o} = T_{h_f}$)

$$\frac{\epsilon_{h_f}}{\epsilon_{h_o}} = \frac{P_f}{P_o} \quad | \quad T = \text{const.}$$

An alternate form for $\epsilon_{h_f}/\epsilon_{h_o}$ is:

$$\frac{\epsilon_{h_f}}{\epsilon_{h_o}} = \frac{P_f}{P_o} \left[1 - \frac{T_{c_o}^4 - T_{c_f}^4}{T_{h_f}^4 - T_{c_f}^4} \right]$$

The case of parallel squares or discs connected by nonconducting but reradiating black walls can then be used as a reasonably good approximation for a typical experimental set-up. Thus [27] $F_\epsilon \approx \epsilon_h \epsilon_c$

In a typical experiment the nonconducting walls are made up on three sides by the vacuum with the black cold vacuum chamber walls in the background. The L-shaped plate also has $F_\epsilon \sim \epsilon_1 \epsilon_2$. Such a calibrating arrangement precludes the sample plate from viewing the thruster body during calibrations.

3.6.2 Absorptance Measurements: Hall [2] presented a technique for in-situ absorptance measurements which could possibly be used for the pulsed plasma thruster. A (Xenon) light source could be used to irradiate a test sample. Supplementary electric heating of the sample would also be required to obtain any desired test sample temperature. If one can assume negligible heat losses through the suspension system and the instrumentation and heater leads, then from a power balance one has at equilibrium:

$$\alpha G_L A_s + P_o + \sigma A_s F_A F_\epsilon F_w^4 = \sigma A_s F_A F_\epsilon T_s^4$$

where

α = absorptance to the source being used

G_L = source (lamp) irradiance (watts/cm²)

A_s = area of test sample

P_o = electric power input to get to a temperature T_s

T_w = temperature of surrounding chamber

Another expression is obtained by turning the light source off and varying the electric power input P_f so that the test sample is restored to the same temperature T_s . For this second test condition

$$P_f + \sigma A_s F_A F \epsilon T_w^4 = \sigma A_s F_A F \epsilon T_s^4$$

Upon subtracting the second relation from the first, one can find the relation

$$\alpha = \frac{P_f - P_o}{G_L A_s}$$

This two step calibration procedure can be carried out before and after exposing the sample to the thruster's plume. One then obtains the change in absorptivity of the sample due to the source as the ratio

$$\frac{\alpha_a}{\alpha_b} = \frac{(P_f^1 - P_o^1)_a}{(P_f - P_o)_b} \frac{G_{L_a}}{G_{L_b}}$$

The respective power inputs P to the sample are those required to maintain the test sample at constant temperature. If the lamp irradiance G_{L_a}/G_{L_b} can be kept constant, it will not be necessary to know its value and the relative change in absorptivity is then

$$\frac{\alpha_a}{\alpha_b} = \frac{(P_f^1 - P_o^1)_a}{(P_f - P_o)_b}$$

To check constancy of lamp irradiance before and after exposure to the plume one could monitor the temperature of a protected reference test sample irradiated by the light source. The input power to the light source could be appropriately modified to assure constancy of temperature of this reference test sample.

The treatment thus far has assumed heat conduction from the test plate through its support and also through the heater and instrumentation leads can be neglected. This assumption will now be examined.

The thermal conductivity along these conducting elements can be calculated from the relation

$$q = KA \Delta T / \Delta \ell$$

where K = thermal conductivity, A cross sectional area, $\Delta T / \Delta \ell$ is the temperature gradient along the respective conductor. If the respective conductors originate from some location at temperature T_0 and terminate at the test plate a distance $\Delta \ell$ from the source, the total conduction loss will be

$$q_t = \Sigma KA \left(\frac{\Delta T}{\Delta \ell} \right)$$

This expression can now be evaluated for the various conductors.

- 1) Heater element feed wires: suppose one uses a pair of #28 AWG copper leads to heat the test plate.

$$K_{\text{copper}} \approx 196 \text{ to } 226 \frac{\text{BTU-ft}}{\text{ft}^2 \text{ hr } ^\circ\text{F}} \quad (\text{using a value } 200)$$

$$A_{\#28} = 8.659 \times 10^{-7} \text{ ft}^2$$

$$\text{or } q \approx 1.732 \times 10^{-4} \frac{\Delta T}{\Delta \ell} \frac{\text{BTU-ft}}{\text{hr } ^\circ\text{F}} \quad \text{per lead}$$

$$\text{or } 3.464 \times 10^{-4} \frac{\Delta T}{\Delta L} \frac{\text{BTU-ft}}{\text{hr } ^\circ\text{F}}$$

- 2) Thermocouple leads #28 copper - Constantan thermocouple leads are available in the LN₂ cooled test facility. The conduction along these will be

$$K_{\text{Constantan}} \approx 13.2 \frac{\text{BTU-ft}}{\text{ft}^2 \text{ hr } ^\circ\text{F}}$$

For the #28 copper-constantan pair,

$$q \approx 3.689 \times 10^{-4} \frac{\Delta T}{\Delta L} \frac{\text{BTU-ft}}{\text{hr } ^\circ\text{F}}$$

- 3) Support rod: If a 0.25 in. diameter Teflon rod is used to support the test plate

$$K_{\text{Teflon}} \approx 0.14 \frac{\text{BTU-ft}}{\text{hr } ^\circ\text{F}}$$

Hence,

$$q \sim 4.77 \times 10^{-6} \frac{\Delta T}{\Delta L} \frac{\text{BTU-ft}}{\text{hr } ^\circ\text{F}}$$

If all of these items are of the same length and experience the same temperature gradient, the conductive heat loss would be

$$q \approx 7.2 \times 10^{-4} \frac{\Delta T}{\Delta L} \frac{\text{BTU-ft}}{\text{hr } ^\circ\text{F}}$$

$$\text{or } \approx 2.11 \times 10^{-4} \frac{\Delta T}{\Delta L} \frac{\text{Watts-ft}}{^\circ\text{F}}$$

It can be seen that the magnitude of the temperature gradient between the test sample and a general support should be kept as small as possible. If no precautions are taken, the test sample may be at a typical spacecraft temperature (say 20°C) and the general support could be at the LN wall temperature (~ -180°C). If this difference occurs over a distance of 2 inches (~ 5 cm), the conductive loss would be equivalent to about 0.75 watt! Such a loss is not negligible as can be shown. For example, suppose the test sample area is 4 in.², is at 20°C, is black (ε ~ 0.95) and loses heat only by radiation to the cold wall of the chamber. The approximate

heat input required to maintain a constant temperature of 20°C will be about 1.0 watts. Thus it is seen that it will be imperative to virtually eliminate the temperature gradient along the leads and support. Such a gradient can be virtually eliminated if the support and instrumentation leads are attached to a backing plate which is heated and controlled to be essentially at the test sample temperature at all times. This backing plate would be behind the testing plate. Such an approach was used by Sadler [28] et al., in their emissiometer.

The analysis presented above defines the parameters and test conditions for performing "calorimetric-type" in-situ calibrations. After such in-situ tests are carried out, one could briefly expose the test sample to air and then restore the original test conditions for the purpose of checking the effect of exposing the "contaminated" test sample to air.

3.6.3 Beam Energy Distribution Study: Besides contaminating a thermal control surface by changing its emissivity or absorptivity, it is also important to know how much heat would be transferred to such a surface if it were located in the plume. Studies with the QCM and glass capture cups have revealed that their temperature was increased when they were located within the plume. Thus an independent diagnostic technique that can be used to define the plume and its effect on a spacecraft surface is to locate small calorimeters in the beam. Since, ideally, a small surface located in the plume brings the incoming flow of plume mass to rest, the temperature rise of the surface is related directly to the total energy (i. e. kinetic plus thermal) of the plume. Thus one can think of the resultant temperature distribution of a number of small surfaces located in the plume as being representative of the energy distribution of the plume. Since a complicated flow pattern does take place around the surface, not all of the incoming energy is actually transferred to the disc. Thus the simple approach of distributing a number of small surfaces in the plume should be considered to provide only a first-order indication of the plumes energy distribution. Nevertheless a knowledge of such a distribution is relevant to the operation of thermal control surfaces.

A number of 1 inch (2.54 cm) diameter "calorimeter discs" were located on the movable rake and the plume was surveyed. The "calorimeters" were copper discs mounted on a Nylon screw in order to reduce conductive heat transfer from

the disc to the rake. A shiny radiation shield was located behind the polished back face of the disc to reduce heat loss by radiation. This shield was thermally isolated from the disc by a fiberglass washer. A thermocouple was used to record the temperature of the copper disc facing the plume. Figure 31 shows one of the complete assemblies. Fourteen of these "calorimeters" were mounted on the rake at following location θ : 80° , 55° , 40° , 30° , 20° , 10° , 5° , 0° , -10° , -20° , -30° , -40° , -50° and -75° .

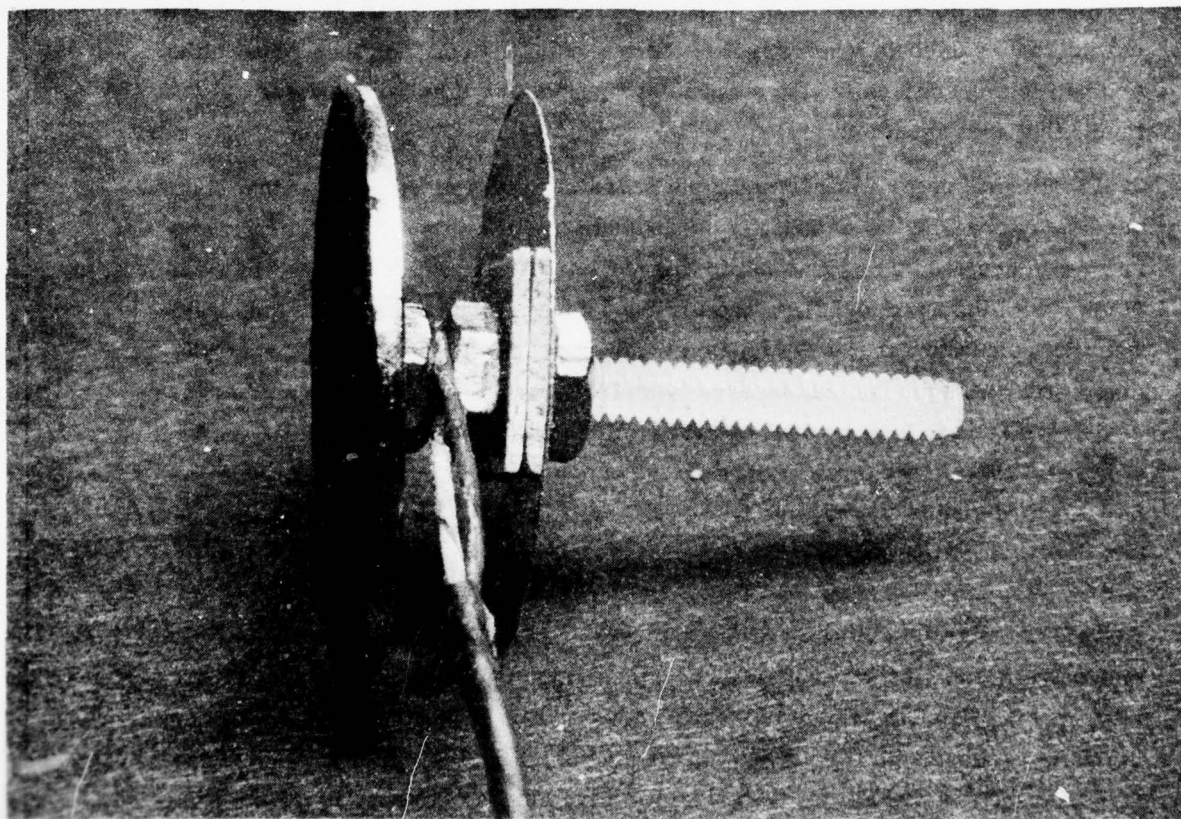


Figure 31. Calorimetric Disc

A typical test was to monitor the discs temperature while the thruster was firing at a constant pulse rate. The temperatures of the discs were recorded once thermal equilibrium was reached. Typically, thermal equilibrium was reached in about 3 hours of exposure to the plume. The rake was then moved to some new angular location ϕ and the procedure was repeated to obtain a new set of equilibrium data. This diagnostic technique allowed a large amount of data to be generated within a relatively short period of testing time. Data was generated to provide following information:

- a) The temperature distribution as a function θ for several values of angular position- ϕ (Fig. 32).
- b) A comparison of the temperature distribution for equal values of ϕ to either side of the geometric center line of the nozzle (Fig. 33).
- c) The temperature distribution in the plume $\phi = 0$ for two different distances in the flow direction (Fig. 34).
- d) A comparison of the temperature distribution due to the normal exhaust cone used during this program with the distribution obtained by adding a box extension to the exhaust cone (Fig. 35).
- e) A test was also performed to determine the temperature gradient between the calorimetric disc and the aluminum rake to which the calorimetric assembly was attached to (Fig. 36).

Figure 32 presents the temperature distribution obtained by swinging the rake through one quarter of a hemisphere. The angles swept out are from $\phi = 0^\circ$ to $\phi = -90^\circ$. This test data reveals that the major part of the plumes energy is within a cone angle of about 30° . This result obtained by the calorimetric technique agrees with the results obtained by the Langmuir probe and the QCM. It is believed that the boundaries of the plumes energy distribution would have been more sharply defined if collimating tubes had been used in conjunction with the calorimetric discs.

Figure 33 compares the thermal data at equal angular locations $\pm\phi$ about the geometric center of the nozzle. The data presented shows that the energy in the plume is not symmetric about the geometric center of the thruster nozzle but tilted toward the cathode (i.e. $\theta = 7^\circ$) and slightly toward positive angles ϕ . This unexpected result

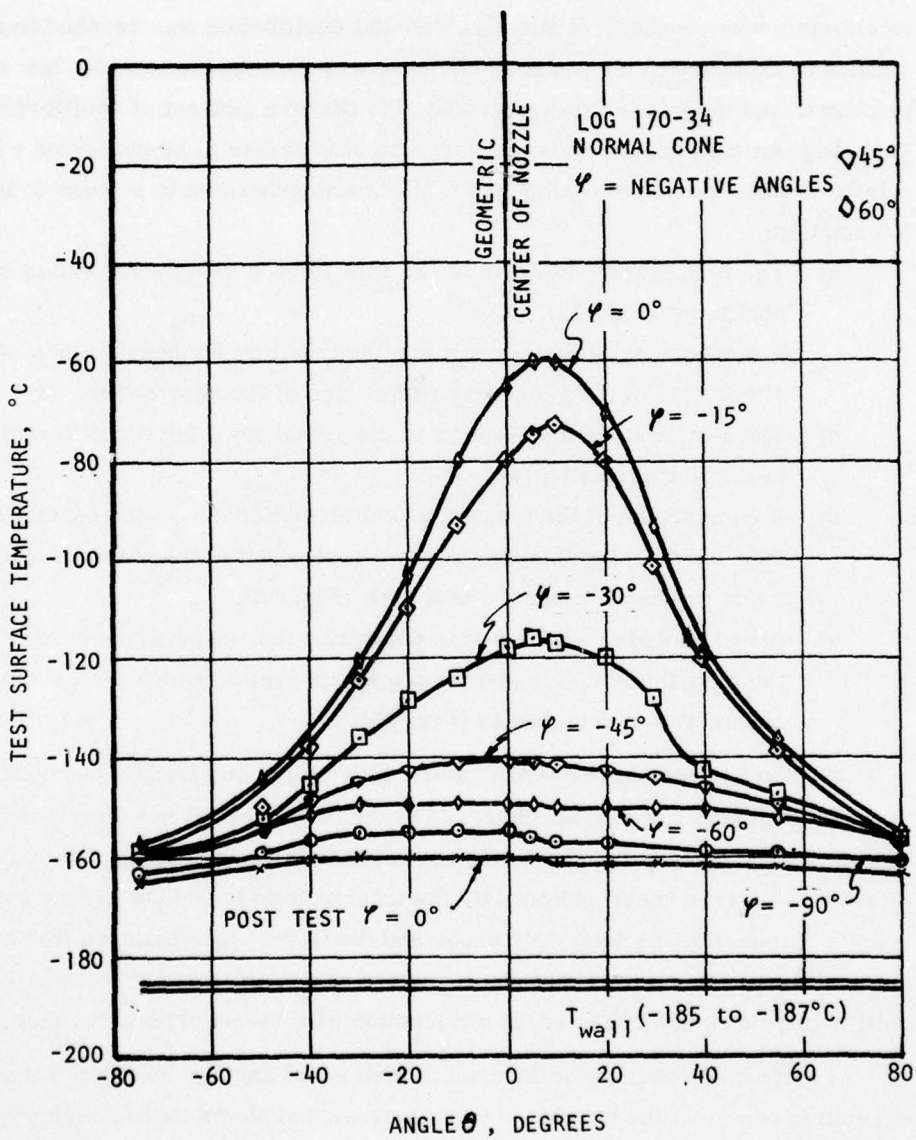


Figure 32. Temperature Variation for Angles θ and φ

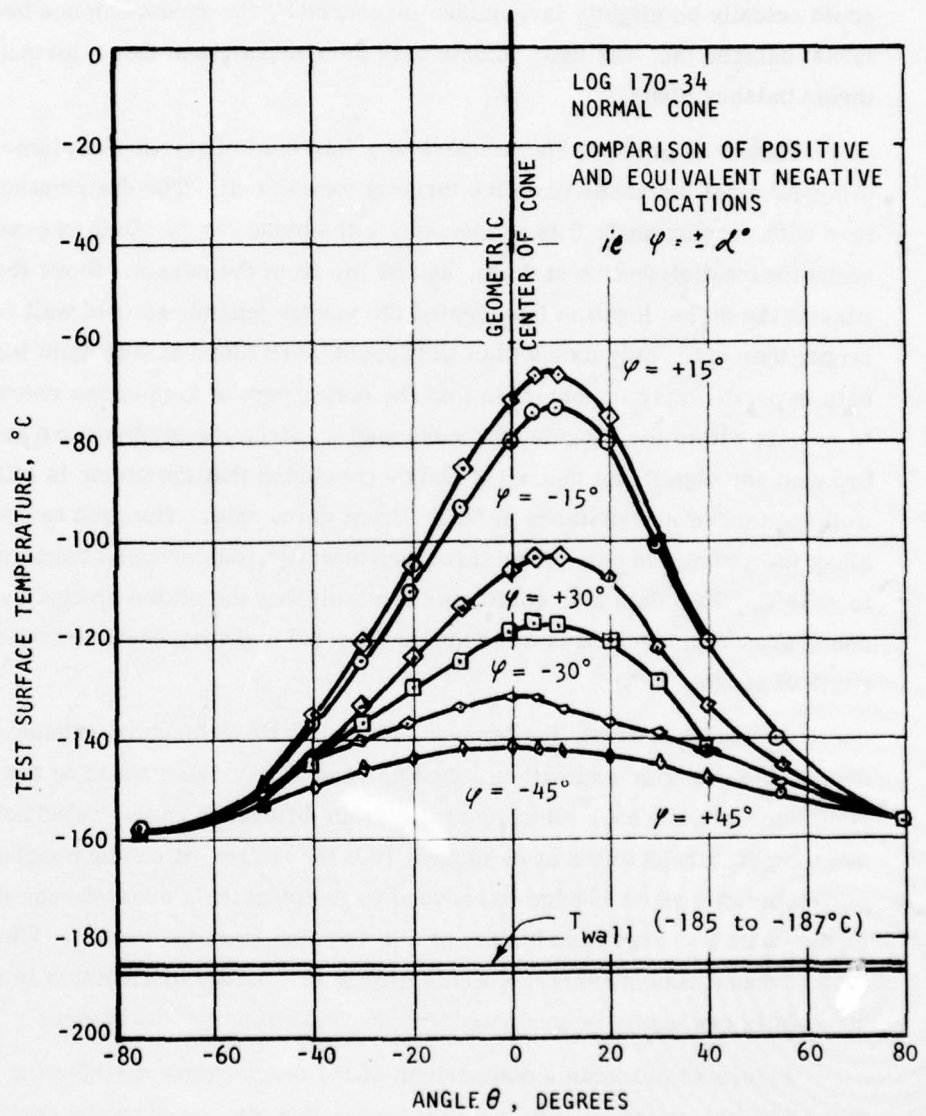


Figure 33. Temperature Variation Comparison

suggests that the amplitude of the impulse bit being generated by the thruster could actually be slightly larger than measured by the thrust balance because the thrust balance that was used detects only the component of force normal to the thrust balance plane.

Figure 34 presents the temperature distribution across the plume at two different axial distances from the thruster nozzle exit. The distribution of temperature with varying angle θ is presented for the plane $\phi = 0$. Data is presented of the temperature distribution at 28 in. and 56 in. from the nozzle. Since the circular rake at the 56 in. location intercepted the vacuum chambers cold wall for angles larger than $\pm 28^\circ$, only data within $\pm 28^\circ$ could be obtained at that axial location. The data is particularly important in that the major part of the plumes energy is seen to remain within the roughly $\pm 30^\circ$ cone angle. Since the temperature profile did not broaden any significant amount it can be concluded that the plume is still rather well collimated at a distance of 56 in. from the nozzle. The peak temperature along the geometric axis of the thruster, however, has dropped from roughly -60°C to -114°C . This data also confirms the result that the plume ejected by the milli-pound peaked plasma thruster is highly directed and very energetic within a cone angle of roughly 30° .

Figure 35 presents the temperature data with the normal exhaust cone used during this program and with a 2 inch horizontal extension added to the outer perimeter of that cone. Since essentially no difference can be noted between the two temperature profiles at 28 inches from the nozzle, it can be concluded that this particular geometric change introduced to the thruster's exhaust cone had no effect on the beam's energy distribution at that location from the nozzle. Whether or not other exhaust cone geometries would change the energy distribution in the plume apparently can easily be evaluated by this "calorimetric" technique.

Figure 36 presents a comparison of the temperature distribution noted on the individual calorimeters with the distribution that was noted on the continuous aluminum support tube of the rake. Since the temperature gradient from the disc to the rake at any given angular location θ is never more than about 20°C very little heat transfer is expected to take place from the disc to the rake. The thermal

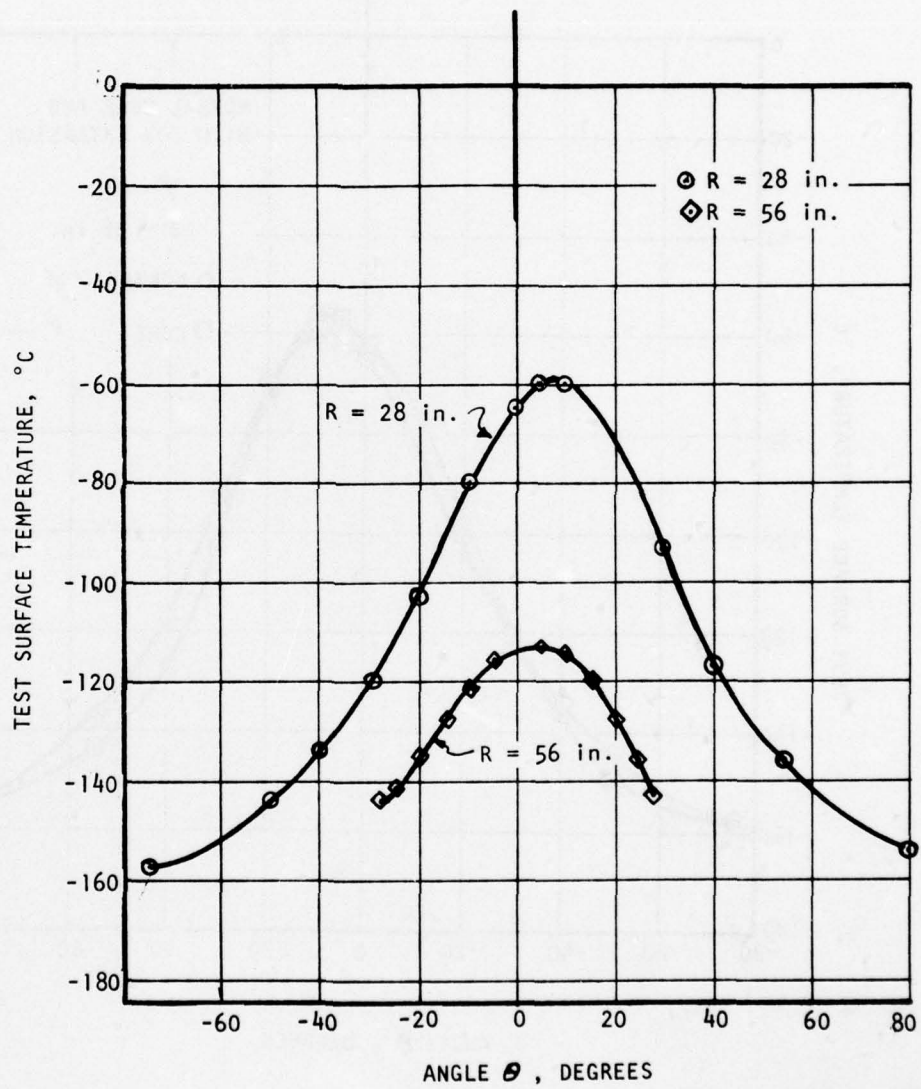


Figure 34. Axial Variation of Temperature

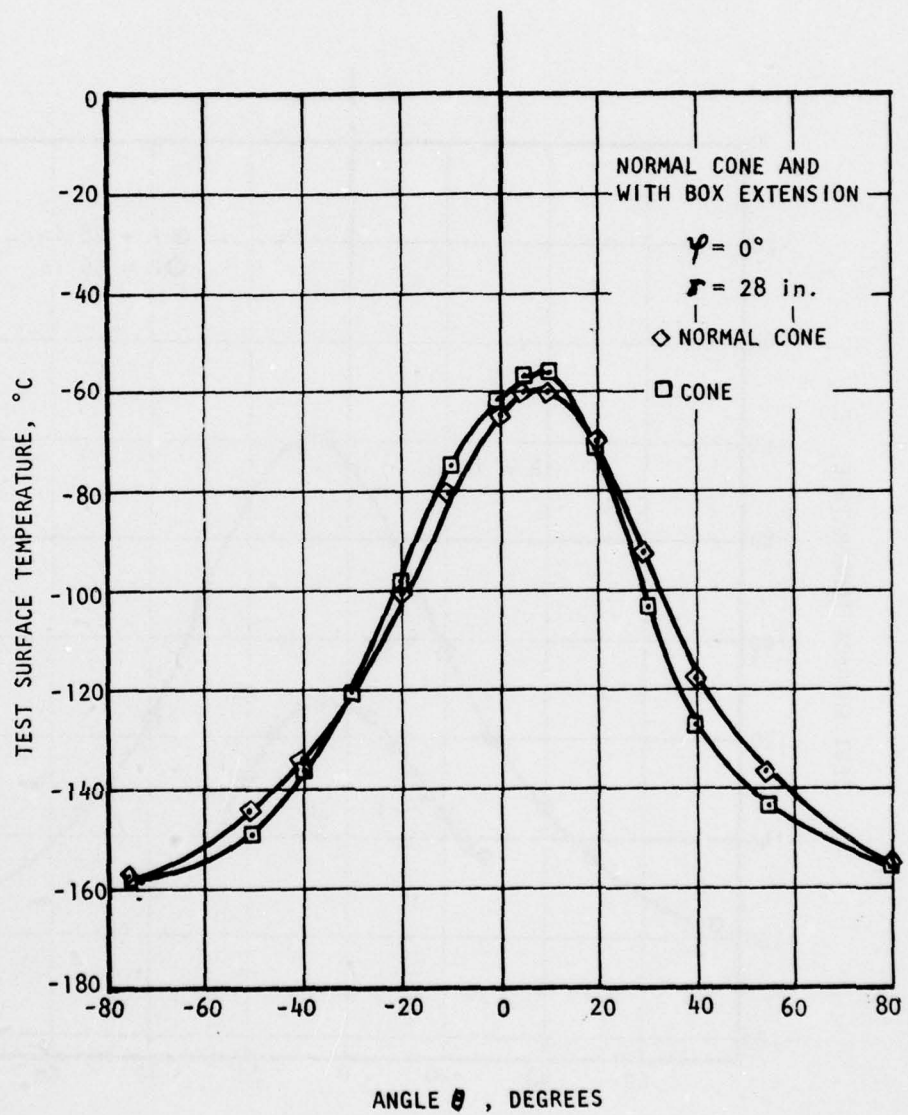


Figure 35. Effect of Cone Geometry

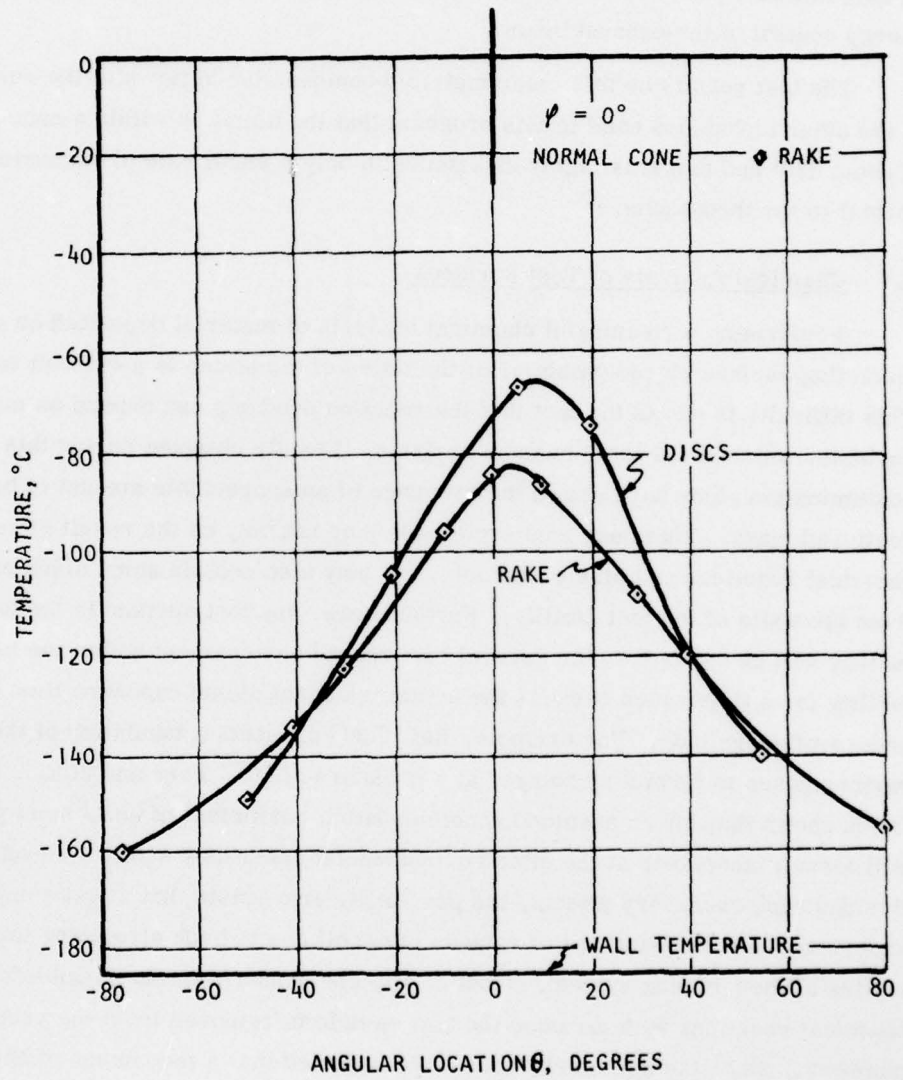


Figure 36. Temperature of Discs and Rake

isolation provided is therefore expected to be adequate for the exploratory study carried out. It is not possible at this time to assess the "capture" coefficient of an uncollimated calorimetric disc in its ability to provide a true measure of the energy content of the exhaust beam.

The test results by this calorimetric technique also agree with the results of the other techniques used in this program that the plume is within a cone angle of about $\pm 30^\circ$ and that it is highly directed with only a small rate of expansion normal to the thrust axis.

3.7 Chemical Analysis of Test Surfaces

Performing a meaningful chemical analysis of material deposited on a collecting surface placed within or at the edges of the plume is a difficult task. This difficulty is due to the fact that the reaction products can depend on many variables which could enter such an analysis. Results obtained during this plume contamination study have shown the presence of an appreciable amount of back scattered mass. This back scattered mass may not only be the result of secondary chemical reactions and plume products, but may also contain some black paint from the walls of the test facility. Furthermore, any test surface in the test facility will be exposed to the general background environment within the test facility for a time which exceeds the actual transient plume exposure time by many orders-of-magnitude. For example, Ref. [20] presents a tabulation of the time for various gases to form a monolayer at a pressure of 10^{-6} Torr and 20°C . The tabulation shows that for an assumed accommodation coefficient of unit, most gases will form a monolayer at the cited environmental conditions within 3 seconds. Besides such secondary effects, the possibility also exists that a test sample could experience minute quantities of vacuum pump oil due to back streaming through the baffles of the pumping system. Most of all, one cannot rule out possible secondary chemical reactions with air once the test sample is removed from the vacuum chamber. Since the same reference cited revealed that a monolayer of Nitrogen forms in about 3×10^{-9} seconds at atmospheric conditions, a technique involving a vacuum or inert gas containment of a test sample until a chemical analysis is carried out would not be feasible. Since a chemical analysis of a "contaminated" specimen would eventually involve exposure to air, it was decided to enclose the test specimen within a collimating system to reduce the effects due to scattered

mass impinging directly on the test sample while testing in the vacuum test facility. Special shipping containers were fabricated to support the test samples in such a manner that it was impossible for any foreign matter (other than air) to contact the samples from the time they are removed from the vacuum chamber until they are analysed.

Early in the program GTE Laboratories* considered carrying out the chemical analysis of the contaminated test samples to be provided by Fairchild Republic. As the plume study progressed and early glass capture cup data became available, it became evident that much less mass was being deposited on test samples than expected. GTE required an absolute minimum of 1 milligram of deposit for an analysis. They desired about 50 milligrams for an optimum analysis. If the glass capture cups were to be used, over 130,000 thruster pulses (11 days of continuous operation) would have been required for a minimum analysis. In order to carry out the optimum analysis involving infrared spectroscopy, elemental analysis, thermal analysis, x-ray diffraction and mission spectroscopy would have required more than 50 days of collection time with the glass capture cups. Rather than increasing the size of the capturing sample, alternate techniques of analysis were sought. GTE was helpful in that they recommended thin film analysis by either ESCA (Electron Spectroscopy for Chemical Analysis) or Fourier Transform - Infra Red Spectroscopy. Digilab* who fabricates such equipment referred us to the Battelle Memorial Institute in Columbus, Ohio.

Dr. R. J. Jakobsen of the Battelle Columbus Laboratories performed a Fourier Transform - Infra Red analysis of test samples sent to him to establish feasibility of this diagnostic technique to analyze test specimens and also to provide the results of such an analysis. This analysis allows one to identify the molecular structure of the contaminant rather than just citing the elements present.

Four 7075-T6 Alclad aluminum test samples were prepared. The aluminum sample represented a likely spacecraft surface. The samples were 0.76 mm thick, 10 mm wide and 45 mm long. The pre-test cleaning procedure used by Fairchild Republic was to polish the surface on a 600 grit wheel followed by a polish with Chromic Oxide #3 to provide a high lustre surface finish. Two of the four samples were kept as clean reference units. The remaining two were located inside a collimating tube at the edge of the plume (i. e. $\theta = 30^\circ, 35^\circ$) as established by the QCM and other diagnostic studies. The temperature of the aluminum capture speci-

*Waltham, Mass.

mens was kept between -120°C to -122°C while being exposed for 12,000 consecutive thruster pulses (i. e. 24 hours of continuous operation). The background cold walls of the test facility was kept at -187°C during the test. After the test was completed the liquid nitrogen was turned off and the facility with the test specimens were brought to room temperature before the vacuum chamber was vented to atmospheric pressure.

The clean and "contaminated" specimens were shipped in the special containers to Battelle. Figure 37 presents the spectra in absorptance units from 3600 to 600 wave numbers (2.78 microns to 16.67 microns). Figure 38 presents the resultant spectra obtained by subtracting various (as indicated) ratio's of the contaminated and uncontaminated spectra.

Dr. Jakobsen provided the following information: Four hundred scans (about 12 minutes) of each sample were signal averaged on the FT-IR instrument and the absorptance spectra are expanded only 4X. This implies that the spectra were relatively easy to obtain, and even smaller amounts of contaminant than the present amounts (due to 12,000 thruster pulses) could be detected. No detailed interpretation with the spectra was attempted because of the presence of contamination on the clean surface as will be discussed. However, two results are instantly evident:

- 1) The uncontaminated (i. e. clean sample) provided by Fairchild Republic is not clean
- 2) The contaminated sample shows the presence of a metallic salt or carboxyl (COO^-) ion

In the spectrum of the uncontaminated sample aliphatic CH bands ($\sim 2930\text{ cm}^{-1}$) and a carboxyl vibration (1745 cm^{-1}) are observed (see Fig. 37). Phllate esters are common contaminants from human beings (i. e. finger prints) or from laboratory air. These bands are not observed in the spectra of the contaminated sample possibly because: 1) this sample has been washed, 2) the contaminant is covered up by the formation of the metal salt, or 3) the metal salt is formed from the ester contaminant.

The strong 1590 cm^{-1} band and the weaker 1440 cm^{-1} band are good indications of the presence of a metal salt (anti-symmetric and symmetric COO^- vibrations) in the spectrum of the contaminated sample.

Other differences exist between the contaminated and uncontaminated sample (especially in the low frequency region extending from 1400 cm^{-1} to 600 cm^{-1}).

*Cambridge, Mass.

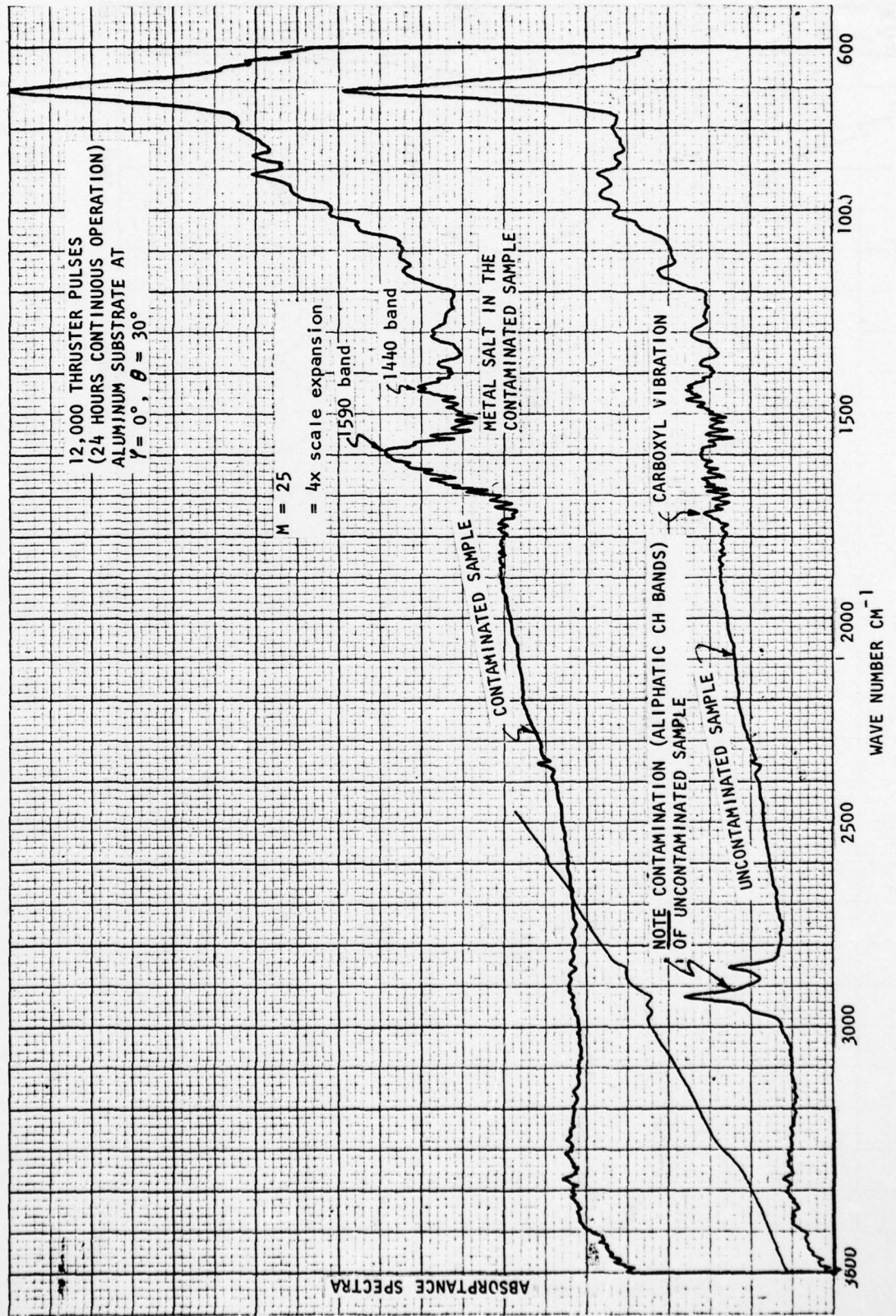


Figure 37. Absorbance Spectra by FR-IR Technique

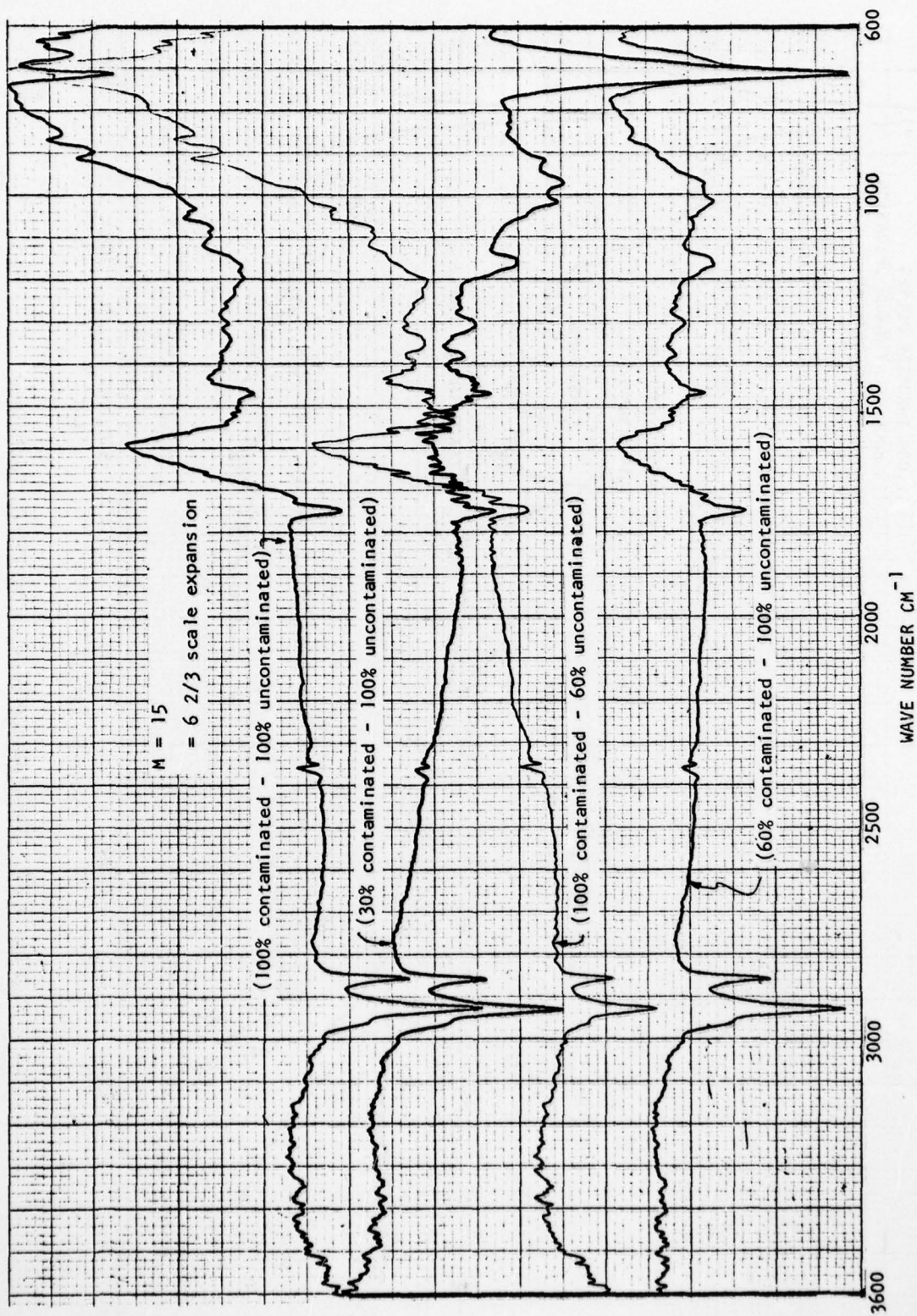


Figure 38. Subtracted Absorbance Spectra by FR-IR Technique

However, without a detailed study, one cannot tell whether:

- a) These differences are also due to the ester of the uncontaminated sample plus the metal salt of the contaminated sample, or
- b) New species

The results of the chemical analysis that was performed reveal that the Fourier Transform - Infra Red analysis can easily be used to study changes in a sample of a spacecraft surface and to identify the molecular structure of the contaminant. Since the uncontaminated sample which was cleaned and polished revealed contamination which the test sample exposed to the plume did not, it is obvious that further refinements in the experimental technique are called for. In particular, the source of oxygen in the contaminated sample must be determined and the FT-IR technique itself should be used to define when a "cleaned" control sample can be considered to be chemically clean before a plume contamination analysis is carried out.

With regard to the presence of oxygen, several sources could account for it:

- 1) Oxygen could have been obtained from the oxide layer in the aluminum test samples reacting with the energetic beam of plasma, 2) it could have been in the Teflon (Dr. Jakobsen mentioned that DuPont uses peroxide as an initiator in the polymerization of Teflon), 3) water vapor could have been trapped on the surface, 4) a secondary oxidation process may have occurred after the "contaminated" test sample was exposed to air. The presence of oxygen allows many competing reactions to occur with CF groups. In any future studies it is recommended that

- a) An analysis of a sample of unused Teflon propellant be made to determine whether or not oxygen can originate from it.
- b) Similarly, the metal electrodes and ceramic Mykroy insulation should be analyzed individually.
- c) Some tests should be carried out with an oxide free capturing sample (i. e. a gold plated surface).
- d) The oxide free capture sample should be heated in the vacuum test facility to about 500°C to 600°C to drive off any organic contaminants before a contamination study is initiated.
- e) A cleaning and handling procedure should be developed with the Fourier Transform - Infra Red diagnostic tool making the judgment on the cleanliness realized.
- f) Study and, if possible, assess the ex-situ technique of analysis with respect to the possible results one might encounter with an in-situ analysis (if such an analysis could ever be performed).

AD-A036 904

FAIRCHILD REPUBLIC CO FARMINGDALE N Y
PULSED PLASMA PLUME STUDIES.(U)
MAR 77 W J GUMAN, M BEGUN

F/G 21/3

UNCLASSIFIED

AFRPL-TR-77-2

F04611-75-C-0037
NL

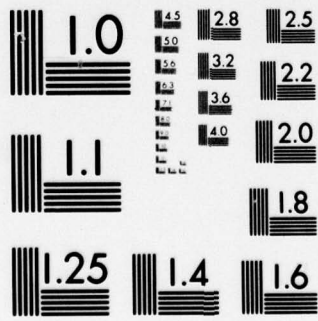
202
AD
A036904



END

DATE
FILMED
4-77

3690



MICROCOPY RESOLUTION TEST CHART
NATIONAL BUREAU OF STANDARDS-1963-A

- g) Establish whether or not different reactions might be occurring in the plume at different distances from the nozzle exit.

It should be evident from the latter list of questions that could be considered in future studies that a comprehensive unambiguous chemical analysis of plume contamination is a program in itself.

Other than the stronger 1590 cm^{-1} (6.29 microns) band and the weaker 1440 cm^{-1} (6.94 microns) band whose origins have not been positively identified, plume contamination of a test surface was not observed over the broad range of wave numbers extending from 3600 cm^{-1} (2.78 microns) to 600 cm^{-1} (16.67 microns). This range of wave numbers covers the range in which it is possible to identify the molecular structure of organic contaminants such as may be generated by the propellant used in the thruster.

4.0 CONCLUSIONS AND RECOMMENDATIONS

The major source of contamination of surfaces placed inside the LN cooled vacuum chamber has been identified to be mainly due to mass being scattered off the walls of the test facility. However, by using collimators and time resolved instrumentation, it became possible to carry out contamination studies within such a facility. It might be desirable to carry out an additional evaluation of a collimator. In particular with respect to its effect of perturbing the local transient flow in the plume and an analysis of the accuracy of the results obtained with a collimator.

By means of a Langmuir probe, calorimetric discs, a collimated QCM and collimated glass capture cups it was found that the transient plume is fairly well collimated and that the outer extremities of the plume are located within $\pm 30^\circ$ to $\pm 40^\circ$ with respect to the geometric center line of the thruster that was studied. Whether or not major changes of the exhaust cone would change this location was not examined.

Time resolved studies of the plume by a Langmuir probe and a photocell has shown the life of the plume at a region in space to be only a few tens of microseconds. This result reveals that a spacecraft surface exposed over a 5 to 7 year period to the plume of a North-South station keeping thruster will actually see an accumulated plume flow time for only about 5 minutes during that mission time.

By means of a collimated QCM and glass capture cups it was noted that like with an ion engine erosive effects of a surface can occur if that surface is located within the outer boundaries ($\pm 30^\circ$ to $\pm 40^\circ$) of the plume.

Calorimetric disc studies have shown the peak value of the energy content of the plume to be a few degrees off the geometric center line of the thruster nozzle. This result suggests that the actual impulse bit amplitude may be slightly larger than the reported one. The thrust vector should be defined by a thrust vector balance and compared with the result obtained by the calorimetric technique.

The present results from the glass capture cup technique developed can only be considered to be useful qualitatively. It was found that the inability to remove all deposits from the cup prevented repeatable data to be had with this technique.

The in-situ Langmuir probe cleaning technique that was developed was successful in the development of one of the most valuable diagnostic tools developed during this program. The maximum instantaneous value of the transient ion density noted in the plume was about 3.5×10^{14} ions/cm³ at a distance of 0.7m from the thruster nozzle. The peak instantaneous density drops to about 5.7×10^{13} ions/cm³ at an axial distance of 1.42m. The maximum transient electron temperature noted was about 4.3×10^4 K. The lowest detectable density of the present set-up is about 10^{12} ions/cm³. Results obtained show the transient ion density to last only several tens of microseconds on axis within the plume at a distance of 0.7m from the nozzle. It is recommended that a pulsed probe be developed to significantly reduce the data reduction time and the overall accuracy of the technique.

Chemical analysis of a contaminated sample using Fourier Transform-Infra Red technique has identified contamination of an aluminum sample at only two absorption bands. A stronger absorptance was noted at 1590 cm^{-1} (6.29 microns) and a weaker band at 1440 cm^{-1} (6.94 microns). These bands are good indications of the presence of either a metal salt or a carboxyl ion (COO^-). The source of oxygen in the contaminated sample needs to be resolved and since the uncontaminated control sample was also found to be contaminated (the latter source, phtalate esters, was different than the source cited above for the test sample), it is important that future contamination studies develop procedures for pre-test cleaning of test samples.

Since transient pressure surges were noted on a nude ionization gauge which was hidden behind the thruster, it has been concluded that any back flow noted in the test facility was due to wall scattering rather than from direct plume effects. It would be desirable to develop a transient nude ionization gauge along with a pulsed Langmuir probe as general time-resolving instrumentation for back flow measurements.

Exposing collimated flight quality solar cells to regions extending from 15° off the thrust axis to 80° off the axis has not shown any changes in the AMO calibration short-circuit current. Minor changes noted are within the calibration accuracy of Spectrolabs LAPSS (Large Area Pulsed Simulator System). Since the cells were exposed to the plume for 8 and 24 hours of thruster operation, it might

be desirable to increase the exposure time in future tests providing back scattered mass in the test environment does not contaminate the cells.

None of the experimental data generated revealed the plume of the pulsed plasma thruster to be "dirty" or highly contaminating. This result supports flight experience with pulsed plasma micro thrusters. Most contaminating effects noted during this study were due to facility effects. However, erosive effects of a surface can occur if the surface is positioned within the energetic transient plume which is fairly well collimated within about $\pm 30^\circ$ to $\pm 40^\circ$.

Since features of the plume of a pulsed plasma thruster differ from features of other propulsive devices, it is recommended that detailed studies of scattering effects due to the test facility be carried out in future contamination studies if such studies are carried out in a different test facility.

5.0 REFERENCES

1. Komatsu, G.K., Sellen, Jr., J.M., Beam Efflux Measurements, NASA CR-135038, 1 June 1976.
2. Hall, D., Cohen, E., Evaluation of Electric Propulsion Beam Divergence and Effects on Spacecraft, Final Report 08965-6013-R0-00, Sept. 2, 1969, TRW Systems Group, Redondo Beach, Calif.
3. Reynolds, T., Richley, E., Contamination of Spacecraft Surfaces Downstream of a Kaufman Thruster, NASA TN-D-7038, January 1971.
4. Weigland, A., Mirtich, M., Measurement of Sputtered Efflux from 5, 8 and 30 cm Diameter Mercury Ion Thrusters, AIAA Paper 75-358, AIAA 11th Electric Propulsion Conference, New Orleans, La., March 1975.
5. Kemp, R., Luedke, E., Hall, D., Miller, W., Effects of Electrostatic Rocket Deposited Impacted Materials on Solar Cells, AIAA paper 72-447, AIAA 9th Electric Propulsion Conference, Bethesda, Md., April 1972.
6. Stevens, J., Determination of the Extent of Ion Thruster Efflux Deposition on Spacecraft Surfaces from the SERT II Flight Thermal data, NASA TM-71642, 1975.
7. Zafran, S., Colloid Advanced Development Program - Appendix H Compatibility of Colloid Thruster Exhaust with Spacecraft Surfaces, AFRPL-TR-76-19, June 1976, TRW Defense and Space Systems Group, Redondo Beach, Calif.
8. Scialdone, J., Determination of Molecular Contamination Performance for Space Chamber Tests, NASA TN D-7250, Washington, D.C., May 1970.
9. Demichev, V., Matyukhin, V., A Study of the Properties of Rapidly Moving Plasma Blobs, Soviet Physics - Doklady, Vol 8, No. 5, Nov. 1963 p. 457.
10. Lyon, W.C., A Study of the Effects of Teflon Thruster Exhaust upon Spacecraft, Report HIT-443, Hitman Associates, Inc., Columbia, Md., April 1970, (Final Report contract NAS 5-9479, Goddard Space Flight Center, Greenbelt, Md.)
11. Visentine, J., Ogden, J., Ritter, M., Smith, C., Preparation, Verification and Operational Control of a Large Space Environment Simulation Chamber for Contamination Sensitive Tests, Paper 33 in "Space Simulation" NASA-SP-298, 1972.
12. Dawbarn, R., Busby, M., Kinslow, M., Study of High Energy Gases Impinging on Various Cryo Surfaces, AEDC-TR-72-33, April 1972, Arnold Engineering Development Center, AFSC, Tennessee.
13. Palumbo, D.J., Begun, M., Guman, W., Pulsed Plasma Propulsion Technology, Interim Report, 10 May 1973 - 10 July 1974, AFRPL-TR-74-50, Air Force Rocket Propulsion Laboratory AFSC, Edwards, Calif.

14. Wentink, T., High Temperature Behavior of Teflon, AVCO Research Report 55, Avco Everett Research Laboratory, Mass., July 1959.
15. Palumbo, D., Guman, W., Pulsed Plasma Propulsion Technology, Report AFRPL-TR-73-79, Air Force Rocket Propulsion Laboratory, Edwards, Calif., September 1973.
16. Johnson, E.O. and Malter, L., Phys. Rev., Vol. 80, p. 58-68 (1950).
17. F. Maisenholder and W. Mayerhoffer, Jet Diagnostics of a Self Field Accelerator with Langmuir Probes, AIAA Journal, Vol. 12, #9, September 1974.
18. Pulsed Electromagnetic Gas Acceleration, Princeton University, Semi Annual Report #634R.
19. Electrical Probes for Plasma Diagnostics, J.D. Swift, M.J.R. Schwar, American Elsevier Publishing Co., Inc., New York, Chapter 9 and Chapter 6.
20. Dennis, N. and Heppell, T.A., Vacuum System Design, Chapman and Hall Ltd., London, 1968 (Distributed by Barnes & Noble, Inc.), p. 5.
21. Guman, W., Nathanson, D., Pulsed Plasma Microthruster Propulsion System for Synchronous Orbit Satellite, J. Spacecraft & Rockets, Vol. II, No. 10, Oct. 1974, pp. 729-731.
22. Allen, W., Personal Communication, John Hopkins University, Applied Physics Lab., September 11, 1974.
23. Curtis, H., Effect of Error in Spectral Measurements of Solar Simulators on Surface Response, NASA TN-5904, Washington, D.C., July 1970.
24. Norman, C.F., Design and Initial Operation of a Large Low Cost Solar Simulator using Tungsten Lamps with Collimating Tubes, AEDC-TR-69, 198, Dec. 1969.
25. Moffett, Personal Communication, 213-365-4611, Spectrolab, Sylmar, Calif., Nov. 11, 1976.
26. Goetzel, C., Rittenhouse, J., Singleton, J., Space Materials Handbook, 3rd Edition, NASA SP-3051, 1969, p. 90.
27. Hsu, S.T., Engineering Heat Transfer, D. Van Nostrand Co., Inc., New York, 1963, p. 147.
28. Sadler, R., Hammerdinger, L., Rando, I., "Emissometer, a Device for Measuring Total Hemispherical Emittance," In Measurement of Thermal Radiation Properties of Solids, NASA SP-31, 1963.